R-7
6/01

QEA

Quantitative Environmental Analysis, LLC

REVIEW OF KALAMAZOO RIVER PCB FATE MODEL DEVELOPED BY LIMNO-TECH, INC.

Prepared for:

Michigan Department of Environmental Quality
Lansing, Michigan

June 2001

TABLE OF CONTENTS

TABLES

LIST OF FIGURES

SECTION 1
INTRODUCTION

A PCB fate model was developed for and applied to the Kalamazoo River by Limno-Tech, Inc. (LTI). Development, calibration and application of the LTI model was documented in "Modeling Analysis of PCB and Sediment Transport in Support of the Kalamazoo River Remedial Investigation/Feasibility Study" (LTI 2000). That report, i.e., LTI (2000), will be referred to as the "LTI report" herein.

A review of the LTI model has been conducted by QEA for Michigan Department of Environmental Quality (MDEQ). This work was performed under a contract that was administered by Camp, Dresser & McKee (CDM). Todd King of CDM was the project manager, who also provided technical guidance and support. QEA appreciates the technical advice provided by Warren Lyman of CDM.

The model review included the following activities: review of the LTI report; evaluation and testing of various models (e.g., HEC-6, KALSIM and bank erosion models); a meeting at LTI in Ann Arbor on January 9 and 10; review of additional information provided by LTI; and various informal discussions with LTI personnel. The technical interchanges with LTI were very helpful; the open technical discussions at the January 2001 meeting were productive. QEA appreciates the effort made by Mike Erickson and his colleagues at LTI in providing model documentation and answering the many questions that were posed to them.

The focus of the model review was determining the answer to the following question: *Is the LTI model sufficiently reliable for use as a management tool to evaluate remedial alternatives?* To answer this question, the review concentrated on evaluating the primary components of the PCB fate model: HEC-6 hydraulics, bank erosion model and KALSIM. For comparative purposes, a description of a reliable PCB fate modeling framework is presented in Section 2; comparisons between this model framework and the LTI model are useful for identifying potential weaknesses in the LTI model. The capabilities and accuracy of the LTI

model are more fully understood if some basic knowledge about PCB fate and transport processes in the Kalamazoo River is used in the model evaluation process. A preliminary analysis of PCB fate and transport data from the river was conducted for this purpose and the results are discussed in Section 3. The fourth section of the report contains a detailed discussion of the PCB fate model and its primary components. Conclusions about the reliability of the LTI model and an answer to the question posed above are presented in the last section of the report.

SECTION 2
DESCRIPTION OF A RELIABLE PCB FATE MODEL

Development of a reliable PCB fate and transport model for the Kalamazoo River, or any river, requires more than simply applying a computer model, adjusting various input parameters during model calibration, and then using the model to make forecast predictions for different remedial alternatives. A reliable model is able to accurately and realistically simulate PCB fate processes over temporal and spatial scales that are relevant to the management questions for a particular contaminated sediment site. The details of a model will vary from site to site but, in general, a reliable model will contain the components and processes described below. This information may be used as a standard to which the LTI model can be compared and aid in determining the reliability of that model.

2.1 COMPONENTS OF A QUANTITATIVE MODEL

A quantitative model of PCB fate in a river will consist of the following submodels: hydrodynamic, sediment transport, PCB fate and transport, and bioaccumulation. A generalized schematic for a PCB fate model framework that includes these submodels is illustrated on Figure 2-1. An important component of any PCB fate model, in addition to the four submodels, is the procedure used to specify flow and solids loads from the surrounding watershed. Often, long-term changes in sediment and fish PCB concentrations in a river, i.e., natural attenuation rate, are primarily controlled by the sediment loading rate from tributaries.

The complexity of each submodel depends on site conditions, e.g., river geometry and sediment bed properties, and the level of uncertainty that can be tolerated in the assessment. However, a minimum level of model complexity is necessary for developing a credible model that is capable of producing realistic simulations. Important fate and transport processes that must be included in a model to achieve this minimum level of credibility are described in the following sub-sections.

One truism about modeling is that "a model is only as good as the data that are used in it." Thus, it must be remembered that a significant level of effort is typically required for data analyses to support the development and calibration of a computer model. Not only must data be analyzed to develop model inputs, e.g., site-specific PCB parameters and tributary solids loads, but analyses need to be conducted to develop an understanding of the processes controlling PCB fate in a particular river. This type of analysis is referred to as development of a conceptual model for the site.

A conceptual model for a contaminated sediment site provides a qualitative understanding of transport processes in the river. This assessment provides information on the primary processes that control temporal and spatial differences, usually at relatively large scales, in PCB concentrations in water, sediment and biota. Even though a conceptual model only provides a qualitative understanding of PCB fate and transport, this qualitative model is critical for development of a reliable quantitative model. Results of the computer model are compared to the conceptual model to ensure that the quantitative model is producing realistic results. Without adequate agreement between these two models of the system, the computer model cannot be used as a reliable management tool.

While a conceptual model and the data analyses used for its development are important, these qualitative analyses must not be used in isolation to evaluate PCB fate at a site or to make management decisions. The conceptual model and associated data analyses need to be used in conjunction with a quantitative model because a computer model constrains and synthesizes the data.

2.2 HYDRODYNAMIC PROCESSES

A hydrodynamic model simulates the movement of water in a river. This submodel predicts temporal and spatial variations in current velocity, water depth and bottom shear stress. The level of spatial resolution represented by the model, i.e., one-, two- or three-dimensional, depends upon the complexity of the river geometry and flow conditions. Typically, density-driven circulation in a river is of minimal importance, making it possible to accurately simulate

flow in a river using a one-dimensional or two-dimensional hydrodynamic model. Generally, a time-dependent model is required for contaminated sediment applications.

Accurate simulation of sediment transport processes is of critical importance for development of a reliable contaminant fate model. As discussed in the next sub-section, bottom shear stress is a primary factor in controlling sediment deposition and resuspension processes. Bottom shear stress is a measure of the force exerted by river currents on the sediment bed due to water column turbulence. In many rivers, including the Kalamazoo River, significant spatial variations in bathymetry, e.g., lateral variations in water depth, and sediment bed type, e.g., cohesive and non-cohesive sediments, can affect local bottom shear stress. In many cases, it is important to simulate these spatial variations in bottom shear stress, making it necessary to use a two-dimensional, vertically-averaged hydrodynamic model.

2.3 SEDIMENT TRANSPORT PROCESSES

Suspended sediment particles in a river have a large range of sizes, from less than 1 μm clays to medium sands on the order of 400 μm. Simulation of the entire particle size spectrum is impractical. Therefore, particles can be broadly segregated into two groups: silt and clay that may interact and form flocs (cohesive sediment) and sand that is transported as discrete particles (non-cohesive sediment). "Class 1" particles include all the cohesive particles, i.e., clays and silts, with disaggregated particle diameters of less than 62 μm, while the "class 2" particles include coarser, non-cohesive sediments, primarily fine and medium sand with diameters between 62 and 425 μm. In the past, many contaminant fate models have only used one sediment size class, an approximation that may not produce realistic results. Significant temporal and spatial variations in suspended sediment composition can occur in a river, making it necessary to use at least two sediment size classes.

As mentioned above, cohesive sediments in the water column range from clay particles smaller than 1 μm up to ~62 μm silts. The discrete particles aggregate and form flocs that can vary greatly in size and effective density. Variations in concentration and shear stress affect both floc diameter and settling speed (Burban et al. 1990). Previous modeling studies (Ziegler and

Nisbet 1994, 1995; Gailani et al. 1996; QEA 1999) have shown that an effective approximation is to treat suspended cohesive sediments as a single class. This approach assumes that the settling and depositional characteristics of cohesive sediments can be represented by average values of a distribution of properties. Using this approximation, the deposition flux (D_1) of cohesive (class 1) sediments to the sediment bed is expressed as (Ziegler and Nisbet 1994)

$$D_1 = P_1 W_{s,1} C_1 \tag{2-1}$$

where C_1 = suspended sediment concentration, class 1; $W_{s,1}$ = cohesive sediment settling speed; and P_1 = probability of deposition for cohesive sediments.

Settling speeds of cohesive flocs have been measured over a large range of concentrations and shear stresses in freshwater (Burban et al. 1990). The Burban settling speed data for cohesive flocs in freshwater were analyzed to develop a formulation to approximate the effects of flocculation on settling speed (QEA 1999). This analysis indicated that the settling speed is dependent on the product of the concentration (C_1) and the water column shear stress at which the flocs are formed. Using this formulation, class 1 sediments have settling speeds that range from about 1 to 10 m/d.

Modeling suspended cohesive sediments as a single class makes it necessary to use a probability of deposition (P_1) to parameterize the effects of particle/floc size heterogeneity and near-bed turbulence on the deposition rate. The complex interactions occurring in the vicinity of the sediment-water interface cause only a certain fraction of the settling cohesive sediments, represented by P_1, to become incorporated into the bed (Krone 1962, Partheniades 1992). An experimentally-based formulation that represents the effects of variable floc size on probability of deposition was developed by Krone (1962)

$$P_1 = 1 - \frac{\tau}{\tau_{cr,dep}} \quad , \quad \tau \le \tau_{cr,dep} \tag{2-2}$$

where τ = bottom shear stress and $\tau_{cr,dep}$ = critical shear stress for deposition. A typical value for $\tau_{cr,dep}$ is 1 dyne/cm^2, which corresponds to a current velocity of approximately 20 cm/s. Non-mechanistic solids transport submodels have used a constant effective settling speed (O'Connor et al. 1983, Velleux and Endicott 1994), an approximation which neglects the important effects of near-bed turbulence on deposition and can produce unrealistic results because significant temporal and spatial variations in τ and P_1 occur in any river.

Class 2 particles, i.e., fine and medium sand, suspended in the water column have an effective settling speed ($W_{s,2}$) that depends on the effective particle diameter (d_2). A relationship between $W_{s,2}$ and d_2 was developed by Cheng (1997). The depositional flux (D_2) for this sediment class is estimated as

$$D_2 = P_2 W_{s,2} \Gamma C_2 \qquad (2\text{-}3)$$

where C_2 = suspended sediment concentration, class 2; P_2 = probability of deposition for non-cohesive sediments; and Γ = class 2 stratification correction factor. Details concerning methods for calculating Γ, $W_{s,2}$ and P_2 are presented in QEA (1999), however, general descriptions of these parameters will be given here. The settling speed of sand increases with particle diameter, with settling speeds ranging from about 200 to 1,000 m/d for suspended sands. Similar to cohesive sediments, probability of deposition of sand particles decreases as current velocity (or τ) increases, with $P_2 = 1$ for quiescent conditions. Significant vertical stratification of class 2 sediment can occur in the water column due to the high settling speeds of fine and medium sand. This characteristic means that accurate calculation of class 2 deposition flux requires use of the near-bed concentration ($C_{a,2}$), where $C_{a,2} = \Gamma C_2$ and $\Gamma > 1$. Note that Γ is dependent upon $W_{s,2}$, τ, bottom roughness and local depth.

It should be noted that the "effective" settling speed of class 1 ($P_1 W_{s,1}$) is typically one to two orders of magnitude lower than that of class 2 ($P_2 W_{s,2} \Gamma$). This differential has significant impact on simulation results and underscores the importance of using two sediment size classes as opposed to a single size class as has been typically used in many contaminant fate models.

Experimental results have shown that a finite amount of material will typically be resuspended from a fine-grained, cohesive sediment bed exposed to a constant bottom shear stress. This phenomenon, referred to as bed armoring, has been observed and quantified in a number of laboratory (Parchure and Mehta 1985, Tsai and Lick 1987, Graham et al. 1992) and field studies (Hawley 1991, Amos et al. 1992). The amount of fine-grained sediment resuspended from a cohesive deposit can be predicted using (Gailani et al. 1991)

$$\epsilon = \frac{a_o}{T_d^N}\left(\frac{\tau - \tau_{cr}}{\tau_{cr}}\right)^n \quad , \quad \tau \geq \tau_{cr} \tag{2-4}$$

where ε = net mass of resuspended sediment per unit surface area (resuspension potential); a_o = site-specific parameter; T_d = time after deposition in days; N,n = exponents dependent upon the deposition environment; and τ_{cr} = effective critical shear stress. Previous studies have shown that the resuspension properties of cohesive beds in different aquatic systems can differ substantially (Ziegler and Nisbet 1994, 1995; Lick et al. 1995; QEA 1999), with the shear stress exponent (n) ranging from 2 to 3 and the parameter a_o possibly varying by an order of magnitude.

The non-linear relationship between resuspension potential and bottom shear stress in Equation (2-4) is important. Bottom shear stress increases as the square of the current velocity (u_c). Thus, for a current-dominated environment, e.g., a river, the mass of resuspended cohesive sediment (ε) is a highly non-linear function of the current velocity, with ε being proportional to u_c raised to the fourth to sixth power. For rivers, this non-linear dependence on current velocity, or equivalently flow rate, generally causes rare floods to be of great importance.

Many contaminant fate models have used a resuspension velocity that is empirically determined during model calibration (O'Connor et al. 1983, Velleux and Endicott 1994). This procedure can produce highly inaccurate results because: 1) site-specific data are not used to determine erosion parameters (and, thus, constrain the resuspension process); 2) bed consolidation effects are neglected; and 3) bed armoring effects are not simulated. In addition,

spatial variations in bed properties, e.g., cohesive and non-cohesive sediment, are usually neglected.

Simulation of non-cohesive resuspension in many rivers is necessary because: 1) non-cohesive bed areas, composed primarily of sand and gravel, typically compose a majority of the sediment bed area and 2) cohesive and non-cohesive resuspension processes are very different. Typically, non-mechanistic solids transport submodels have not accounted for spatial variations in resuspension properties and have used a spatially constant resuspension velocity. This approach is generally inadequate and should not be applied to most rivers.

Extensive work has been done on modeling suspended load transport of non-cohesive sediment, with many different models available. One model that has been shown to be useful for contaminant fate studies in rivers was developed by van Rijn (1984), see QEA (1999) for computational procedure details. The van Rijn method has been shown to yield good results for predicting suspended load transport of sands (van Rijn 1984, Garcia and Parker 1991, van Rijn et al. 1993).

Non-cohesive areas of the sediment bed in many rivers typically contain a significant fraction of non-suspendable coarse sand and gravel. When erosion occurs in these areas, the suspendable sediment in the near-surface layer, referred to as the active layer, is depleted. Continuous depletion of suspendable sediment in the active layer will eventually reduce the erosion rate to zero. At this point, the active layer is composed entirely of non-suspendable sediment, and the sediment bed has become armored (Karim and Holly 1986, Jain and Park 1989, van Niekerk et al. 1992). The bed armoring process has been modeled by assuming that the sediment bed is composed of an active layer, which interacts with the water column, and a parent bed, which is below the active layer (Karim and Holly 1986, van Niekerk et al. 1992). Interactions between the parent bed, active layer and water column cause the grain size distributions in the active layer and parent bed to change with time. The thickness of the active layer is of critical importance in applying this type of bed armoring model. Various formulations have been proposed for the active layer thickness (Borah et al. 1982, Karim and Holly 1986, Jain

and Park 1989). An expression for the active layer thickness, which is a linear function of the local bottom shear stress, was developed by van Niekerk et al. (1992).

In summary, resuspension processes need to be represented by formulations that depend upon bottom shear stress and local sediment bed properties. Erosion is an episodic process, with significant resuspension occurring when the bottom shear stress exceeds a critical value, which is dependent upon bed properties. Significant differences exist between the resuspension properties of cohesive and non-cohesive sediments, with a reliable model accounting for these differences. Finally, site-specific data are needed to adequately parameterize bed properties for both types of sediment.

2.4 PCB FATE PROCESSES

A quantitative mathematical model of PCB fate will consider all of the processes depicted in Figure 2-2. The various transport, transfer and reaction processes, as well as forcing functions (such as loadings) external to the area of study, affect PCB concentration. A quantitative mathematical model is constructed by combining the principle of conservation of mass with mechanistic descriptions of the various processes.

PCB fate processes may be divided into two general categories: (a) transport and (b) transfer and reaction. Transport is the physical movement of PCBs caused by the net movement of water and solids to which PCBs are adsorbed. The processes involved in transport are flow and dispersion in the water column (hydrodynamics) and settling, resuspension and burial of solids (sediment transport) as discussed in the previous two sections. Generally, transport process specifications are supplied by the coupled hydrodynamic and sediment transport models. Transfer and reaction include movement of PCBs among the air, water, and solid phases of the system and biological transformation of the compound. The processes involved in transfer and reaction are volatilization, adsorption, dechlorination and biodegradation.

Adsorption

As shown on Figure 2-2, PCBs are generally present in three interacting phases: 1) freely dissolved; 2) sorbed to particulate matter or solids; and 3) sorbed or complexed with dissolved or colloidal organic carbon (DOC). Adsorption is generally treated as a rapid process relative to other processes affecting PCBs. Equilibrium partition coefficients are typically used to determine the partitioning of chemical between the three phases. Thermodynamic considerations suggest that equilibrium partition coefficient should be a function of temperature. The conventional conceptual model of sorption is a biphasic process, consisting of a fast stage (minutes to hours) and a slow stage (weeks to months). The fast stage is adequately described by equilibrium partitioning (DiToro and Horzempa 1982), whereas the resistant component is not. Ignoring biphasic sorption will result in an over-estimation of desorption of PCBs from sediments, but in some cases this error is small and can be neglected. For this reason, it is preferential to obtain site-specific partitioning relationships.

Volatilization

Typically, a chemical's tendency to volatilize is determined by the ratio of its equilibrium activities in air and water. The rate at which volatilization occurs is dependent on the mass transfer coefficient at the air-water interface and the concentration of PCBs in the water column. Only freely-dissolved PCB can be transported across the interface and sorption to particulate or dissolved organic carbon reduces volatilization. The equation used to describe PCB flux due to volatilization is generally specified by a two-film theory through two relatively thin boundary layers. The water-phase mass transfer coefficient can be determined either by water flow conditions or surface wind conditions, depending on the system and the controlling mechanism of surface turbulence. The water-vapor equilibrium constant (Henry's Constant) will generally have a positive dependency on temperature due to basic thermodynamics. Volatilization at waterfalls and dams can also be a significant fate mechanism of PCB, depending on river flow rate and height of dam.

Dechlorination

The most significant biodegradation process that affects PCBs is the biotransformation associated with dechlorination. Anaerobic dechlorination of PCBs has been studied in numerous laboratory and field experiments. A good review is presented by Bedard and Quensen (1995). The process depends on the chlorine substitution pattern of the PCB congener(s) and site-specific environmental conditions. An accurate model of dechlorination requires consideration of the dechlorination pathways and rates for individual congeners, but often is approximated as an overall first-order rate process. However, for PCB fate models that consider total PCBs (i.e., sum of all PCB congeners), dechlorination is typically not a major mass loss mechanism. For example, USEPA has estimated that it accounts for about a 10% loss in the Upper Hudson River (USEPA 1997). Ignoring dechlorination will generally result in a underestimation of fate processes such as desorption and volatilization.

PCB Exchange at the Sediment-Water Interface

PCB exchange across the sediment-water interface occurs as a result of numerous physical, chemical, and biological mechanisms. Hydrodynamically-induced resuspension dominates sediment-water exchange during periods of elevated flow. During low-flow periods, a number of possible mechanisms contribute to sediment-water exchange, including:

- molecular diffusion of PCBs contained within sediment pore waters;
- transport of natural colloids to which PCBs have sorbed;
- groundwater advection of contaminated pore-water; and
- bioturbation induced pore-water and particulate transport.

Often, these mechanisms are grouped together in a single Fickian formulation that specifies the total transfer as a product of the concentration gradient between the sediment pore-water and water column dissolved (truly dissolved and DOC) PCBs and an overall diffusive transfer coefficient. A large seasonal dependence has been observed in this coefficient that may be correlated to biological activity in the bed.

Vertical Diffusion within the Bed

Similar to sediment-water diffusive transport, pore-water diffusive transport of PCBs within the sediment is described as the product of the vertical gradient of dissolved plus DOC bound pore-water PCB concentration and a diffusion coefficient, typically based on the molecular diffusion coefficient.

Particulate Mixing within the Bed

The dominant mixing in the sediment bed active layer is primarily due to particulate mixing caused by the activities of benthic invertebrates in the sediment. This process of bioturbation is mathematically described as a "particle diffusion" process.

2.5 BIOACCUMULATION PROCESSES

The goals of developing a quantitative analysis of bioaccumulation generally include:

- quantifying the relative importance of alternative contaminant sources to the biota, for example local sediments versus water;
- evaluation of historical trends in contaminant levels in biota; and
- predicting the rate of natural recovery and the response of fish contaminant levels to remedial actions.

The transfer of PCBs through the food web can be described in various ways. The simplest description is a bioaccumulation factor, which corresponds to a ratio of the contaminant concentration in the species of interest to the concentration in the exposure source. A more sophisticated approach involves a dynamic model.

Bioaccumulation factors

Two bioaccumulation factors are generally used, one to describe accumulation from sediment (biota-sediment accumulation factor or BSAF) and one to describe accumulation from the water column (bioaccumulation factor or BAF). The accumulation of PCBs from the water column is described by

$$BAF = \frac{v_L}{c}(1000) \qquad (2\text{-}5)$$

where BAF = bioaccumulation factor (L/kg lipid); v_L = concentration of PCBs in the organism (mg/kg lipid); and c = concentration of dissolved PCBs in the water column (µg/L). The accumulation of PCBs from sediments is described by

$$BSAF = \frac{v_L}{r_{soc}} \qquad (2\text{-}6)$$

where BSAF = biota-sediment accumulation factor (kg organic carbon/kg lipid); and r_{soc} = concentration of PCBs on sediment bed particles (mg/kg organic carbon).

Concentrations in the sediments are represented on an organic carbon basis because PCBs preferentially associate with the organic matter fraction of the sediment bed and because benthic organisms derive their energy from sediment organic matter. Therefore, the amount of PCBs ingested by the organism is proportional to the amount of PCBs present in the organic matter fraction, which is represented by r_{soc}.

Bioaccumulation factors are often used as screening-level descriptors of bioaccumulation for all aquatic biota. These factors are most useful in describing bioaccumulation in small, short-lived organisms that accumulate a chemical from one exposure source and that respond rapidly to changes in exposure concentrations. Examples of appropriate organisms include benthic and water column invertebrates. BAFs and BSAFs have been developed for the Kalamazoo River,

and these indicate that it is probable that the water column constitutes a more important direct source of PCBs to the fish than do local sediments in the Kalamazoo River (see Section 3.4 for more discussion).

Dynamic mechanistic models

The application of bioaccumulation factors to describe the bioaccumulation process is subject to a number of limitations. First, if both the water column and sediments contribute to overall exposure and if PCB concentrations in the two media change at different rates, then a single bioaccumulation factor may not characterize concentrations in the biota accurately. This is important in developing estimates of the future rate of recovery of the system under natural attenuation and subject to remediation. Second, if exposure concentrations, organism physiology (especially lipid content and body weight) or the food web change on a time scale commensurate with the response time of the food web, then bioaccumulation factors will not accurately describe the bioaccumulation process: chemical levels in the organism may not be able to keep pace with changes that occur on a time scale similar to the response time of the organism.

Under these conditions, therefore, a time-variable model provides the best tool for making projections, especially of short-term responses to changes in exposure (e.g., during remediation). Furthermore, a model can aid in the analysis of long-term historical trends, which may be confounded by short-term variation in lipid content, body weight and food web structure.

Time-Variable Mechanistic Model

The accumulation of PCBs by aquatic animals is described by

$$\frac{dv_i}{dt} = K_{ui}c + \alpha_c \sum_{j=1}^{n} C_{ij}v_j - (K_i + G_i)v_i \qquad (2\text{-}7)$$

where i,j = indices for predator and prey, respectively; v_i = concentration of chemical in species i (µg/g(w) where g(w) is grams wet weight); K_{ui} = rate constant for respiratory chemical uptake by

species i (L/g(w)-d); c = concentration of chemical dissolved in water (μg/L); K_i= rate constant for excretion of chemical by species i (1/d); α_c = efficiency at which ingested chemical is assimilated from prey; C_{ij} = predation or consumption rate of species i on species j, (g(w)prey/g(w) predator-d); G_i = growth rate of species i (g(w)/g(w)-d); and n = number of species (including different year classes of a single species) preyed upon by species i.

The first term of Equation (2-7) represents the direct uptake of PCBs by the animal from water. The second term represents the flux of PCBs into the animal through feeding. The third term represents the loss of chemical due to diffusion across the gill and the change in concentration due to growth. The gill is the major site of depuration; the fecal elimination rate is much less than the growth rate and is not included in the model. The dynamic bioaccumulation model is applied to each fish species, accounting for species-specific differences in growth rate, consumption rate, and elimination rate. The individual processes within Equation (2-7) have been discussed in detail elsewhere (Connolly 1991, Connolly et al. 1992, QEA 1999).

The information necessary to develop a reliable model include the following:

A model framework, or computer code. The model framework should permit dynamic (time-variable) simulation. Ideally, the entire life cycle of the key species should be simulated, as this permits greater realism as well as comparison of model results with data collected for fish of varying ages. The model should be mechanistic, incorporating bioenergetics and toxicokinetics principles. The model should permit multiple trophic levels and complex dynamic diets. Finally, the model should provide for the possibility of movement among regions with varying exposure levels.

Values for parameters describing species bioenergetics. Bioenergetics refers to the processes underlying energy intake and use, primarily growth and respiration. These are critical to several components of a bioaccumulation model: the respiration rate contributes to the calculation of the food consumption rate, as well as the rates of uptake and loss of PCBs across the gill surface. The growth rate contributes to the food consumption rate; in addition, growth dilution can be a dominant negative term in Equation (2-7). In general,

published information is available concerning the respiration rates of many species and generic formulae are also available. Growth rates vary among species and locations, and should in general be measured in the fish that are being modeled. Such measurements are relatively simple, involving calculating ages in individual fish based on scale or spine annuli.

Characterization of food web structure. Food web structure is another critical component of the model that should be characterized to the extent possible using site-specific information. The food web consists of the species of interest, their prey, the prey of their prey, and so on. In general, water column and sediment particulate matter are the first trophic level of the food web. These particles consist of allochthonous particulate matter that enters the river from the watershed, as well as autochthonous matter that is produced within the river itself (i.e., phytoplankton, periphyton and macrophytes). These resources are consumed by invertebrates that reside in the water column as well as within and on the surface of the sediment bed. Invertebrates are consumed by fish, which in turn can be consumed by larger predatory fish. Fish may feed on a combination of sediment-dwelling invertebrates and water column-based invertebrates.

It is not necessary in general to model every species. Species of particular interest should be modeled individually. The prey of these species may be modeled as trophic groups, for example bottom-feeding forage fish and water column-feeding forage fish, benthic and water column invertebrates. The choice of groups depends on the extent of the available contaminant data, as well as the extent of the available information describing the bioaccumulation process. For example, there are several studies available that quantify bioaccumulation in benthic and water column invertebrates, but there is in general insufficient information to model individual species of invertebrates in a manner that will improve the overall precision of the model.

Field natural history information is sometimes sufficient to specify reasonable diets for the key species groups. Often, however, food web structure cannot be quantified precisely because natural ecosystems are too variable to accurately characterize average

diets in the absence of extensive field investigations. Therefore, one reasonable strategy is to use natural history information to provide bounds on reasonable diets and then adjust the dietary composition within these bounds during model calibration.

Characterization of species movement patterns or exposure areas. In ecosystems with spatially variable exposure levels (e.g., Kalamazoo River), it is important to have some understanding of where the organisms forage in order to develop a realistic model. For example, the impact of targeted remediation of contaminated sediments will depend on the relative contribution of those targeted sediments to the average dose to the fish. Such information can be drawn from natural history observations, from field studies of movement patterns (e.g., tagging and DNA composition), and from gradients in PCB concentrations observed in sediments, water and fish. Often, the last source provides the most precise information: in an ecosystem which exhibits gradients in either sediments or water contaminant concentrations, gradients in contaminant levels in fish that match these gradients indicate relatively limited movement, while the lack of a gradient in fish contaminant levels suggests movement throughout the area.

Values for parameters describing PCB toxicokinetics. These parameters include assimilation efficiencies at the gut surface, uptake efficiencies at the gill surface, and elimination rates. A considerable body of literature exists that permits quantification of assimilation and uptake efficiencies. Elimination rates are subject to greater uncertainty, as long-term studies are rare and indicate PCB elimination rates that are considerably lower than short-term studies. The PCB elimination rate is a reasonable choice for adjustment during calibration, although consistency with previous modeling studies should in general be maintained.

PCB exposure levels. Depending on the goal of the modeling, exposure levels can be determined from available contaminant data for sediments and water, or from the results of a fate and transport model. With sufficient historical sediment and water data, a model of historical trends in fish may be developed based upon those data. For projecting the rate of natural recovery and the response of fish contaminant levels to remediation

actions, sediment and water column contaminant levels projected by a fate and transport model are necessary.

2.6 SUCCESSFUL APPLICATIONS

While the contaminant fate modeling framework described in the above sub-sections is sometimes considered to be 'state-of-the-science', and thus not easily applied to practical problems such as the Kalamazoo River, experiences at other contaminated sediment sites demonstrate that this type of model can be successfully applied. Previous applications of a comprehensive contaminant fate model that incorporated the important characteristics and processes discussed above into the various submodels include: 1) PCB and heavy metal fate in the Pawtuxet River, Rhode Island (Ziegler and Nisbet 1994, HydroQual 1996); 2) PCB fate in the Lower Fox River, Wisconsin (Gailani et al. 1991); 3) PCB fate in Watts Bar Reservoir, Tennessee (Ziegler and Nisbet 1995); 4) mercury fate in Lavaca Bay, Texas (HydroQual 1998); and 5) PCB fate in the Upper Hudson River, New York (QEA 1999, Connolly et al. 2000, Ziegler et al. 2001). These applications show that reliable models can be developed and used with confidence as management tools.

SECTION 3
PRELIMINARY OBSERVATIONS CONCERNING PCB FATE IN KALAMAZOO RIVER

As discussed in Section 2, development of a reliable model for a contaminated sediment site depends on the development of a conceptual model for the site so that the quantitative (computer) model results can be qualitatively validated. Review and evaluation of the Kalamazoo River PCB fate model developed by LTI cannot be accomplished by solely relying on model details and simulation results presented in the LTI report. While development of a comprehensive conceptual model for this site is beyond the scope of this review, some knowledge of PCB fate and transport processes in the river is necessary for proper evaluation of the LTI model. Thus, analyses of available Kalamazoo River data were conducted to develop a preliminary understanding of PCB fate in the river. This section describes the various analyses of sediment transport, PCB fate, and biota data that were carried out. Preliminary conclusions about PCB fate processes, based on these analyses, are also presented. The observations and conclusions developed in this section will be useful for evaluating the credibility and reliability of the LTI model as discussed in Sections 4 and 5.

3.1 NATURAL RECOVERY

Temporal trends indicate that fish PCB concentrations in the Kalamazoo River are decreasing. The rate of decline in biota levels, typically referred to as the rate of natural recovery, varies with location in the river and with the time period being considered. Different analyses having been conducted to estimate the natural recovery rate in biota (LTI 2000, Kern 2001). A useful measure of the natural recovery rate is half-life, which represents the period of time required for the average fish PCB concentration to decrease by a factor of two. Ranges of estimated half-lives for PCB levels in carp and smallmouth bass residing in three different regions of the river are shown on Figure 3-1. The half-life ranges presented on this figure were the result of analyses conducted by Kern (2001) that used all available fish concentration data. Uncertainty exists in estimated fish concentration half-life, and the natural recovery rate inferred

from this measure, due to variability between time periods considered in the half-life analyses and variability in sampling location. Different PCB half-life ranges may result from analyses that use data collected during specific time periods.

PCB half-lives in these two species range between approximately 3 and 13 years (Figure 3-1). Based on these results, the nominal range of PCB half-life in the Kalamazoo River is assumed to be 6 to 10 years herein. This range will be useful for comparing the results of data and modeling analyses in other sections of this report. Extrapolation of these PCB half-lives, i.e., natural recovery rates, to future periods is uncertain because PCB exposure sources to the fish may change.

3.2 SEDIMENT TRANSPORT PROCESSES

Natural recovery in the Kalamazoo River is caused by a combination of PCB source reductions (e.g., upstream and tributary sources, bank erosion sources) and burial of surficial sediments by cleaner sediments, as well as other PCB fate and transport processes. Burial is primarily controlled by sediment transport processes. Sedimentation rates in the river, especially in depositional zones such as Lake Allegan, are an important factor in the natural attenuation rate of surficial PCB concentrations. High-resolution sediment cores collected in depositional areas, e.g., Morrow Lake, Allegan City Impoundment and Lake Allegan, during 1994, 1999 and 2000 were geochronologically dated (LTI 2000, Lyman 2001). Average sedimentation rates at the sampling locations were determined based on the geochronologic analysis (LTI 2000, Lyman 2001); burial rates range between about 0.5 and 2.0 cm/yr (Figure 3-2a).

Estimated sedimentation rates were converted by QEA to an equivalent contaminant half-life in the well-mixed surficial bed layer where it was assumed that there were no external contaminant loads to the bed. Half-lives were calculated by assuming well-mixed layers that were 5 and 10 cm thick (Figure 3-2b). The resulting half-life estimates ranged between 2 and 9 years for the 5-cm layer and between 4 and 17 years for the 10-cm layer. These half-lives approximate the natural recovery rate of the Kalamazoo River in the absence of external PCB loads, e.g., upstream and bank erosion sources. In this analysis, the estimated PCB half-life, in

the absence of external PCB loads, is valid for periods during which the sedimentation rate is approximately constant, i.e., no significant changes in sediment loading to the river or in the deposition environment. Generally, half-lives that were estimated based on sedimentation rates with no external contaminant sources were lower than the range of half-lives based on temporal trends in fish concentrations, i.e., 6 to 10 years. This result suggests that an upstream PCB source(s) to zones 9 and 10 (Allegan City Impoundment and Lake Allegan) exists and it is affecting the natural recovery rate in those zones.

Sediment transport processes in the Kalamazoo River can be grouped into two broad categories: free-flowing river and impoundments. Free-flowing river reaches have a relatively high-energy environment, i.e., high bottom shear stress. Typically, the sediment bed in these areas is composed of sand and gravel. Cohesive (muddy) sediment deposits are relatively small; typically, about 10% to 20% of the bed area is composed of cohesive sediment deposits. A relatively low-energy environment exists in impoundment and backwater areas of the river; these areas are conducive to deposition. The sediment bed in these areas is primarily composed of cohesive sediment, with varying amounts of fine sand. Sedimentation rates are relatively high, typically ranging between 0.5 and 2.0 cm/yr.

3.3 PCB TRENDS IN WATER AND SEDIMENT

Spatial trends in water column PCB concentrations and loads during low-flow conditions were evaluated by QEA using data collected from March 2000 through September 2000. Low-flow conditions in the Kalamazoo River are defined as periods when flow rate at the Comstock gauging station is less than 800 cfs (mean discharge at that location is approximately 1,100 cfs). Water column PCB concentration data were regularly collected at eight locations between Morrow Lake Dam and Calkins Dam during this period in 2000. Water column PCB loading rates at the different locations were estimated using measured PCB concentrations and estimates of local flow rate.

Average spatial trends in low-flow water column PCB concentrations and loads during this sampling period are shown on Figure 3-3. The following general trends in PCB

concentrations and loads are observed from the data. Water column PCB load approximately doubles between Morrow Lake Dam (~RM 76) and the upstream end of the former Plainwell impoundment (~RM 58), indicating that the sediment bed between these two locations is a PCB source to the water column. PCB concentrations and loads approximately double again between RM 58 and the former Trowbridge Dam (~RM 46). This load increase is due to a sediment bed PCB source and possibly other sources in the former impoundments. Minimal change in PCB loads is observed between RM 46 and Allegan City Dam (~RM 36), indicating that the water column sources and sinks are approximately in balance during low-flow conditions in this 10-mile reach of the river. A significant decrease, approximately 33%, in PCB load is observed to occur in Lake Allegan. The fact that Lake Allegan is a PCB sink during low-flow conditions is very interesting, with the deposition of biotic and abiotic solids likely being a factor in the observed decrease in load.

Surficial PCB concentration samples were collected at numerous locations in the study area during 1993 and 1994. Organic carbon (OC) content was also measured so that dry-weight PCB concentration data can be normalized with respect to OC content. This normalization tends to remove variability in PCB spatial trends due to spatial variability in OC content, which is generally related to variations in sediment bed type, i.e., cohesive and non-cohesive sediments.

Average surficial PCB concentrations were determined for Aquatic Biota Sampling Areas (ABSA) 2 to 9 (Morrow Lake Dam to Lake Allegan). The spatial distributions of these ABSA averages, for dry-weight and OC-normalized PCB concentrations, are presented on Figure 3-4. Generally, OC-normalized bed concentrations are similar in zones 3, 7 and 10 (means of about 100 to 150 mg-PCB/kg-OC), with bed concentrations in zones 4, 5 and 6 being about two to five times higher (means of about 250 to 500 mg-PCB/kg-OC). The impact of PCB loading from long-term bank erosion in the former impoundments is presumably the primary cause of the elevated bed concentrations in zones 4, 5 and 6.

3.4 PCB TRENDS IN FISH

Spatial gradients of fish PCB concentrations were evaluated by QEA using carp and smallmouth bass samples collected at several locations during 1993 and 1994. Average wet weight and lipid-normalized PCB concentrations for both species were computed on an ABSA basis. Fish PCB concentrations were lipid-normalized because PCBs are preferentially stored in fats and normalization tends to reduce variability due to variability in lipid content.

Lipid-normalized concentrations in carp are similar in zones 2 to 6 and in Lake Allegan (means between 100 to 200 mg-PCB/kg-lipid), with concentrations about twice as high in zone 7 (350 mg-PCB/kg-lipid upstream of Trowbridge Dam), see Figure 3-5. Similarly, the highest PCB levels observed in smallmouth bass occur in zone 7 (Figure 3-6). Zone 7 is a former impoundment; elevated lipid-normalized PCB levels observed in carp and smallmouth bass are presumably due to higher PCB levels observed in the water column and surfical sediments in these areas.

The relative importance of the water column and surface sediments as sources of PCBs to the food web was evaluated by QEA using bioaccumulation factors, that is, ratios of fish tissue levels to levels in water (BAF) and sediment (BSAF; see Section 2.4). Downstream of Morrow Lake, BAF values for carp and smallmouth bass range between 5×10^6 and 30×10^6, a factor of six difference (Figure 3-7a). These values overlap BAF values observed in other systems (HydroQual 1995). BSAF values range from 0.1 to 4 kg-OC/kg-lipid (Figure 3-7b), a factor of 40 difference. These values are, in general, lower than BSAF values observed in carp in other systems (HydroQual 1995). The fact that BAF values are consistent with values measured in other systems and exhibit relatively little variability, while BSAF values appear to be relatively low and variable, suggests that the water column is the dominant source of PCBs to the fish.

3.5 PRELIMINARY CONCLUSIONS

The preceding results suggest the following conclusions, which must be considered to be preliminary and subject to refinement because of the limited scope during the present study. The

first conclusion that can be drawn from the analyses is that natural recovery is occurring in the river. The natural attenuation rate is spatially and temporally variable but an approximate range of the half-life that is representative of the site is six to ten years. While this half-life range (6-10 years) is based on temporal analysis of available fish PCB concentration data and is uncertain, it is useful for comparative purposes and it will be used to assess the reliability of the LTI model in subsequent sections of this report.

Examination of spatial trends in water column PCB concentrations during low-flow conditions, i.e., discharge less than 800 cfs at Comstock, resulted in the following observations. First, the sediment bed between Morrow Lake Dam and the upstream limit of the former Plainwell Impoundment increases the water column PCB load by about a factor of two; the observed increase is potentially caused by porewater exchange processes between the bed and water column. The areas upstream of the former impoundments contribute an appreciable amount of PCB to the water column during low-flow conditions. Second, the region between the former Plainwell Impoundment and the former Trowbridge Dam results in a relatively steep increase in PCB in the water column due to sediment porewater exchange and, possibly, other non-resuspension mechanisms. The available data do not permit a distinction between possible sources. Lastly, Lake Allegan is a significant sink during low-flow conditions.

Another conclusion is that PCB sources upstream of Lake Allegan apparently reduce recovery rates in portions of the lake. Relatively high sedimentation rates in the lake, i.e., maximum values of 1.5 to 2.0 cm/year, would produce relatively short half-lives of surficial PCB concentrations, i.e., less than 6 years, if there were no significant upstream PCB sources.

Spatial trends in surficial bed and fish PCB concentrations show that similar levels occur upstream of the former Plainwell Impoundment and downstream of the former Trowbridge Impoundment. This situation suggests that PCB loading from bank erosion in the former impoundments does not significantly increase surficial bed or fish PCB levels in the areas downstream of the former Trowbridge Impoundment. However, this does not imply that PCB loads from eroding banks in the former impoundments are not affecting the natural recovery rate in Lake Allegan.

Results of the BAF and BSAF analyses are used to infer the impacts of water column and bed PCB concentrations on fish levels. BSAF values for carp and smallmouth bass are relatively low and variable in most of the Kalamazoo River. In contrast, BAF values are more consistent with values observed in other contaminated sites and less spatially variable than BSAF values. Taken together, these results suggest that fish PCB levels are generally more closely tied to water column concentrations than to surficial bed concentrations.

SECTION 4
REVIEW OF LIMNOTECH MODELS

The focus of this review has been on the reliability of the PCB fate model and its usefulness as a management tool to evaluate the effectiveness of various remedial alternatives for the Kalamazoo River. The review will therefore present results of examinations and analyses of the primary components of the PCB fate model; the HEC-6 hydraulic, bank erosion and KALSIM submodels constitute the model framework and will be examined in detail. This review is not intended to provide a detailed critique of the LTI report, i.e., line-by-line examination of the report with comments on details. However, significant errors in the report will be documented.

Review of the LTI model includes: 1) model formulation and structure; 2) development of model inputs and parameter values, including input files; 3) computer code; 4) quality control issues; 5) calibration results; and 6) consistency with the preliminary conceptual model. Also included in this section are discussions of the sediment stability analyses. It should be noted that LTI personnel have provided additional material and information that were not included in the original report, which has helped to facilitate this review.

4.1 GENERAL COMMENTS

Specific comments concerning the LTI model will be provided in the following sub-sections. However, several general comments about the LTI report can be made. First, the scientific credibility of the LTI report is compromised to some extent because of the advocacy tone of the text in places. Two examples of this problem are: 1) assertions concerning the extent of natural attenuation in the river are numerously repeated and 2) model inadequacies are frequently blamed on schedule constraints imposed by MDEQ. Second, insufficient information concerning some model inputs and parameters was presented in the LTI report to effectively evaluate model performance and reliability. Important details concerning the specification and application of various parameters and inputs were not included in the report. This problem has

been resolved for the purposes of this review through interactions between QEA and LTI personnel. Third, vertical and horizontal scales used in the figures tend to be inconsistent, which makes it very difficult to compare trends or correlations between different plots. Spatial plots should use a single, consistent horizontal scale for distance along the river; the LTI report uses a mixture of model segment number and river mile (with at least two different river mile indexes used). Vertical scales for TSS or PCB concentration can vary significantly, even on multi-panel plots.

4.2 DESCRIPTION OF LTI MODELING FRAMEWORK

The PCB fate model that was developed for the Kalamazoo River is a one-dimensional model that consists of four submodels: 1) HEC-6 hydraulics; 2) bank erosion; 3) KALSIM sediment transport; and 4) KALSIM PCB fate and transport. The linkages between these submodels are shown on Figure 4-1. At the present time, a PCB bioaccumulation model has not been developed. Short descriptions of the information transferred between the various submodels will be given here. Additional details about the individual submodels is provided in the following sub-sections.

While not generated by a model, watershed flow and solids loads are shown on Figure 4-1 to emphasize the importance of these model inputs for the accurate simulation of PCB fate in the river. Watershed flow and solids load inputs were determined using estimation techniques (see Sections 4.3 and 4.5.3).

The HEC-6 hydraulic model produced the following information: 1) bottom shear stress to be used for sediment resuspension calculations in the KALSIM sediment transport model and 2) water depth and current velocity for use in volatilization calculations in the KALSIM PCB fate model. A grid collapse was performed on HEC-6 output prior to input to KALSIM; HEC-6 results, which are on a finer grid scale, were combined to produce representative, or average, values for the coarser numerical grid used in KALSIM.

The bank erosion model calculated annual loads of sediment and PCBs that were used as input to sediment transport and PCB fate submodels, respectively, in KALSIM. Predicted bank erosion loads were processed before input to KALSIM.

The sediment transport submodel in KALSIM predicted the resuspension, deposition and water column transport of suspended sediment in the river. Only one sediment-size class was used and differences in sediment bed type were neglected, i.e., the model did not distinguish between cohesive and non-cohesive beds. Relatively simplistic, empirical formulations were used to describe resuspension and deposition processes. Predicted resuspension and deposition fluxes (or velocities) across the sediment-water interface were transferred, within KALSIM, from the sediment transport submodel to the PCB fate submodel.

The transport and fate of PCBs in the Kalamazoo River was simulated using the PCB fate submodel in KALSIM. This model includes the transport processes controlling the fate of PCBs in the river depicted in Figure 2-2.

4.3 REVIEW OF HEC-6 MODEL

4.3.1 Overview

The HEC-6 model developed by U.S. Army Corp of Engineers (USACOE) is used to simulate Kalamazoo River hydraulics and to predict current velocity and bottom shear stress as functions of flow for use in KALSIM. HEC-6 is a one-dimensional, steady-state model that simulates open channel flow and sediment transport. The model was developed to simulate a 15-year period extending from 1985 through 1999.

The model was segmented into 156 grid cells from downstream of Morrow Lake Dam to Lake Allegan Dam, with each grid cell having an approximate length of 0.3 miles. Model segmentation was primarily based on transect data collected during the 1993-94 sediment survey. During the survey, channel geometry data were collected at each of the 141 transects.

4.3.2 Hydraulic Submodel

River geometry data were collected during the 1993-94 sediment survey. These data were specified at 141 of the 156 transects (downstream of Morrow Lake Dam to Lake Allegan Dam) represented in the model. Bed elevations were generally measured at five to eight locations along a transect and channel geometry for model input was determined from these data. Supplemental transect geometry at each dam was used to specify the geometrical properties of the dam.

Water surface elevation at Calkins Dam was held constant, based on measured elevations during the 1993-94 survey. A dam rating curve, which determines water surface elevation as a function of discharge rate, was developed for Allegan City Dam. Similar rating curves were developed for the other dams, however, more accurate predictions of water surface elevations were achieved by treating these dams as run-of-the-river dams.

Flow rates were specified at the upstream boundary, located approximately one mile downstream of Morrow Lake Dam, and six tributaries, i.e., Portage Creek, Silver Creek, Gun River, Pine Creek, Schnable Brook, and Rossman Creek. Daily flow data were available at three USGS gauging stations: Kalamazoo River at Comstock, Kalamazoo River at Fennville, and Portage Creek. Inflow at the upstream boundary of the model was specified using the Comstock gauge data. Portage Creek inflows were determined from data collected from that tributary. The other five tributary inflows were estimated using the drainage area ratio (DAR) method. Due to tributary flow estimation uncertainty, adjustment of the tributary flows was needed at times to maintain a flow balance between the upstream and downstream gauges on the Kalamazoo River (i.e., Comstock and Fennville, respectively). This adjustment was done on a seasonal basis and resulted in the DAR method performing reasonably well in approximating cumulative long-term tributary flow.

The HEC-6 hydraulics and sediment transport models were calibrated in parallel due to the feedback between models, i.e., water depth changes are caused by bed elevation changes due to sediment resuspension and deposition. Hydraulic model-data comparisons were made for

water surface elevations and current velocities. The data used in calibration were collected in 1993-94. The calibration process consisted of eight steps:

- multi-channel cross-sections were replaced with idealized cross-sections;
- averaging of bed particle size distribution data;
- adjustment of critical shear stresses for cohesive deposition and erosion;
- adjustment of Manning's n coefficients;
- adjustment of particle size distribution of main-stem solids load;
- adjustment of sediment loads during high flows;
- addition of estimated cross-sections upstream of dams; and
- modeling former dams as run-of-the-river dams.

Detailed discussions of many of the calibration adjustments were not provided in the LTI report, therefore, it cannot be determined if all adjustments were reasonable or realistic.

The removal and replacement of multi-channel cross-sections with idealized cross-sections occurred where complex channels were encountered (e.g., marshes and islands). If the cross-section was not located in a critical area it was removed, otherwise the river channel was refined. The modified cross-sections were based on the same channel width as the original cross-section and a depth approximately equal to the average depth of the multiple channels in the original cross-section.

Manning's n coefficient varied by reach based on areas with similar bed slope and grain size distributions. This coefficient was adjusted during model calibration, which consisted of comparing observed and predicted current velocities and water surface elevations. Main channel values ranged from 0.025 to 0.055 and over-bank values ranged from 0.07 to 0.08.

Abrupt changes in bed elevation upstream and downstream of the dams were possible. To more accurately model these areas, additional model cross-sections were added immediately upstream of each dam. This modification provided a more realistic representation of river geometry.

Model-data comparisons were made of water surface elevations and current velocities. Available water surface elevation data were compiled and the entire data set was used for model calibration. The LTI report stated that 70% of the model predictions were within one foot of the corresponding measured values. A graphical comparison of measured and predicted water surface elevations was presented as Figure 5-3 in the LTI report (reproduced here as Figure 4-2).

Several potential problems exist with the calibration results for water surface elevation. First, the vertical scale on Figure 4-2 has a range of 160 ft. This range is extremely large and has the effect of vertically compressing predicted and observed water surface elevations. This figure cannot be used to adequately evaluate model performance. An alternative graphical or statistical presentation of model-data comparisons must be developed to provide an effective means for determining model accuracy. For example, the results in a specific reach of the river could be expressed as a relative error with respect to an appropriate datum in that reach. Second, the ability of the model to reproduce observed temporal variations in water surface elevation, due to changes in flow rate, at specific locations has not been demonstrated. This type of model-data comparison should have been included in the LTI report. Finally, model error was greater than one foot at 30% of the sampling locations. It is unclear how large the maximum errors were and if these errors indicate that the model produces unrealistic locations at those locations. More discussion and detail should have been provided regarding the maximum error locations.

To perform a model-data comparison of current velocities, the data were averaged because multiple velocity measurements were taken on the same day for each transect. In averaging the data, individual velocity measurements were weighted by water depth at each sampling location to provide a better comparison to the laterally-averaged velocities predicted by the model. Model-data comparisons for current velocity were presented on Figure 5-4 in the LTI report (reproduced here as Figure 4-3). Generally, the model appears to satisfactorily predict current velocity at the locations where model performance was evaluated.

4.3.3 Sediment Transport Submodel

The objective of the HEC-6 sediment transport submodel was to provide an overall characterization of sediment transport in the Kalamazoo River, purportedly to provide insight for other data and modeling analyses. The value of comparing HEC-6 and KALSIM sediment transport results is unclear because of significant differences between the two models and, also, because of weaknesses in the HEC-6 submodel. No results from this submodel were used in PCB fate and transport simulations; deposition and resuspension fluxes were not transferred from HEC-6 to KALSIM. Thus, the HEC-6 sediment transport results are not highly relevant to this review, which is focused on PCB fate issues. Therefore, a detailed review of this submodel will not be presented herein.

4.3.4 Summary of Model Strengths and Weaknesses

Generally, model calibration results appear reasonable and the hydraulic submodel seems to provide usable results for KALSIM. A primary strength of using HEC-6 hydraulics is that this approach provides a mechanistic method for specifying temporal and spatial variations in bottom shear stress that are used in the resuspension formulation of the KALSIM sediment transport submodel.

The model does have several weaknesses, however. First, HEC-6 is a one-dimensional, steady-state model. The report states that use of a steady-state model "is a minor limitation of the model because transient effects are relatively unimportant in most of the Kalamazoo River" (p. 5-2 in LTI 2000). No support for this assertion is provided in the LTI report. The impact of this approximation on model results is uncertain. Second, calibration results were not adequately presented, i.e., water surface elevation comparisons, and the adequacy of model performance could not be determined from the graphical results presented in the report. Third, the model's ability to simulate water surface elevation changes due to flow rate variations must be demonstrated to provide added confidence in its predictive capabilities.

4.4 REVIEW OF BANK EROSION MODEL

4.4.1 Overview

Accurate simulation of bank erosion processes in a river is a difficult and challenging task. A wide range of bank erosion models have been developed for various types of bank materials and riverine conditions; a generalized model applicable to most bank erosion situations has not yet been developed. Application of a bank erosion model to a particular site is difficult for the following reasons: specification of model parameters; spatial and temporal variability of bank properties; sparsity of calibration data; impact of vegetation on bank erosion properties; and calculation of bank shear stress due to river currents. Successful applications of bank erosion models have generally been limited to relatively limited reaches of a river, e.g., a single meander bend, that have been extensively surveyed and possess a significant data base.

The model developed for application to the Kalamazoo River was based on the theoretical framework presented in Osman and Thorne (1988). The Osman and Thorne bank erosion model is a mechanistic bank erosion model that simulates two primary processes. First, soil erosion (i.e., lateral erosion) due to shear stress exerted on the bank by river currents. Second, bank failure caused by a combination of bank toe undercutting by bed degradation, lateral erosion, and weakening of bank cohesive strength by wet-dry and freeze-thaw processes.

Formulations presented in Osman and Thorne (1988) were incorporated into a computer model developed by LTI. Bed degradation at the bank toe was simulated using the Lick equation, i.e., Equation 4 of Appendix B in LTI (2000). This equation is used to calculate the erosion of a cohesive sediment bed and includes the effects of bed armoring (Ziegler and Nisbet 1994). Bed and bank shear stresses were calculated using shear velocity estimated from an open channel flow equation.

It should be noted that LTI provided source code and input files for the bank erosion model to QEA for this review. Input files for 27 transects in the former impoundments were

transferred to QEA for model evaluation. In addition, LTI responded to QEA questions concerning the model and its use (Dierks 2001).

4.4.2 Model Development, Calibration and Application

The LTI bank erosion model was used to simulate bank erosion in former impoundments at Plainwell, Otsego and Trowbridge, i.e., transects 58 to 104. The model was calibrated over a six-year period, from 1994 through 1999. This period corresponded to a time span over which bank erosion rates at various transects in the former impoundments could be estimated from site observations (LTI 2000). Observed bank erosion rates in those areas ranged from approximately zero to 33 in/yr during this period (Dierks 2001).

Various site-specific physical parameters were specified for each transect. A summary of the eight physical parameters is presented in Table 4-1. The range of values for each physical parameter, i.e., most parameters were spatially variable, is also given in that table. These values were obtained from the LTI model input files. Determining the accuracy or validity of the physical parameters specified in the input files was beyond the scope of this effort.

Table 4-1. Site-specific inputs for bank erosion model.

Parameter	Description	Range
B_{wo}	Initial bottom width	36 → 77 m
Lsl	Left bank slope	0.37 → 12.24
Rsl	Right bank slope	0.42 → 5.49
β	Bank angle	18° → 69°
S	Longitudinal bed slope	-0.0010 → 0.0044
H_o	Initial bank height	0.15 → 2.07
r	Meander bend radius	0 → 524 m
ρ_s	Bank soil density	0.4 → 1.6 g/cm^3

Eleven parameters in the LTI bank erosion model were estimated or adjusted during model calibration (Table 4-2). Critical shear stresses for bed and bank erosion were treated as calibration parameters. Both of the critical shear stresses were spatially variable. Manning's n coefficients were also spatially variable; values for each transect were determined using an open

channel equation and water surface elevation data collected during the 1993-94 survey. Values of two parameters that affect bank stability calculations, i.e., angle of internal friction (ϕ) and effective bank cohesion (c), were specified with no reference to site-specific data or literature-based values. When bank failure occurs, the volume of bank soil that slumped into the river was distributed over 5% of the channel width (parameter *redist*). This value appears to be arbitrary. Similarly, the Nikuradse roughness height, which is used to calculate shear velocity and shear stress, was arbitrarily set at 1 cm with no justification or support.

Table 4-2. Bank erosion model parameters.

Parameter	Description	Value
τ_o	Bed critical shear stress, Lick equation	$2 \rightarrow 6$ dynes/cm^2
τ_{cr}	Bank critical shear stress	$12 \rightarrow 45$ dynes/cm^2
n	Manning's n coefficient	$0.0144 \rightarrow 0.1611$
ϕ	Angle of internal friction	15^o
c	Effective bank cohesion	2 kPa
redist	% of bottom width over which bank failure is redistributed	5%
K	Nikuradse roughness height	1 cm
a_o	Constant, Lick equation	0.28 mg/cm^2
t_d	Time after deposition, Lick equation	5 days
N	Time after deposition exponent, Lick equation	1.1
m	Excess shear stress exponent, Lick equation	3.1

Bed erosion at the bank toe was calculated using the Lick equation (Equation 4 in Appendix B). This equation is applicable for predicting cohesive bed erosion, which means that it was implicitly assumed that cohesive sediments exist in the nearshore region of all transects in the former impoundments. No support for this assumption was presented in the LTI report. Four parameters (a_o, t_d, N and m) must be specified in the Lick equation. Ideally, a shaker study is conducted so that site-specific values of a_o and m can be determined, e.g., QEA (1999). Alternatively, values from other rivers can be used to estimate these parameters if site-specific data are not available (Ziegler 2001). It is unclear how the parameter values for the Lick equation listed in Table 4-2 were determined; no explanation or references were provided in the LTI report concerning specification of these parameters. Generally, the values used in the bank erosion model are within the range of values determined from studies in other rivers.

Prior to using the bank erosion model in this review, the source code and input files supplied by LTI were examined. Errors were found in both the source code and input files. Two programming errors were discovered in the LTI code. First, the parameter *phi* (angle of internal friction, ϕ) is input as degrees but not converted to radians, which is necessary for correct calculation of trigonometric functions in Fortran. Second, the equation for calculating H' ($= H_o - \Delta W \tan\beta$) was not coded correctly; in the source code provided to QEA, $H' = H_o - \Delta W / \tan^{-1}\beta$. Note that $1/\tan^{-1}\beta \neq \tan\beta$ because $\tan^{-1}\beta$ is arc tangent, not inverse tangent. These code errors were corrected and the effect of these errors on model results is discussed below.

Errors were also found in several input files. The *redist* parameter, i.e., fraction of bottom width over which bank failure is redistributed, was incorrectly specified in the files for transects 65, 66, 85, 96 and 97. In those five input files, *redist* had a value of 5, whereas in all other input files it was set at 0.05. The value of redist was set at 5%, but the code required this parameter to be specified as a fraction, i.e., 0.05. Thus, *redist* was incorrectly set at 500% instead of 5% for the five transects listed previously. The value of a_o was incorrectly specified as 0.00030 in the file for transect 58. The impact of these input file errors on model results is discussed below.

A more serious error in the LTI bank erosion model concerns use of the Lick equation. In discussions with LTI personnel in January 2001, it was determined that the Lick equation had been incorrectly applied in the model and that bed armoring effects were not being simulated. This error causes significant overprediction of bed erosion at the toe bank, which would presumably cause an overprediction of bank erosion due to slumping. This error was not corrected by QEA and, hence, impacts on model performance cannot be quantitatively assessed. Correcting the error would entail significant code development and then recalibration of the model. Note that the results presented in this report include this error in the bank erosion model.

The bank erosion model was calibrated for the six-year period from 1994 through 1999. The bed critical shear stress (τ_o) was adjusted for each transect, with a range of 2 to 6 dynes/cm^2. These values are higher than the value determined from studies in a number of rivers. Typically, the critical shear stress used in the Lick equation is approximately 1 dyne/cm^2 (Ziegler and

Nisbet 1994, 1995; Gailani et al. 1991; QEA 1999). The higher values of τ_o used in the bank erosion model is probably attributable to the neglect of bed armoring effects. Bank critical shear stress (τ_{cr}) ranged from 12 to 45 dynes/cm^2.

Calibration results were presented on Figure 2 of Appendix B (reproduced here as Figure 4-4), which compared predicted and observed erosion rates for the six-year period at each transect. Generally, those results demonstrated that the bank erosion model was adequately predicting bank erosion at the 19 transects for which comparisons were done. Data-based erosion rates for these transects are presented in Table 4-3, along with model results provided to QEA by LTI personnel. It is assumed that those model results correspond to results presented in Figure 2 of Appendix B. A comparison of LTI-provided results to erosion rate data is presented on Figure 4-5. This comparison is very similar to the figure in the LTI report (Figure 4-4).

Table 4-3. Observed and predicted bank erosion rates for 1994 to 1999 (in/yr).

Transect	Data-Based[1]	LTI-Provided[2]	QEA-Original[3]	QEA-Corrected[4]
58	2.3	4.2	2.2	2.3
59	6.7	9.5	2.8	2.6
60	11	14	7.5	7.5
62	9.9	13	4.2	3.6
65	0.6	1.7	0.2	0.0
66	15	5.0	3.6	3.6
83	2.6	6.2	2.1	1.7
87	28	15	6.0	5.7
88	5.3	6.6	0.8	1.1
89	7.8	6.9	0.0	0.0
90	10	7.5	3.1	3.1
91	2.3	4.6	1.8	1.3
92	3.9	6.3	1.4	0.0
94	0.2	0.0	0.0	0.0
99	11	12	0.6	0.1
101	3.0	5.0	1.6	1.2
102	33	13	14	13
103	6.1	7.1	22	23
104	2.4	6.5	0.0	0.0

(1) Data provided by LTI (Calibrate_Param_Compare.xls file)
(2) Model results provided by LTI (Calibrated_Param_Compare.xls file)
(3) QEA results using original LTI source code and input files
(4) QEA results using corrected LTI source code and input files

An attempt was made to reproduce the calibration results presented in the LTI report. Calibration-period simulations were conducted using the original source code and input files provided to QEA (QEA-original) and those results are presented in the fourth column of Table 4-3. Comparison of those results with LTI-provided results shows that a significant discrepancy exists between these two sets of predictions (see Table 4-3 and Figure 4-6). The cause of this discrepancy is unclear. The QEA-original results are compared to data-based erosion rates on Figure 4-7.

As noted above, source code and input file errors were corrected by QEA. Those corrections did not have a significant impact on model results (see Table 4-3 and Figure 4-8). When the corrected model (QEA-corrected) was used to simulate the calibration period, the model-data comparison is significantly different from the reported or LTI-provided calibration results (Figures 4-4 and 4-5). These corrected results indicate that the model significantly under predicts erosion rates, generally by a factor of two or greater.

Overall, the errors discussed above raise concerns about quality control in the LTI work products. In addition, the inability to reproduce calibration results is problematic. More discussion about quality control issues is presented in Section 4.6.

Additional analyses of model predictions were conducted to further evaluate the behavior and credibility of the bank erosion model. Only results using the QEA-corrected version of the model are presented. Model predictions will be presented for two periods: six-year calibration period from 1994 through 1999 and 30-year forecast period starting in 1994.

Frequency of bank erosion, i.e., percent of time that erosion was occurring, during the calibration period at the 27 transects in the former impoundments is shown on Figure 4-9. Bank erosion is predicted to be highly episodic at a majority of the transects, with erosion occurring less than 5% of the time during this six-year period at 24 of the 27 transects. However, at transects 85, 95 and 96, bank erosion is predicted to occur relatively frequently. In particular,

erosion is simulated 100% of the time at transect 85, which seems unrealistic. Note that these three transects were not in the calibration data set.

Spatial distributions of bank height changes, channel width changes and bank erosion rates at the end of the 6- and 30-year periods are shown on Figures 4-10 and 4-11, respectively. Significant spatial variability exists in predicted changes in bank height and channel width (erosion rate) during both periods. Model results at several transects appear to be unrealistically high, with bank height changes greater than 3 m (greater than 400% increase relative to initial bank height) and relative channel width changes greater than 100% increase (with respect to initial width).

Model behavior at different locations is illustrated by temporal plots of bank height changes and erosion rates at transects 58, 85 and 97. Results at transects 58 and 97 represent typical behavior at most locations (Figures 4-12 and 4-13). Generally, erosion is episodic and significant bank erosion only occurs during high-flow events that occur approximately once every three to five years. Long-term average erosion rate approaches an approximately constant value after about 10 to 15 years (about 2 in/yr for both of these transects). Bank height increases during the 30-year period at both locations. At transect 58, an increase of ~2.5 m is predicted by 2023, with this increase occurring nearly linearly in time. A bank height increase of about 1 m is predicted at transect 97 at the end of the 30-year simulation, however, bank slumping during erosion events causes periodic decreases in bank height.

As mentioned above, model predictions for transect 85 appear to be unrealistic. Figure 4-14 illustrates model behavior at this location during the 30-year forecast period. An extremely large amount of erosion (~600 in.) occurred during the first year of the simulation. The initial bottom width of transect 85 was 47 m, which means that a 33% increase in width occurred during the first year. Erosion occurred continuously at this transect but the rate decreased with time as the channel width increased, which is qualitatively correct. However, during the last ten years of the simulation, erosion rates at transect 85 were comparable to rates at other transects (~10 to 30 in/yr). Overall, the channel width at transect 85 increased by about 76 m, which represents an increase of ~160% with respect to the initial width. Bank height increased by over

7 m during the 30-year period, with the final bank height being approximately 4.5 times greater than the initial height of 2 m. These large changes do not appear to be realistic.

4.4.3 Linkage to KALSIM

Predictions of the bank erosion model were processed to develop sediment and PCB load inputs for KALSIM. Daily sediment and PCB loads from bank erosion in the three former impoundments, i.e., Plainwell, Otsego and Trowbridge, were specified as external sources to six KALSIM segments, i.e., segments 12, 13, 18, 19, 20 and 21. The linkage between the bank erosion model and KALSIM involved several steps that are described below. Included in the description of the linkage procedure is discussion of assumptions and approximations that were used in constructing the coupling between the two models.

The calibrated model simulated bank erosion for the seven-year period used to calibrate KALSIM (1993 through 1999). Annual bank erosion rates were predicted for transects in six KALSIM segments (Table 4-4). The predicted transect erosion rates were transformed into representative erosion rates for each KALSIM segment using a length-weighted average (LWA) procedure. The following assumptions and approximations were used in the LWA calculations: erosion only occurred between the transects, no bank erosion occurred in areas of the KALSIM segment that were upstream or downstream of the transects; bank erosion rate between adjacent transects was equal to the average of the rates at those two transects; if little or no erosion occurred at a transect, zero erosion was assumed for the entire section between the adjacent transects; and bank erosion between two transects in a river bend was only active along half of the bank area. This approach resulted in bank erosion being simulated in 41% to 76% of the bank area in the six KALSIM segments encompassing the former impoundments (Table 4-4). An inconsistency exists in the assumption of zero erosion between adjacent transects when one transect has negligible erosion. To be consistent with the approximation that erosion between adjacent transects equals the average of the two erosion rates, the same calculation should be done irrespective of the erosion rate magnitude.

Table 4-4. Length-weighted averaging information for bank erosion model linkage.				
KALSIM Segment	Transects included in KALSIM segment	KALSIM segment length (ft)	Total bank length with erosion (ft)	Portion of KALSIM segment with erosion (%)
12	56, 57, 58, 59, 60, 61	4,488	3,424	76
13	62, 63, 64, 65, 66	4,910	3,671	75
18	83, 84, 85, 86, 87, 88, 89	7,218	4,507	62
19	90, 91, 92, 93, 94	5,333	3,509	66
20	95, 96, 97, 98, 99, 100	10,243	4,207	41
21	101, 102, 103, 104, 105	7,339	5,006	68

The annual erosion rates resulting from the LWA procedure were used to generate an exponential function describing the temporal decline in erosion rates for each KALSIM segment. Subsequently, the exponential erosion rate equations were used to generate similar functions that predicted declining sediment and PCB loads used as external sources to KALSIM. Sediment loads, e.g., metric tons/year, were calculated as the product of erosion rate, bank dry density and bank area. PCB loads, e.g., kg/year, were calculated as the product of sediment load and bank PCB concentration. The reason for developing these exponential functions for sediment and PCB loads was "to facilitate its input into the KALSIM model" (LTI 2000). Details concerning the development of these exponential functions, or the coefficients used in the equations, were not provided in the LTI report. One consequence of using the exponential load functions was to minimize, or eliminate, potential effects of episodic bank erosion that was predicted by the bank erosion model. It is unknown at this time what impact this approximation has on PCB fate model predictions of long-term natural recovery rates in the river.

The final step in specifying load inputs for KALSIM was to distribute the estimated annual loads on a daily basis over the course of a year. This task was accomplished by applying the following method to each of the six KALSIM segments with bank erosion loads. First, the number of days in a year for which the bottom shear stress exceeded the critical bed shear stress was determined. The critical bed shear stress used here corresponded to the value determined during calibration of the KALSIM sediment transport submodel; critical shear stresses from the

bank erosion model were not used in this calculation. Second, the bank erosion load for a given day was determined based on the relative magnitude of the excess shear stress on that day, i.e., excess shear stress is equal to the difference between the bottom shear stress and critical shear stress. This process is best explained with the following numerical example. Assume for a given KALSIM segment that the critical shear stress equals 1 dyne/cm^2 and that the critical shear stress is exceeded on three days in a year, with values of 4, 6 and 8 dynes/cm^2. Thus, the excess shear stress is 3, 5 and 7 dynes/cm^2 for these three days, with the total excess shear stress for the year being 15 dynes/cm^2. Therefore, the annual bank erosion load is distributed over these three days as 3/15 (20%), 5/15 (33%) and 7/15 (47%) of the total yearly load.

Several potential problems exist with this method. First, using critical bed shear stress determined from calibration of the KALSIM sediment transport submodel instead of critical shear stress used in the bank erosion model as a threshold value for bank erosion loading in KALSIM is inconsistent. Second, extensive processing of bank erosion model results prior to use as external loads in KALSIM creates uncertainty in the magnitude and timing of the loads. Third, processing of bank erosion model results negates benefits and constraints associated with the use of a mechanistic model that simulates episodic bank erosion processes.

Sediment and PCB loads from bank erosion sources that were input to KALSIM during the seven-year (1993 through 1999) calibration period are listed in Table 4-5. These loads were provided to QEA by LTI (Dierks 2001). Note that the loads were generated using the exponential functions discussed above.

Table 4-5. Bank erosion loads input to KALSIM during 7-year calibration period.

Former impoundment	Sediment load (MT)	PCB Load (kg)	Mean PCB Concentration (ppm)
Plainwell	2,986	39.9	13.0
Otsego	2,410	29.4	12.2
Trowbridge	2,707	33.3	12.3
Total	8,104	101.6	

4.4.4 Summary of Model Strengths and Weaknesses

The primary strength of the bank erosion modeling approach was the development and application of a mechanistic model to simulate episodic bank erosion processes. In addition, model calibration results presented in LTI (2000), i.e., Figure 2 in Appendix B, show that the predictive capability of the model is acceptable.

A number of significant weaknesses exist in the development, calibration and application of the bank erosion model. First, the bank erosion model is relatively unconstrained. Of 11 parameters specified in the model, two were adjustable calibration parameters and eight parameters were set arbitrarily with no justification. Second, errors exist in the original source code and input files provided to QEA by LTI. Generally, these errors did not cause significant differences in model results. However, neglect of bed armoring in application of the Lick equation for predicting cohesive bed erosion at the bank toe is a significant error that causes overprediction of bed erosion. Third, model calibration results could not be reproduced. Calibration results using the corrected source code and input files were significantly different from results presented in LTI (2000); the results presented herein are less accurate than the original results, with the model typically underpredicting erosion rates by a factor of two or greater. Fourth, significant processing of bank erosion model results prior to use in KALSIM negates use of a mechanistic model for predicting bank erosion. The added complexity to the modeling framework, i.e., a mechanistic bank erosion model, has probably not increased the reliability of the PCB fate model. Fifth, the bank erosion model produces unrealistic results at some transects, primarily at locations not used for model calibration. Finally, the above weaknesses contribute to produce external PCB loads to KALSIM from bank erosion in the former impoundments that have a large uncertainty associated with them. A primary consequence of this uncertainty, as will be discussed in Section 4.5, is that PCB loads from bank erosion input to KALSIM are probably too low.

4.5 REVIEW OF KALSIM MODEL

4.5.1 Overview

KALSIM is a one-dimensional, time-dependent model that is composed of two submodels: sediment transport and PCB fate. The sediment transport submodel provides suspended solids concentration, resuspension flux and deposition flux information to the PCB fate submodel. Additional details about the structure of these two submodels are presented below.

The model domain for KALSIM extends from Galesburg, located near the upstream end of Morrow Lake, to Calkins Dam, located at the outlet of Lake Allegan, and encompasses approximately 54 miles of the Kalamazoo River. The river was discretized into 35 grid cells, with the average grid cell length being 1.5 mi (2,500 m). Lateral (cross-channel) variations in sediment transport or PCB fate were not resolved by the model.

Temporal variations in water volume were neglected in KALSIM; a constant volume approximation was used for water column transport of solids and PCBs. This approximation is necessary because of limitations in the basic structure of the model. Use of the constant volume approximation may introduce significant errors into model calibration results. Overprediction of water column concentrations during high-flow events is a direct consequence of this model limitation. It is uncertain what effect this has on long-term PCB fate.

4.5.2 Sediment Transport Submodel

The critical link in any contaminated sediment model is the sediment transport submodel and this holds true for KALSIM. Validity and reliability of PCB fate simulations for the Kalamazoo River are highly dependent on the sediment transport submodel. Therefore, this submodel was a primary focus of the model review.

Necessary components of a credible sediment transport model were presented in Section 2. The sediment transport submodel in KALSIM lacks many of these components. Generally, simplistic representations of resuspension and deposition processes are used in KALSIM. The model is highly empirical and poorly constrained. In addition, some of the sediment transport formulations in KALSIM are inconsistent with known sediment transport behavior.

Only one sediment size class is simulated in the model, with this size class aggregating the effects of suspended cohesive and non-cohesive sediment, as well as biotic solids. This approximation neglects temporal and spatial variations in the composition of suspended sediments, both within the model domain and in external sediment loads from upstream and tributary sources. Similar to other rivers, significant variations in suspended sediment composition, i.e., relative fractions of cohesive and non-cohesive sediment, probably occur in the Kalamazoo River (and tributaries that supply sediment to the river), particularly during high-flow events when external sediment loading is large. Neglecting the effects of variable composition by using a single sediment size class reduces the accuracy of the model. The ability of KALSIM to accurately simulate sediment deposition, i.e., magnitude and spatial distribution, is compromised by this approximation.

Deposition processes in KALSIM are simulated using

$$D_s = V_s C_s \qquad (4\text{-}1)$$

where D_s = sediment deposition flux; V_s = effective settling speed; and C_s = suspended sediment concentration. The effective settling speed (V_s) was adjusted during model calibration. A constant settling speed of 2 m/d was used in Morrow Lake and Lake Allegan. In all other parts of the river, V_s was a function of flow rate (Figure 4-15). Low-flow ($V_{s,low}$) and high-flow ($V_{s,high}$) settling speeds were specified for each model segment (other than segments in Morrow Lake and Lake Allegan). In each segment, V_s varied with normalized flow rate, where the flow rate was normalized with respect to the mean flow rate in that segment (Figure 4-15). The values of $V_{s,low}$ and $V_{s,high}$ were adjusted in each segment during model calibration; $V_{s,low}$ ranged from 0.05 to 1.0 m/d and $V_{s,high}$ ranged from 0.1 to 5.0 m/d (Table 4-6).

The variation in effective settling speed with flow rate is qualitatively correct. A shift to a higher effective settling speed during high flow events has been determined from modeling results on the Upper Hudson River (QEA 1999). The magnitudes of $V_{s,low}$ and $V_{s,high}$ are approximately in the range of effective settling speeds determined in other modeling studies; $V_{s,low}$ and $V_{s,high}$ are lower, but not significantly lower, than effective settling speeds determined from the Upper Hudson River model (QEA 1999). Values of $V_{s,low}$ and $V_{s,high}$ were determined on a segment-specific basis by adjustment during model calibration. No discussion was presented in the LTI report concerning the criteria or a procedure used to specify these two parameters in model segments 4 to 30. The spatial variations of $V_{s,low}$ and $V_{s,high}$ are presented on Figure 4-16. It is unclear whether the spatial variation in these two parameters is random or consistent with spatial variations in deposition conditions in the river. A weak correlation exists between $V_{s,low}$ and $V_{s,high}$, with $V_{s,low}$ increasing as $V_{s,high}$ increases (Figure 4-17). Bottom shear stress at the local mean flow rate, determined from the HEC-6 relationships between shear stress and flow rate, was used as a measure of the deposition environment in a specific segment. Relationships between $V_{s,low}$ and $V_{s,high}$ and bottom shear stress at the local mean flow rate are presented on Figure 4-18. These plots show that there is a weak correlation between effective settling speed and bottom shear stress, with effective settling speed generally decreasing as bottom shear stress increases, which is qualitatively correct. However, this empirical approach introduces uncertainty into KALSIM predictions of the magnitude and location of deposition in the river.

Table 4-6. Spatial variation of deposition and resuspension parameters.					
Model segment	Q_{low} (m^3/s)	$V_{s,low}$ (m/d)	Q_{high} (m^3/s)	$V_{s,high}$ m/d)	τ_c (dynes/cm^2)
4	64.1	0.05	96.1	0.1	25
5	64.2	0.05	96.3	0.1	25
6	64.5	1.0	96.8	3.0	14
7	70.0	0.5	105.0	3.0	8
8	70.8	0.5	106.2	1.0	14
9	75.1	0.05	112.6	0.1	25
10	76.9	0.05	115.4	0.1	25
11	77.9	0.1	116.9	0.5	40
12	78.0	0.1	117.0	0.5	40
13	78.1	0.5	117.2	2.0	20
14	78.2	0.1	117.3	0.1	20
15	78.2	1.0	117.3	1.0	2
16	86.5	1.0	129.7	2.0	4.5
17	86.7	0.1	130.1	0.5	25
18	87.0	0.1	130.5	0.5	15.5
19	93.8	0.1	140.6	1.0	8
20	93.9	0.1	140.9	0.5	25
21	96.1	0.1	144.2	0.5	12
22	96.4	1.0	144.6	3.0	12
23	96.5	0.05	144.8	0.1	25
24	97.2	0.05	145.8	0.1	38
25	97.5	0.05	146.2	0.1	25
26	97.5	0.5	146.3	1.0	6
27	97.6	0.25	146.3	0.5	8
28	98.0	1.0	146.9	5.0	2
29	99.0	0.25	148.5	0.5	8
30	99.1	0.5	148.6	1.0	7

Sediment resuspension was simulated in KALSIM using a resuspension velocity (V_r) that was adjusted during model calibration. The effects of bed armoring were not included in the model. Flow-independent resuspension velocities were used in Morrow Lake and Lake Allegan. Lower V_r values were specified during the winter (0.10 to 0.20 cm/yr for December 1 through March 15) than during the rest of the year (0.25 to 0.50 cm/yr) in the two lakes, presumably to account for the effects of ice cover.

Flow-dependent resuspension velocity was simulated in the rest of the river (segments 4 to 30) using

$$V_{rH} = \beta_3 \left(\frac{\tau - \tau_c}{\tau_c} \right)^{\beta_4} \quad , \quad \tau > \tau_c \qquad (4\text{-}2)$$

where V_{rH} = high-flow resuspension velocity (cm/yr); τ = bottom shear stress (dynes/cm^2); and τ_c = critical shear stress (dynes/cm^2). The constant (β_3) and exponent (β_4) in Equation (4-2) were spatially constant and had values of 0.0511 cm/yr and 2.75, respectively. It is unclear how the values β_3 of β_4 and were determined, presumably these parameters were adjusted during model calibration. Critical shear stress was spatially variable and adjusted during model calibration. Values of τ_c ranged from 2 to 40 dynes/cm^2 (Table 4-6). A comparison between the resuspension velocity formulations applied to lakes and the river channel (Equation 4-2) is presented on Figure 4-19.

The empirical relationships used to simulate sediment resuspension in KALSIM are problematic for several reasons. First, assuming a flow-independent resuspension velocity (or, alternatively, V_r that is not dependent on bottom shear stress) in the lakes is physically incorrect. Erosion does not occur continuously in the lakes, as this approximation assumes, but resuspension is an episodic event. While it may be argued that the magnitude of V_r in the lakes is small (0.1 to 0.5 cm/yr), these resuspension rates are of the same order of magnitude of net sedimentation rates in the lakes (predicted values of about 0.1 to 0.6 cm/yr). Imposing continuous resuspension in the lakes, with V_r comparable to the deposition rate, significantly affects PCB fate and transport in two ways. First, continuous resuspension, at a rate that is similar to the net sedimentation rate, artificially increases the interaction of particle-bound PCBs between the sediment bed and water column. Second, continuous resuspension will reduce the burial rate predicted by the model, causing an increase in the residence time in the bioavailable surface layer of the bed, which, ultimately, affects the predicted natural recovery rate.

The second problem with the resuspension formulations is that bed armoring processes are neglected. Previous applications of contaminated sediment models to rivers have shown that inclusion of cohesive and non-cohesive bed armoring processes is important and necessary for accurate simulations of long-term contaminant fate (Ziegler and Nisbet 1994, 1995; QEA 1999;

Ziegler et al. 2001). Third, KALSIM neglects the significant differences between the resuspension properties of cohesive and non-cohesive sediments. Fourth, this approach is purely empirical; site-specific data were not used to estimate resuspension parameters used in the model. This empirical approach causes resuspension to be unconstrained and, thus, the accuracy of scour predictions is highly uncertain.

Critical shear stress (τ_c) was a primary calibration parameter for the sediment transport submodel. This parameter was spatially variable and adjusted on a segment-specific basis. The spatial distribution of τ_c is shown on Figure 4-20. For comparative purposes, critical shear stresses for the suspension of 500 and 1,000 μm sand particles, i.e., 6.5 and 21 dynes/cm^2, respectively, are included on that figure. This comparison shows that 82% and 63% of the segments have τ_c greater than the critical shear stresses for 500 and 1,000 μm sand, respectively. Generally, suspended load transport of sand is restricted to particle diameters less than 500 μm, i.e., fine and medium sand; τ_c for fine and medium sand is less than about 6-7 dynes/cm^2. Critical shear stress for cohesive sediments has a typical range of about 1 to 5 dynes/cm^2. Thus, values of τ_c used in KALSIM are unrealistically high in a majority of the model segments. Neglecting bed armoring in the model could be the reason that unrealistic τ_c values had to be used to achieve acceptable calibration results.

It is unclear how the spatial distribution of τ_c was specified. The correlation of τ_c to τ at the mean flow rate in a segment is shown on Figure 4-21. This result indicates that the spatial variation of τ_c is consistent with increasing turbulent energy (because τ is a measure of local turbulent energy). This relationship is realistic because coarser bed material tends to occur in areas of higher turbulent energy in a river.

Accurate determination of incoming sediment loads to the Kalamazoo River is of critical importance for the development of a credible PCB fate and transport model of this river. The reason for this focus on sediment loads is that the solids loading rate, primarily from upstream and tributary sources, is a key factor in controlling the natural recovery rate in the system. Increasing (or decreasing) sediment loads to the river will increase (or decrease) the natural

recovery rate. Solids sources included as model input were: upstream, tributary, and direct drainage sources; biotic solids production; bank erosion; and point sources.

Available TSS concentration data were used to develop sediment rating curves for upstream and tributary sources. Sediment loads at the upstream boundary of the model (near Galesburg) were specified using a sediment rating curve developed from TSS concentration data collected on the Kalamazoo River at Augusta, which is about five miles upstream of Galesburg. Seasonal variations in sediment loading were accounted for by developing a rating curve for each month of the year. This approach produced unrealistic results for March, April, May and June. The rating curve analysis produced a negative correlation between TSS concentration and flow rate during these four months, i.e., TSS concentration decreases with increasing discharge. This result is inconsistent with known behavior on many other rivers, including the Black River (a tributary to the Kalamazoo River and a reference tributary for this study), where a positive correlation between TSS concentration and flow rate exists. This type of behavior, i.e., increasing TSS concentration with increasing discharge, would be expected during these four months because of high sediment loads associated with high flows during the spring runoff. It should be noted that the negative correlation in the sediment rating curves for these four months is probably due to limited TSS concentration data collected during high flows; additional high-flow sampling would probably produce a more realistic and accurate rating curve for the upstream boundary.

Tributary sediment loads were specified using rating curves developed from data collected on Portage Creek and South Branch Black River. Kalamazoo River tributary and direct drainage sediment loads were estimated using the South Branch Black River rating curve as a reference. Monthly variation in tributary loads was included, similar to the upstream boundary load. An adjustment was made to the Pine Creek rating curve to account for sediment trapping in the impoundment that is upstream of the creek mouth; estimated TSS concentrations for the Pine Creek load were reduced by about 45%.

This approach to estimating watershed sediment loading to the Kalamazoo River produced an average annual sediment load of about 27,400 MT/yr for the period between 1985

and 1999. About 47% of the total load (12,800 MT/yr) was specified at the upstream boundary at Galesburg. The tributary and direct drainage loading rate (14,600 MT/yr) corresponds to a sediment yield of 25 MT/yr-mi^2 for the watershed between Galesburg and Calkins Dam. It is unknown if this sediment yield is reasonable for the Kalamazoo River watershed. However, this yield is low compared to tributary sediment yields for the Upper Hudson River, which typically range between 50 and 100 MT/yr-mi^2.

A Simplified Primary Productivity (SPP) model was used to estimate solids loads that are generated in the water column due to biotic processes. Sediment loading due to bank erosion was also included in the model (see Section 4.4). Point source loads were estimated from available data.

The total sediment load input to the model during the seven-year calibration period (1993-1999) was 242,200 MT. The distribution of this load between the various sources is shown on Figure 4-22. The major source of sediment to the model was from watershed sources (71%). Biotic solids production, estimated using the SPP model, contributed to 22% of the total load.

The sediment transport submodel was calibrated during the seven-year period between 1993 and 1999. An important factor about KALSIM calibration is that the sediment transport and PCB fate submodels were calibrated simultaneously. More discussion about this approach, and its validity, is presented in Section 4.5.4.

Sediment transport model performance was evaluated through these comparisons: 1993-1994 TSS concentrations, 1993-99 burial rates, and erosion-deposition patterns predicted by HEC-6. The value of comparing HEC-6 and KALSIM sediment transport results is unclear because of uncertainty in the accuracy of HEC-6 predictions. It is doubtful that this comparison provides added confidence in the reliability of the KALSIM sediment transport simulations.

Temporal comparisons between observed and predicted TSS concentrations during 1993 and 1994 were made at six locations in the river (see Figures 7-3a-f in the LTI report). One of

the better model-data comparisons was at M-118 in Allegan City (reproduced here as Figure 4-23). Spatial profiles of suspended sediment concentration for two low-flow and four high-flow periods were also presented (see Figures 7-4 and 7-5 in the LTI report). Generally, model performance would be characterized as poor to fair in those comparisons.

Predicted average burial rates for the seven-year calibration period were compared to average sedimentation rates estimated from geochronologic dating of high-resolution sediment cores. Comparisons were made for these locations and model segments: Morrow Lake (segments 2 and 3); Allegan City Impoundment (segment 28); and Lake Allegan (segments 32, 33 and 35). The model significantly underpredicts burial in all six of these segments (Figure 4-24). Generally, sedimentation rates are underpredicted by a factor of two to four in these depositional zones. These results strongly suggest that sediment loads from watershed sources are significantly underpredicted, which is probably due to sediment rating curves that were constructed using limited high-flow TSS concentration data.

KALSIM sediment transport results for the seven-year calibration period were analyzed to gain further understanding of model performance. A sediment mass balance for the modeling domain (segments 1 through 35) was constructed for the period from 1993 through 1999 (Figure 4-25). During this seven-year period, the Kalamazoo River, between Galesburg and Calkins Dam, was predicted to have a 75% trapping efficiency, i.e., 75% of the incoming sediment was deposited in the system. About 91% of the total mass of deposited sediment (182,200 MT) was deposited in Morrow Lake (60,100 MT) and Lake Allegan (106,200 MT), which had trapping efficiencies of 58% and 64%, respectively. Mass balances were constructed for each of the ten zones in the study area (Figures 4-26 to 4-28). Zones 3 (~RM 57 to 72) and 6 (former Otsego Impoundment) were predicted to be net erosional during this period. Zones 2, 4, 5, 7 and 8 had relatively low trapping efficiencies (less than 4%). Overall, the mass balance analysis indicates that the general pattern of deposition in the river was predicted qualitatively correctly by the sediment transport submodel.

4.5.3 PCB Fate and Transport Submodel

This submodel is run in parallel with the sediment transport submodel to simulate the fate and transport of total PCBs in the river. Hydrodynamic information required by KALSIM is obtained from the HEC-6 model, i.e., water depth and current velocity used in PCB volatilization formulations. Bank erosion model results are included as PCB loads input to KALSIM.

The KALSIM PCB submodel uses the same numerical grid as the sediment transport submodel. Underlying each water column grid cell, twenty-nine 1.67-cm thick layers are used to discretize the sediment bed. The top seven sediment layers are computationally active while the lower 22 layers act as archive layers. The archive layers are computationally inactive unless there is transfer of sediment into or out of them due to burial or erosion processes. The well-mixed surface layer was assumed to be 5 cm thick, i.e., top three layers. The thickness of the well-mixed layer controls the residence time (half-life) of surficial PCB concentrations in the model.

KALSIM models PCBs in the water column and sediment bed as either dissolved or particle-bound. PCB fate and transport mechanisms simulated by KALSIM are: advection, dispersion, resuspension, deposition, partitioning, volatilization, diffusion and vertical mixing in the bed as shown on Figure 2-2.

Two-phase equilibrium partitioning was assumed in the model. The PCB partition coefficient (K_{poc}) was set at $10^{5.45}$ L/kg, i.e., log K_{poc} = 5.45. This is incorrectly cited in the LTI report as K_p. Site-specific data were not used to estimate K_p or K_{poc}. The partition coefficient was estimated using literature values and Upper Hudson River data, assuming that Kalamazoo River PCBs are mainly composed of Aroclor 1242. This is probably a reasonable estimate of K_{poc}. However, K_{poc} can be highly variable between river systems and, often, at different locations in the same system; site-specific partitioning data should be used whenever possible.

An important aspect of building a reliable PCB fate model is accurately specifying initial conditions for PCB concentrations in the sediment bed. Sediment PCB concentration data were

collected in 1993-94 at 170 transects downstream of Morrow Lake. These data were analyzed to determine initial PCB concentrations in each layer of the sediment bed for model input. Representation of the sediment bed in each grid cell of the model encompasses a relatively large surface area that includes a variable number of transects with PCB concentration data. Determining average PCB concentrations for each sediment layer in a particular grid cell required making some assumptions during the data analysis. The following procedure was used to specify initial PCB bed concentrations in KALSIM. Samples collected at each transect were first length-weighed along the transect to get an average PCB concentration value and then area-weighted for each model grid cell, depending on how many transects occurred in the model grid cell. A similar approach was used to vertically length-weight the samples in each sediment layer. The accuracy of this approach was not determined. However, given the spatial distribution of data, the approach and methodology used seem reasonable.

Two exceptions to this approach were applied by LTI. First, the effect of sediment samples with high PCB concentrations at several locations was limited by using a maximum weighting of 10% of the transect for those samples. Samples collected close to former Plainwell, Otsego City and former Otsego Impoundments were affected by this adjustment. Second, initial PCB bed concentrations were averaged for the following four pairs of grid cells to prevent simulation problems: model grid cells 17 and 18; 20 and 21; 26 and 27; and 29 and 30. These grid cells represent about 20% of the total river length. It is unclear why the sediment data were averaged on a different spatial resolution than the model grid, because the available data supported the model grid resolution. This averaging introduces uncertainty into the model and could significantly affect the consistency between PCB sediment data and initial conditions specified in the model. This spatial averaging may also significantly affect evaluation of remedial options in those segments. Initial conditions specified in the model for surficial PCB concentrations are shown on Figure 4-29.

No PCB data were collected in Morrow Lake in 1993. Initial conditions for PCB bed concentrations in Morrow Lake were based on data collected in 1987 by MDNR. Temporal declines in fish PCB levels were used to adjust the 1987 bed data and estimate 1993 PCB bed concentrations in Morrow Lake. The accuracy of these estimates for Morrow Lake are uncertain.

A two-layer resistance model (Whitman 1923) was used in KALSIM to simulate air-water exchange of PCBs. This procedure assumes that two stagnant layers exist at the air-water interface, with well-mixed compartments on either side of the interface. For the liquid film transfer coefficient, the O'Connor-Dobbins formulation was used. While this is a good estimate for transfer due to advection dominated surface turbulence, it is not a good estimate for large fetch areas (i.e., Morrow Lake and Lake Allegan), where wind effects likely dominate surface turbulence. Henry's Law coefficient was temperature corrected based on an empirical formulation developed by Achman et al. (1993). Volatilization effects at dams were evaluated and, based on the limited effect, volatilization at dams is not simulated in the model.

The sediment-water mass transfer coefficient (K_f) in KALSIM represents the effects of flow-independent, sediment-water exchange processes. This parameter was assumed to be seasonally variable, which is consistent with observed behavior in other riverine systems and is presumably primarily caused by seasonal changes in biotic activity in the sediment bed. This parameter was adjusted during model calibration and assumed to be spatially variable, i.e., higher K_f values in higher energy environments. Temporal and spatial variations in K_f are presented on Figure 4-30 (originally presented as Figure 7-2 in the LTI report). The values for the riverine and impoundment sections of the river are generally higher than those found at other rivers. Typical values of K_f in other rivers range from 1-10 cm/d. In this case, the PCB fate model may not be accurately distinguishing between different transport mechanisms, which can significantly affect long-term PCB fate simulations. Use of high K_f values, relative to other rivers, in the LTI model indicates that some transport mechanisms or model inputs may not be adequately represented in the model, including: inaccurate gross particulate exchange due to sediment resuspension and deposition; significant groundwater upwelling through the sediments; or sediment PCB concentrations are too low. It is not evident what transport mechanism or model input is driving the high transfer rates, but high diffusive rates suggest potential inaccuracies in the representation of PCB transport from sediment to water column.

Three external PCB sources were included in the model: upstream boundary at Galesburg; tributary inflow from Portage Creek; and bank erosion loads. Total external PCB

loading input to the model during the seven-year calibration period (1993 through 1997) was 136 kg. This load was distributed between the three sources as follows: 22% from upstream boundary at Galesburg; 16% from Portage Creek; and 62 % from bank erosion in the former impoundments (Figure 4-31).

External PCB loading was estimated using the following methods. Limited data for water column PCB loads exist at the upstream boundary of the model; data collected in Morrow Lake were used to estimate PCB concentrations at the upstream boundary. Two measurements of water column PCBs were collected in Morrow Lake during 1986 and 1988, each of which were below the detection limits of 10 and 15 ng/L, respectively. Additional water column data were collected in 1999, which showed an average concentration of 3.4 ng/L and a standard deviation of 2.3 ng/L. Based on these data, a first-order decline rate for water column PCB concentrations at Galesburg was estimated by assuming a 1985 concentration of 10 ng/L and a 1999 concentration of 3.7 ng/L; the decline rate was 0.068 yr^{-1}. This approximation was used to specify PCB concentrations at the upstream boundary that are temporally variable but flow independent. Uncertainty exists in this boundary condition because of the limited data and the assumption that the PCB concentration in 1985 was equal to the detection limit of 10 ng/L.

Approximately 240 water column PCB concentration samples were collected in Portage Creek between 1972 and 1994, with about 45% of these samples collected in 1993 and 1994. Multi-variable regression analysis was performed on the 1993-94 data set to develop a relationship between PCB concentration and three variables (i.e., Equation (3-8) in the LTI report): TSS concentration, flow rate and water temperature. Similar to the upstream boundary, temporal variations in Portage Creek PCB concentrations were included in model inputs by assuming a first-order decay rate of 0.042 yr^{-1}, based on PCB concentration decreases between 1985 and 1994. The effects of Bryant Mill Pond dredging in 1998-99 were incorporated into the model inputs by assuming a constant PCB concentration of 6.5 ng/L from June 1 to December 31 in 1999. The average annual PCB load from Portage Creek was estimated to be 3.2 kg/yr during the seven-year calibration period, with the lowest load being 1.0 kg/yr in 1999.

PCB loads from bank erosion in the former impoundments were estimated using the bank erosion model (see Section 4.4 for a detailed discussion). The total bank erosion load was split into two components prior to model input: water column load and sediment bed load. Distribution of the total load between these two components was determined during model calibration. The sediment bed portion of the total PCB load due to bank erosion was assumed to be incorporated directly into the bed. Model sensitivity to this load distribution was not presented in the LTI report.

The PCB fate submodel was calibrated for a seven-year period that extended from 1993 through 1999. The following philosophy for model calibration was expressed in the LTI report (p. 7-4): "Simultaneous calibration to suspended solids and PCB concentrations was conducted. Obtaining a scientifically credible and internally consistent calibration for both solids and PCB often requires simultaneous solids and PCB calibration because processes that control solids also impact PCB." This approach is a significant weakness in the LTI modeling framework because additional degrees of freedom are incorporated into the model, i.e., fewer parameters are constrained by independent data. Sediment transport processes are not affected by PCB transport; conducting a simultaneous calibration of the sediment and PCB transport models suggests that the sediment transport model is deficient. A credible method for calibrating a PCB fate model is to first calibrate the sediment transport model, then use resuspension and deposition information in the PCB fate model calibration with no feedback to the sediment transport model, i.e., sediment transport predictions are independent of PCB fate results. This approach has been successfully applied to a number of contaminated sediment sites, including: PCBs in Upper Hudson River (QEA 1999); mercury in Lavaca Bay (HydroQual 1998); PCBs in Watts Bar Reservoir, Tennessee; PCBs and heavy metals in Pawtuxet River, Rhode Island (HydroQual 1996); and PCBs in Grasse River, New York (Alcoa 2001).

The PCB fate submodel has five primary parameters that affect calibration results: water-bed distribution of bank erosion PCB load; sediment-water mass transfer coefficient (K_f); rate of mixing and thickness of well-mixed layer in sediment; and initial PCB bed concentrations. The optimum distribution of total bank erosion load was determined to be 90% to the water column and 10% to the sediment bed. Spatial variations in K_f were determined through model

calibration and are shown on Figure 4-30. Note that summer values of K_f in riverine sections of the Kalamazoo River, based on model calibration, are high (15 to 40 cm/d) compared to K_f values determined in similar rivers. The thickness of the well-mixed layer was set at 5 cm. This value typically ranges between 5 and 10 cm for freshwater systems; increasing the thickness of this layer increases the residence time (half-life) of PCBs in surficial sediments. Uncertainty exists in the well-mixed layer thickness and no site-specific data were presented in the LTI report to support using a value of 5 cm.

Initial PCB bed concentrations were adjusted during model calibration. As stated on p. 4-5 of the LTI report: "Initial attempts at model calibration suggested an inconsistency between computer water column PCB concentrations and estimated sediment concentrations based on this approach [data processing method used to specify bed PCB concentrations]. This was a result of overestimating concentrations in the segments containing only one or two PCB concentrations that were much higher than concentrations in the other samples. This problem was observed in the former Plainwell Impoundment, Otsego City Impoundment, and the former Otsego Impoundment. ... To more reasonably account for the influence of isolated high PCB measurements, these sample points were assumed to represent a maximum of 10% of the river width in transects in which they occurred."

The PCB fate model was calibrated during a seven-year period (1993 through 1999) using PCB water column data and observed trends in fish PCB levels. Water column PCB concentration data used for model calibration were collected in 1994 and 1999. The 1994 data set had a relatively high detection limit of 25 ng/L, with 71% of the samples below this detection limit. Water column data from 1999 were collected during low-flow conditions and corresponding TSS concentrations were not measured for those samples.

Comparisons of predicted and observed spatial trends in water column PCB concentrations during low-flow conditions were made for five periods during 1994 and 1999 (Figures 4-32 and 4-33, originally presented as Figures 7-6 and 7-8 in the LTI report). Adjustment of K_f values was used to optimize the agreement between predicted and observed spatial trends in PCB concentrations during these five low-flow periods. Generally, the model

predicted increasing water column PCB concentrations as one moves downstream of Morrow Lake, which is approximately consistent with observed trends until about RM 35. However, predicted PCB levels between ~RM 72 and RM 35 are frequently significantly lower than measured values. Downstream of RM 35, the model predicted an increase in PCB concentrations for flow rates less than 500 cfs (i.e., 1999 data sets), which is inconsistent with significant decreases measured between the inlet and outlet of Lake Allegan.

Minimal detectable PCB concentration data were collected during high-flow events in 1994, making it difficult to evaluate model performance during floods. The impact of seasonal variations in K_f is evident in predicted water column PCB concentrations during the calibration period (Figure 4-34, originally presented as Figure 7-11c,d in the LTI report). Most of the temporal variability in predicted water column PCB concentrations appears to be caused by seasonal variations in K_f, with relatively minor increases being simulated during high-flow events at the two locations shown on Figure 4-34.

Calculated changes in surficial PCB concentrations between 1993 and 1999 were analyzed to determine the natural recovery rate predicted by the PCB fate model. Average PCB concentrations in the top 5 cm of the sediment bed in 1993 and 1999 were determined for zones 1 to 10 (Figure 4-35a). The model predicted decreases in average surficial concentrations in all ten zones, with the maximum decrease being about 1 ppm. Half-lives of PCB concentrations in the well-mixed layer were calculated using predicted changes in bed concentrations during this seven-year period (Figure 4-35b). In 50% of the zones, predicted half-lives were within the half-life range (6 to 10 years) assumed to be most representative of the natural recovery rate in the system. In four of the ten zones, predicted half-lives ranged between about 13 and 20 years. These results indicate that the recovery rates predicted by the PCB fate model are in reasonable agreement with data-based recovery rates.

Improved understanding of PCB fate model performance is gained through use of PCB mass balances. The system was predicted to export 247 kg of PCBs over Calkins Dam between 1993 and 1999, which is a 375% increase (52 kg) in the load input at Galesburg (Figure 4-36). This increase (195 kg) in water column PCB load was due to bank erosion sources (84 kg) and

sediment bed sources (189 kg). Bed diffusion processes composed 84% (158 kg) of the total bed PCB source, with net resuspension accounting for only 16% (31 kg) of the total load from bed to water. Volatilization losses to the atmosphere (78 kg) were approximately equal to the bank erosion PCB load.

PCB mass balances for zones 1 to 10 during the calibration period are presented on Figures 4-37 to 4-39. Most of the net burial in the system occurred in Lake Allegan; 321 kg of PCBs were buried in Lake Allegan, which corresponds to 80% of the total burial loss in the system (400 kg). Significant burial was predicted in three other zones: 16 kg in Morrow Lake (4% of total); 27 kg in former Trowbridge Impoundment (7% of total); and 32 kg in Allegan City Impoundment (8% of total). Note that 55% of the total PCB mass loss due to volatilization occurred in Lake Allegan. Sources and sinks of PCBs in the water column and the well-mixed layer for zones 1 to 10 are illustrated on Figures 4-40 and 4-41, respectively. Note the large PCB mass loss from the bed due to resuspension in Lake Allegan, which was caused by the assumption of a high constant resuspension velocity in the sediment transport submodel.

A PCB mass balance on the well-mixed sediment layer (top 5 cm) for the system between 1993 and 1999 is shown on Figure 4-42. This mass balance is critical because it determines the natural recovery rate predicted by the model, and it illustrates the processes that are controlling that rate. Approximately 34% of the net decrease in PCB mass in this surficial layer was due to mass transfer from the bed to the water column, i.e., net resuspension (31 kg) and pore water diffusion (158 kg). A majority of PCB mass loss from the well-mixed layer was caused by burial (400 kg).

Several weaknesses in the PCB fate model are evident when this mass balance (Figure 4-42) is combined with other model results. As noted above, predicted PCB half-lives in surficial sediments are generally in reasonable agreement with data-based estimates of natural recovery rates. However, two primary lines of evidence indicate that this model-data agreement does not accurately reflect the reliability of the PCB fate model. First, the sediment transport model significantly underpredicted sedimentation rates in the deposition areas, i.e., between a factor of 2 and 4 too low (see Figure 4-24), primarily because upstream and tributary sediment loads were

underestimated. Thus, if sedimentation rates were accurately predicted by the sediment transport model due to increased external sediment loads, PCB losses by burial would increase by at least a factor of two and would cause predicted PCB half-lives to decrease and probably produce model-data comparisons that are inferior to current results. Second, uncertainty in predicted bank erosion PCB loads exists, due to a combination of model limitations and errors. The results strongly indicate that the PCB loads from bank erosion are too low. Increasing the bank erosion PCB loads would increase the deposition flux of PCBs to the bed (Figure 4-42). The uncertainty in these loads is consistent with the underprediction of the sedimentation rates.

4.5.4 Summary of Adjustable Parameters

Generally, KALSIM is an empirical model that is poorly constrained. A summary of the adjustable parameters used in the sediment transport and PCB fate submodels is presented here to emphasize this point. In addition, parameters in the bank erosion model are included because of the importance of that model to simulating PCB fate in the Kalamazoo River.

The bank erosion model used the following adjustable parameters:

- two calibration parameters (τ_{cr} for bed and bank); and
- eight parameter values were not based on site-specific data.

The sediment transport submodel had ten adjustable parameters:

- four parameters for river deposition (spatially variable);
- one parameter for lake deposition;
- three parameters for river resuspension (spatially variable); and
- two parameters for lake resuspension (spatially and temporally variable).

The PCB fate submodel had five adjustable parameters:

- water-bed distribution of bank erosion load;
- sediment-water mass transfer coefficient (spatially and temporally variable);
- initial PCB bed concentrations; and
- rate of mixing and thickness of well-mixed layer in sediment bed.

For comparison, a comprehensive PCB fate model for the Upper Hudson River has been developed, calibrated and validated (QEA 1999, Connolly et al. 2000, Ziegler et al. 2001). The sediment transport submodel for that system was calibrated by adjusting two parameters (i.e., settling speed of sand and non-cohesive active layer parameter). Only three parameters were adjusted during calibration for the PCB fate submodel: well-mixed layer thickness and rate of mixing (primary parameters), and one component of external PCB loading during the early years of the calibration period.

4.5.5 Summary of Model Strengths and Weaknesses

The sediment transport submodel had several strengths. First, the predicted overall deposition pattern in the river, on a zone basis, was predicted qualitatively correctly by the model. Second, bottom shear stress was used to calculate sediment erosion in the river channel, i.e., Equation 4-2. Third, the flow-dependent formulation for effective settling speed was qualitatively correct (Figure 4-15).

Strengths of the sediment transport submodel, however, are greatly outweighed by its significant weaknesses. First, the deposition and resuspension formulations are empirical and poorly constrained. The resuspension formulations, and their parameterization, are inconsistent with known sediment transport behavior: bed armoring is neglected; flow-independent resuspension in the lakes; site-specific resuspension data were not used to determine resuspension parameters; and unrealistically high critical shear stresses (i.e., 20 to 80 dynes/cm^2). Second, the impacts of rare floods on bed stability cannot be evaluated because of the empirical approach used to simulate resuspension (see Section 4.7 for more discussion). Third, sediment loads from upstream and tributary sources are underestimated, probably due to limited TSS concentration data during high-flow periods. Fourth, model-data comparisons for suspended

sediment concentrations are generally poor to fair. Finally, predicted sedimentation rates in the major impoundments are typically a factor of two to four lower than observed values. This inaccuracy in the sediment transport submodel has a significant impact on the PCB fate submodel (see Section 4.5.4 and below) because it affects the predicted natural recovery rate in the river.

The primary strength of the PCB fate submodel is that predicted rates of decline in surface sediment PCB concentrations during the calibration period are in reasonable agreement with observed temporal trends in fish concentrations. Using trends in biota PCB levels as a metric for PCB fate model performance assumes that changes in fish PCB concentrations are directly related to changes in surficial bed concentrations. This link is uncertain in the Kalamazoo River; results of BAF and BSAF analyses presented in Section 3 suggest that fish PCB levels are generally more closely tied to water column concentrations than to surficial bed concentrations.

Similar to the sediment transport submodel, weaknesses in the KALSIM PCB fate submodel outweigh the strengths of the model. First, the model is poorly constrained due to data limitations. A main constraint on the PCB fate model is limited bed concentration data; temporal trends in surficial bed concentrations cannot be accurately determined. Second, the predicted spatial distribution of water column PCB concentrations during low-flow conditions in the river is inconsistent with the observed spatial trends. Third, use of simplistic sediment dynamics causes sediment-water interaction due to resuspension and deposition to be misrepresented. Overprediction of resuspension has large impacts in Lake Allegan. Fourth, loss of PCBs from the surficial bed layer due to burial is probably too low because sedimentation rates were underpredicted by the sediment transport model. Fifth, bank erosion PCB loads are probably significantly underestimated.

4.6 QUALITY CONTROL ISSUES

Development and application of a PCB fate model for the Kalamazoo River, or any river, is a complicated undertaking. Numerous data analyses are conducted to develop model inputs.

Computer source code modifications typically must be made. Linkages between different submodels are constructed. Voluminous model output is processed. Errors can occur in any of these model development and evaluation steps, resulting in erroneous model simulations and reported results. Thus, quality control procedures need to be implemented in any modeling study to ensure that error-free simulations and results are produced.

The quality control procedures used during this PCB fate modeling project were not discussed in the LTI report. As has been presented in previous sections, the types of errors found in the LTI model include: source code, input files and non-reproducible results. The presence of these errors suggests that the quality control procedures applied to this project were not wholly successful. Improved quality control should be a goal of future modeling work on this project.

4.7 ASSESSMENT OF SEDIMENT STABILITY

Sediment stability in the Kalamazoo River during a rare flood was evaluated using KALSIM, see Section 6.1, Part II (LTI 2000). The 100-year flood was simulated; this flood was estimated to correspond to a flow rate of 7,000 cfs at Comstock.

Significant limitations in the sediment transport submodel prevent the use of KALSIM as a management tool to reliably evaluate the impacts of a rare flood on sediment stability in the Kalamazoo River. Weaknesses in the model's resuspension formulations include: empirically determined resuspension parameters (i.e., no site-specific resuspension data were used to parameterize the model); neglect of bed armoring; ignoring differences in resuspension properties of cohesive and non-cohesive sediments; and use of unrealistic critical shear stresses at certain locations in the river. Therefore, KALSIM cannot be used with confidence to evaluate the impacts of a rare flood on sediment stability; 100-year flood predictions were not reviewed because of the insufficient reliability of the model.

A rare wind storm may generate relatively large waves at various locations in Lake Allegan. An analysis was conducted to estimate the potential impact of a wind storm on sediment stability in the lake. Wave parameters, e.g., wave height and period, at different

locations in Lake Allegan were estimated using the ACES wind-wave model (CERC 1992). At a particular location in the lake, bottom shear stress was calculated for a given wind speed and fetch (i.e., distance of open water along the wind direction) based on wave height and period predicted by ACES. Bed stability was estimated at that location by comparing the predicted bottom shear stress (τ) to a critical shear stress (τ_{cr}) for cohesive bed erosion. Areas in the lake of potential sediment erosion during an extreme wind storm were assumed to correspond to locations where τ exceeded τ_{cr}, where τ_{cr} was assumed to be 1 dyne/cm^2.

Generally, this procedure provides an adequate screening-level assessment of the potential for a rare wind storm to cause significant sediment erosion in Lake Allegan. One concern with the results presented in the LTI report is the specification of a rare wind storm. Daily-average wind velocity data were analyzed to estimate the return periods of wind storms in the vicinity of Lake Allegan. This analysis yielded a wind speed of 30 MPH, from the northwest, for the 100-year storm. Cohesive resuspension processes typically occur over the period of one to two hours. In addition, wind waves on Lake Allegan will become fully developed, for quasi-steady wind conditions, during a similar time period. Thus, the averaging period for wind speed that is relevant for the sediment stability analysis is approximately one hour; the 100-year storm should be estimated using hourly-average wind speed data, which will probably have a greater magnitude than the daily-average value (30 MPH). The sediment stability analysis should be repeated using a 100-year storm based on hourly-average wind data.

SECTION 5
CONCLUSIONS

The main objective of this review was to evaluate the PCB fate model of the Kalamazoo River developed by LTI and determine the reliability of the model. Ultimately, the following question must be answered:

Is the LTI model sufficiently reliable for use as a management tool to evaluate remedial alternatives?

Based on the results of the PCB fate model evaluation presented herein, the LTI model cannot be used as a management tool at the present time. This judgement is based on various lines of evidence that demonstrate model deficiencies, which have been discussed in detail in Section 4. No single weakness in the modeling framework makes it unreliable as a management tool; a weight-of-evidence approach, based on numerous weaknesses in the LTI model, was used to arrive at the opinion expressed above. A summary of weaknesses in the four submodels that compose the LTI model is provided in Table 5-1. The bank erosion and sediment transport submodels are the primary limitations in the PCB fate modeling framework; errors and weaknesses in those two submodels prevent KALSIM from being a reliable management tool. Specifically, the current version of KALSIM cannot be used to reliably: 1) differentiate between the impacts of PCB loads originating from bank erosion and sediment bed sources or 2) evaluate the effects of rare floods.

Table 5-1. Summary of weaknesses in LTI modeling framework.	
Submodel	Submodel Weaknesses
HEC-6 Hydraulics	• Steady-state model • Calibration results not adequately presented • No demonstration of ability to simulate effects of variable flow rate on water surface elevation
Bank Erosion	• Model is relatively unconstrained • Errors exist in source code and input files • Calibration results could not be reproduced • Processing of model output negates use of a mechanistic bank erosion model • Unrealistic results at some locations • Large uncertainty in predicted PCB loads from bank erosion • Predicted PCB loads from bank erosion are probably too low
KALSIM Sediment Transport	• Deposition and resuspension formulas are empirical and poorly constrained • Resuspension formulations are inconsistent with known sediment transport behavior • Impacts of rare floods on bed stability cannot be evaluated • External sediment loads are underestimated • Model-data comparisons for suspended sediment concentrations are generally poor to fair • Predicted sedimentation rates are typically two to four times lower than observed values in the major impoundments
KALSIM PCB Fate and Transport	• Model is poorly constrained due to data limitations • Predicted spatial trends in water column PCB concentrations during low-flow conditions are inconsistent with observed trends • Sediment-water PCB interaction due to resuspension and deposition is misrepresented • PCB loss from the surficial bed layer is probably too low because sedimentation rates are underpredicted • Bank erosion PCB loads are probably significantly underestimated

A necessary capability for a PCB fate model of the Kalamazoo River is to accurately and realistically predict natural recovery processes in the river. The LTI model appears to simulate temporal declines in surficial PCB concentrations at rates similar to those observed in fish concentrations. However, the mechanisms causing predicted declines in surficial concentrations are not accurately simulated in the LTI model. For example, PCB mass losses from the surficial bed layer due to burial are underpredicted in Lake Allegan because predicted sedimentation rates are two to four times too low. Constant sediment resuspension in Lake Allegan artificially increases PCB interaction between the water column and sediment bed; PCB flux to the water

column is likely overpredicted in the lake. The combined effects of underpredicted burial loss and overpredicted sediment-water interaction cause the net loss rate to be approximately correct. Thus, the model is not realistically predicting natural recovery in the river, even though it appears to be producing accurate simulations. This distinction is important because realistic representations of PCB fate and transport processes must be incorporated into the model if it is to be used to evaluate the efficacy of remedial alternatives. If the LTI model cannot accurately and realistically predict natural recovery rates, then the impacts of various PCB sources, i.e., bank erosion and sediment bed, on natural recovery in the Kalamazoo River and, subsequently, the potential effects of remediating those PCB sources cannot be reliably evaluated using the model.

SECTION 6
REFERENCES

Achman, D.R., K.C. Hornbuckle and S.J. Eisenreich, 1993. Volatilization of polychlorinated biphenyls from Green Bay, Lake Michigan. *Environ. Sci Technol.* 24(1):75-.

Alcoa, 2001. *Comprehensive Characterization of the Lower Grasse River, Volume II: Appendices, Appendix C, A Model of PCB Fate in the Lower Grasse River.* Alcoa, Massena, NY.

Amos, C.L., J. Grant, G.R. Daborn, and K. Black, 1992. Sea carousel – a benthic, annular flume. *Estuar. Coast. and Shelf Sci.*, 34:557-577.

Bedard, D.L. and J.F. Quensen, III, 1995. Microbial reductive dechlorination of polychlorinated biphenyls. In: *Microbial Transformation and Degradation of Toxic Organic Chemicals.* Eds. L.Y. Yound and C. Cerniglia, John Wiley & Sons, Inc.

Borah, D.K., C.V. Alonso, and S.N. Prasad, 1982. Routing graded sediments in streams: formulation. *ASCE J. Hydr. Engrg.*, 108(12): 1486-1503.

Burban, P.Y., Y.J. Xu, J. McNeil and W. Lick, 1990. Settling speeds of flocs in fresh water and seawater. *J. Geophys. Res.*, 95(C10):18,213-18,220.

Cheng, N.S., 1997. Simplified settling velocity formula for sediment particle. *ASCE J. Hydr. Engrg.*, 123(2):149-152.

Connolly, J.P., H.A. Zahakos, J. Benaman, C.K. Ziegler, J.R. Rhea, and K. Russell, 2000. A model of PCB fate in the Upper Hudson River. *Environ. Sci. Technol.*, 34(19):4076-4087.

Connolly, J.P., 1991. Application of a food chain model to polychlorinated biphenyl contamination of the lobster and winter flounder food chains in New Bedford Harbor. *Environ. Sci. & Tech.*, 25:760-770.

Connolly, J.P., T.F. Parkerton, J.D. Quadrini, S.T. Taylor and A.J. Thuman, 1992. *Development and Application of a Model of PCBs in the Green Bay, Lake Michigan Walleye and Brown Trout and Their Food Webs.* Report for Large Lakes Research Station, U.S. Environmental Protection Agency, Grosse Ile, Michigan 48138, Cooperative Agreement CR-815396.

Coastal Engineering Research Center (CERC), 1992. *Automated Coastal Engineering System User's Guide.* Department of the Army, Corps of Engineers, Waterways Experiment Station, Vicksburg, Mississippi.

Dierks, S., 2001. Responses to QEA questions on bank erosion model. LTI memorandum to Kirk Ziegler, QEA. April 3, 2001.

DiToro, D.M. and L.M. Horzempa, 1982. Reversible and resistant components of PCB adsorption-desorption: isotherms. *Environ. Sci. Technol.*, 16:594-602.

Gailani, J., C.K. Ziegler, and W. Lick, 1991. Transport of suspended solids in the Lower Fox River. *J. Great Lakes Res.*, 17(4):479-494.

Gailani, J., W. Lick, C.K. Ziegler, and D. Endicott, 1996. Development and calibration of a fine-grained sediment transport model for the Buffalo River. *J. Great Lakes Res.*, 22:765-778.

Garcia, M. and G. Parker, 1991. Entrainment of bed sediment into suspension. *ASCE J. Hydr. Engrg.*, 117(4):414-435.

Graham, D.I., P.W. James, T.E.R. Jones, J.M. Davies, and E.A. Delo, 1992. Measurement and prediction of surface shear stress in annual flumes. *ASCE J. Hydr. Engrg.*, 118(9):1270-1286.

Hawley, N., 1991. Preliminary observations of sediment erosion from a bottom resting flume. *J. Great Lakes Res.*, 17(3):361-367.

HydroQual, Inc. 1998. *Development and Application of a Modeling Framework to Evaluate Hurricane Impacts on Surficial Mercury Concentrations in Lavaca Bay.* HydroQual report, Mahwah, NJ.

HydroQual, Inc., 1996. *Contaminant Transport and Fate Modeling of the Pawtuxet River, Rhode Island.* HydroQual report, Mahwah, NJ.

HydroQual, Inc. 1995. *Bioaccumulation of Superlipophilic Organic Chemicals: Data Compilation and Analysis.* Prepared for ABT Associates, Bethesda, Maryland, on behalf of USEPA.

Jain, S.C. and I. Park, 1989. Guide for estimating riverbed degradation. *ASCE J. Hydr. Engrg.*, 115(3):356-366.

Karim, M.F. and F.M. Holly, 1986. Armoring and sorting simulation in alluvial rivers. *ASCE J. Hydr. Engrg.*, 112(8):705-715.

Kern, J., 2001. Personal communication with K. Ziegler. Lansing, MI, February 2001.

Krone, R.B., 1962. *Flume Studies of the Transport of Sediment in Estuarial Processes.* Final Report, Hydraulic Engineering Laboratory and Sanitary Engineering Research Laboratory, Univ. of Calif., Berkeley, Calif.

Lick, W., Y.J. Xu and J. McNeil, 1995. Resuspension properties of sediments from the Fox, Saginaw and Buffalo Rivers. *J. Great Lakes Res.*, 21(2):257-274.

Limno-Tech, Inc. (LTI), 2000. *Modeling Analysis of PCB and Sediment Transport in Support of the Kalamazoo River Remedial Investigation/Feasibility Study.* Draft for State and Federal Review, October 2000.

Lyman, W., 2001. Preliminary review of the geochronological data from 2000 sampling. Memorandum to T. King, February 1, 2001.

O'Connor, D.J., J.A. Mueller and K.J. Farley, 1983. Distribution of Kepone in the James River Estuary. *ASCE J. Environ. Engrg.*, 109:396-413.

Osman, A.M. and C.R. Thorne, 1988. Riverbank stability analysis. I: Theory. *ASCE J. Hydr. Engrg.*, 114(2):125-150.

Parchure, T.M. and A.J. Mehta, 1985. Erosion of soft cohesive sediment deposits. *ASCE J. Hydr. Engrg.*, 111(10):1308-1326.

Partheniades, E., 1992. Estuarine Sediment Dynamics and Shoaling Processes. In *Handbook of Coastal and Ocean Engineering, Volume 3.* Ed. J. Herbick, pp. 985-1071.

Quantitative Environmental Analysis, (QEA) 1999. *PCBs in the Upper Hudson River.* Report prepared for the General Electric Company, Albany, NY.

Tsai, C.H. and W. Lick, 1987. Resuspension of sediments from Long Island Sound. *Wat. Sci. Tech.*, 21(6/7):155-184.

U.S. Environmental Protection Agency, 1997. *Phase 2 Report – Review Copy: Further Site Characterization and Analysis – Volume 2C Data Evaluation and Interpretation Report* Hudson River PCBs Reassessment RI/FS. USEPA, Region 2. New York, NY.

van Niekerk, A., K.R. Vogel, R.L. Slingerland, and J.S. Bridge, 1992. Routing of heterogeneous sediments over movable bed: model development. *ASCE J. Hydr. Engrg.*, 118(2):246-279.

van Rijn, L.C., 1984. Sediment transport, part II: suspended load transport. *ASCE J. Hydr. Engrg.*, 110(11):1612-1638.

van Rijn, L.C., M.W.C. Nieuwjaar, T. van der Kaay, E. Nap, and A. von Kampen, 1993. Transport of fine sands by currents and waves. *ASCE J. Wtrwy. Port, Coast., and Oc. Engrg.*, 119(2):123-143.

Velleux, M. and D. Endicott, 1994. Development of a mass balance model for estimating PCB export from the Lower Fox River to Green Bay. *J. Great Lakes Res.*, 20(2):416-434.

Whitman, W.G., 1923. The two-film theory of gas adsorption. *Chemical and Met. Engineering.*29, 147 pp.

Ziegler, C.K., 2001. Evaluating sediment stability at sites with historic contamination. To be published in *Environmental Management.*

Ziegler, C.K. and B.S. Nisbet, 1995. Long-term simulation of fine-grained sediment transport in large reservoir. *ASCE J. Hydr. Engrg.*, 121(11):773-781.

Ziegler, C.K. and B.S. Nisbet, 1994. Fine-grained sediment transport in Pawtuxet River, Rhode Island. *ASCE J. Hydr. Engrg.*, 120(5):561-576.

Ziegler, C.K., P.H. Israelsson, H. Zahakos, D. Glaser and J.P. Connolly, 2001. *Addendum to PCBs in the Upper Hudson River, July 1999.* QEA report prepared for General Electric Company, Albany, NY.

FIGURES

Abbreviations used in spatial plots:

ML	=	Morrow Lake
PC	=	Portage Creek
PI	=	former Plainwell Impoundment
OCI	=	Otsego City Impoundment
OI	=	former Otsego Impoundment
TI	=	former Trowbridge Impoundment
ACI	=	Allegan City Impoundment
LA	=	Lake Allegan

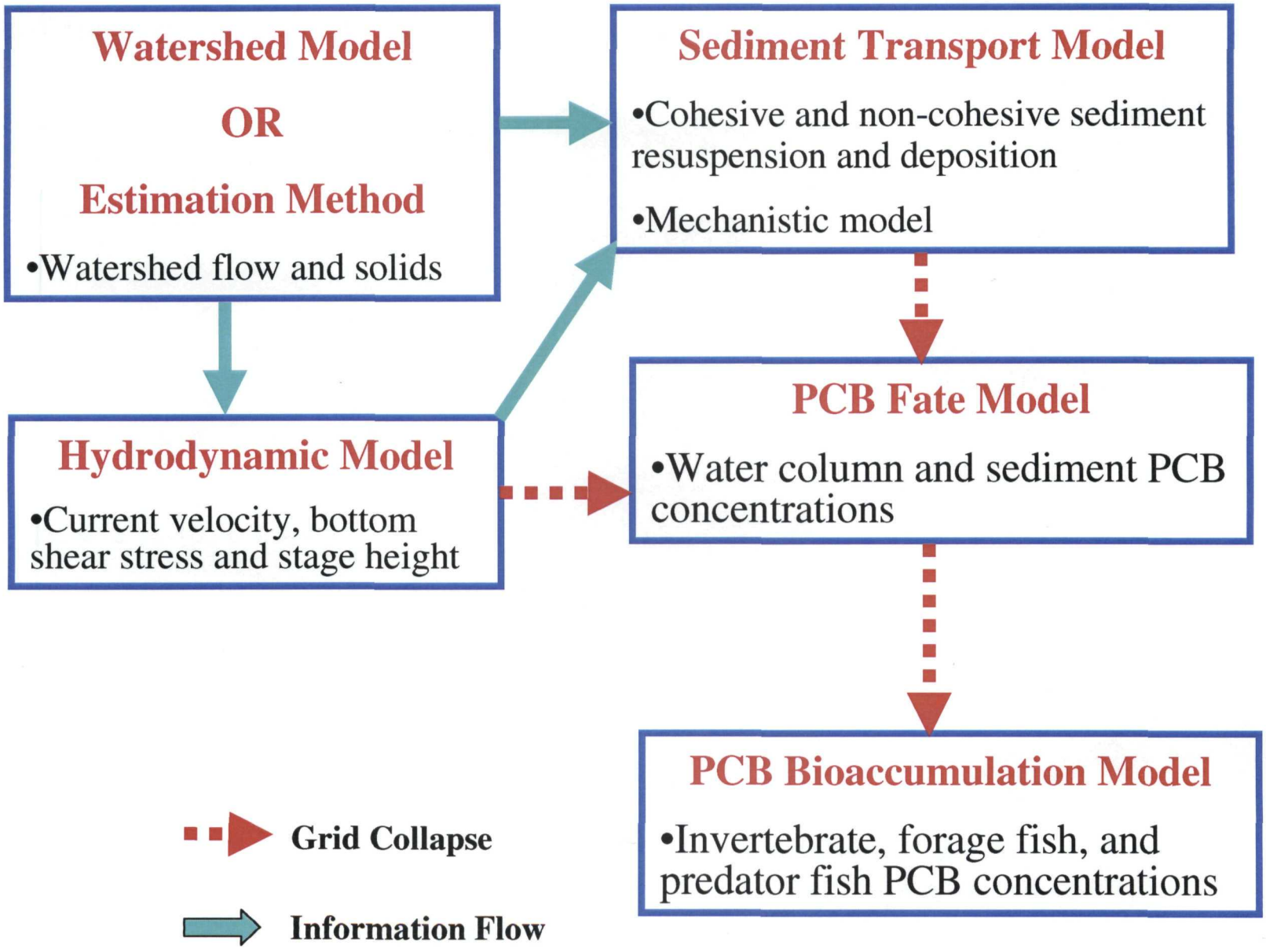

Figure 2-1. Schematic for reliable PCB fate modeling framework.

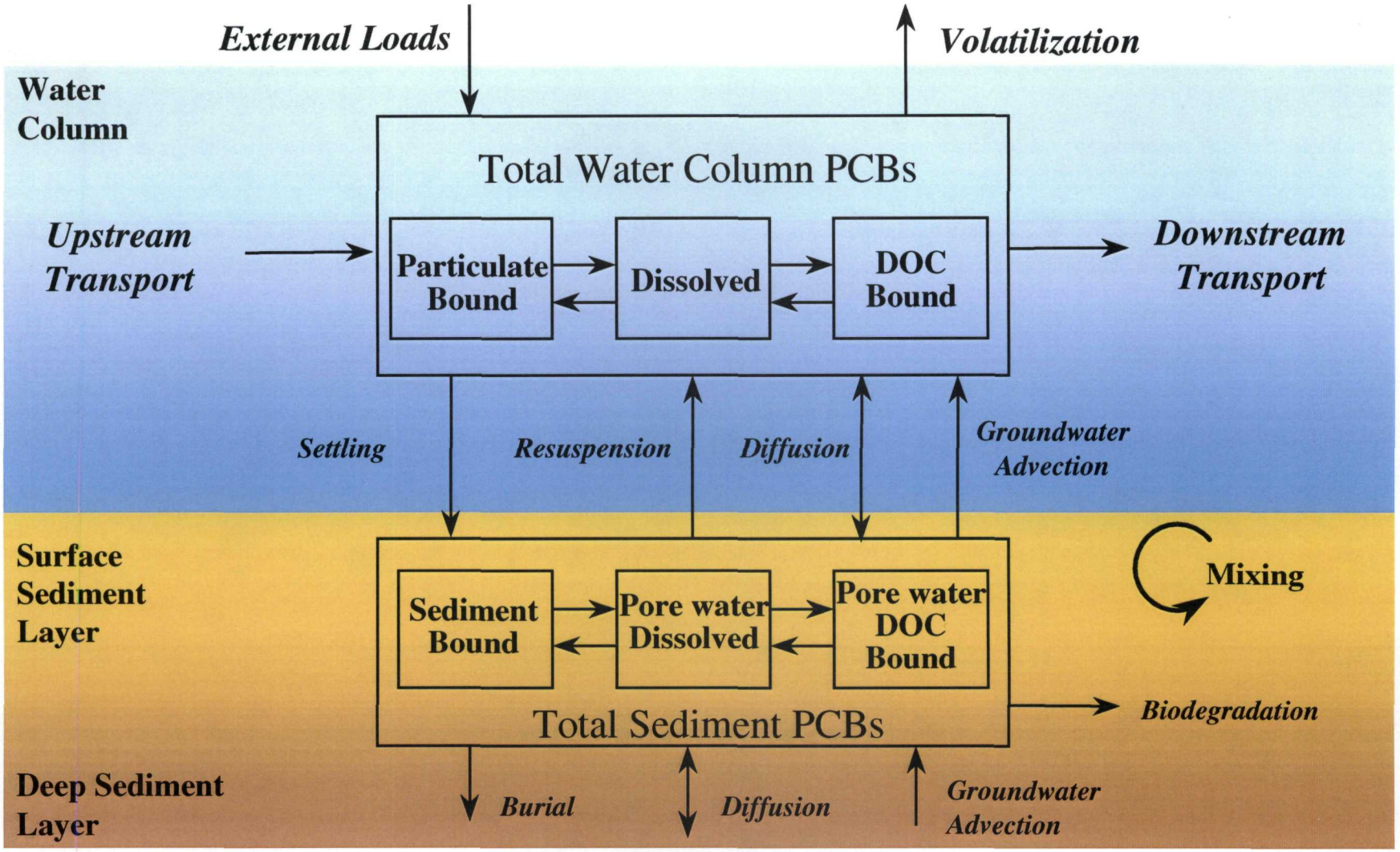

Figure 2-2. Schematic for PCB fate and transport processes to be included in a comprehensive model.

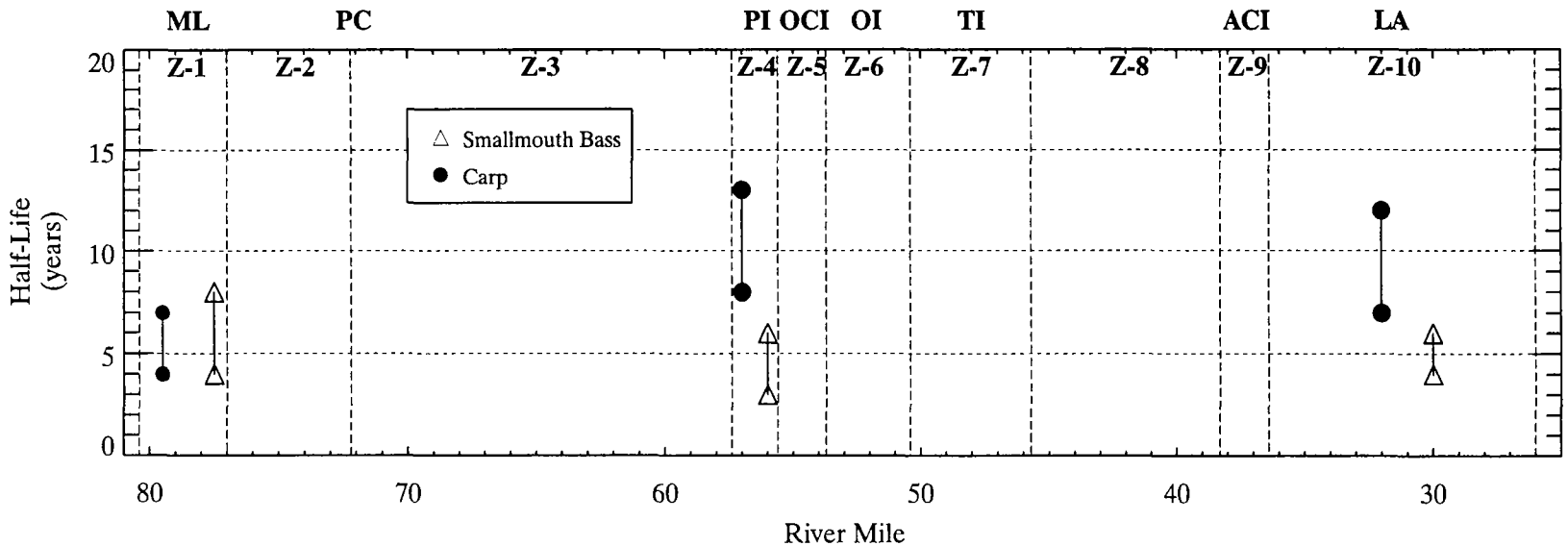

Figure 3-1. Range of estimated half-lives of PCB concentrations in carp and smallmouth bass.

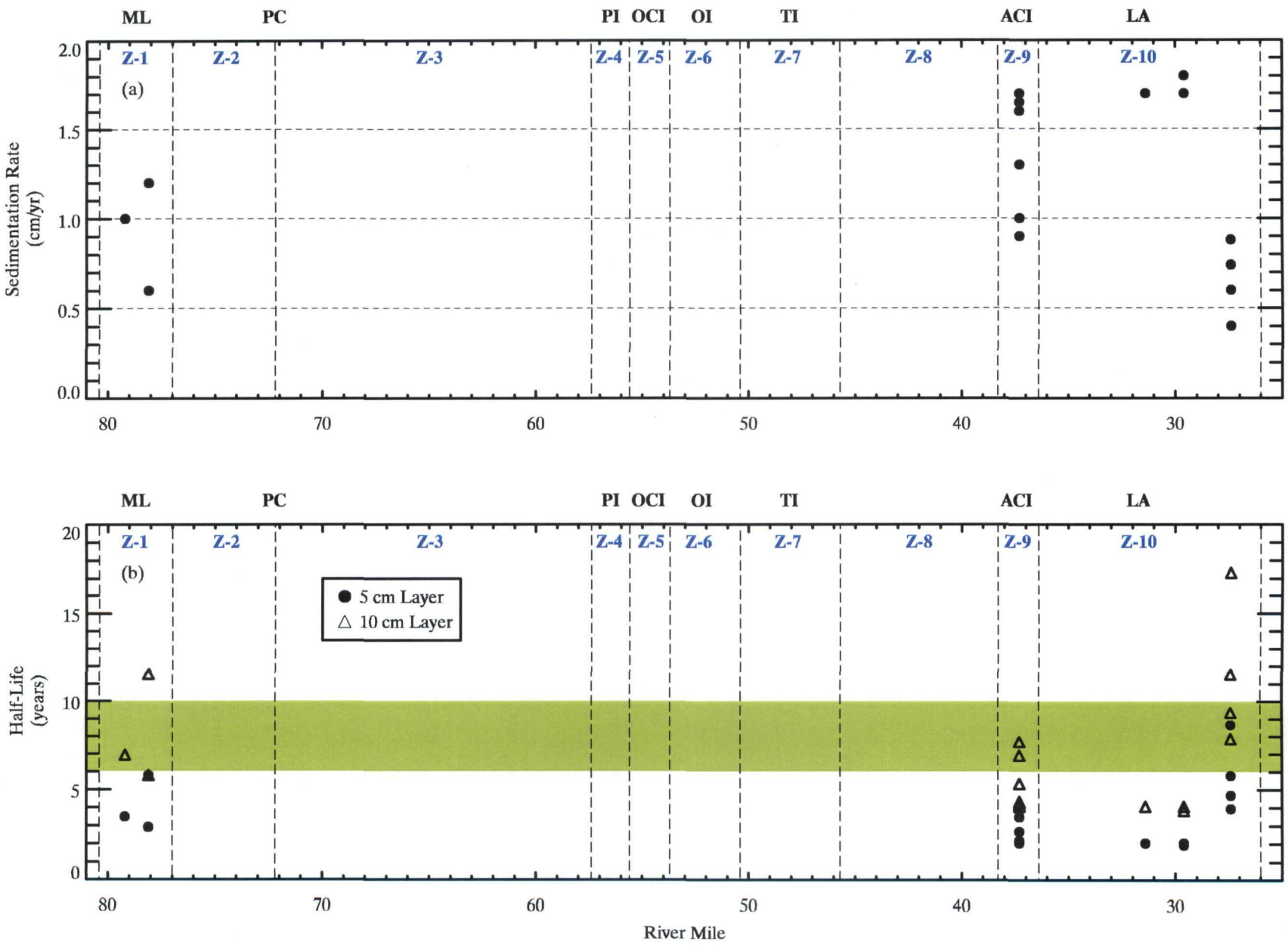

Figure 3-2. Geochronologic analysis of 2000 sediment core data: (a) estimated sedimentation rates and (b) estimated PCB half-lives in surficial sediments assuming no external loads (green band corresponds to PCB half-life range based on temporal analysis of fish data).

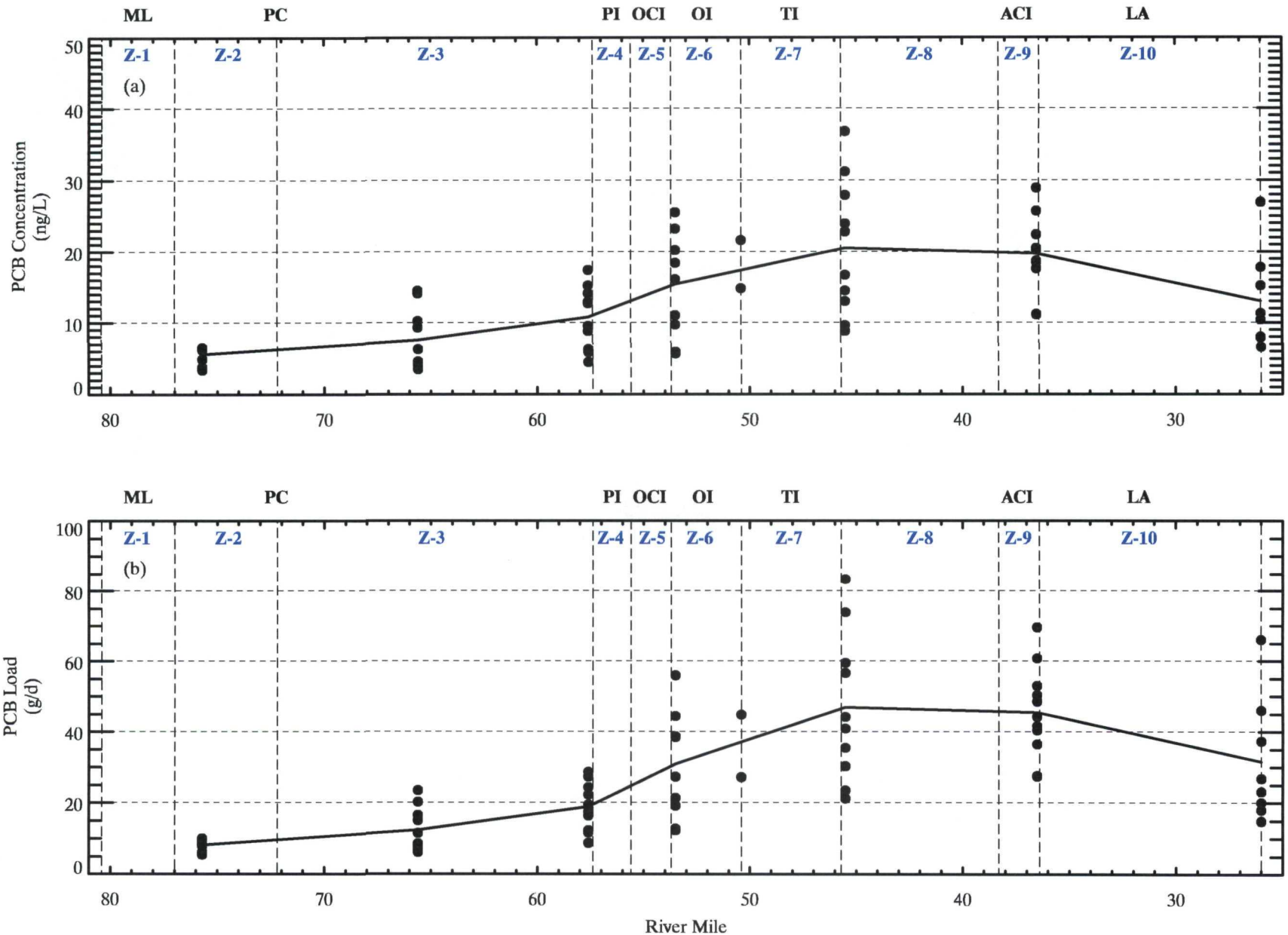

Figure 3-3. Spatial distribution of low-flow water column PCB data: (a) concentrations and (b) estimated loads. Data collected during 2000 for flow rates < 800 cfs at Comstock gauging station. Solid line represents trend through average data.

HM/CFO - E:\CDMkal\documents\Report\cowen\spatial_data_pcbconc.pro
Fri Jun 15 14:33:56 2001

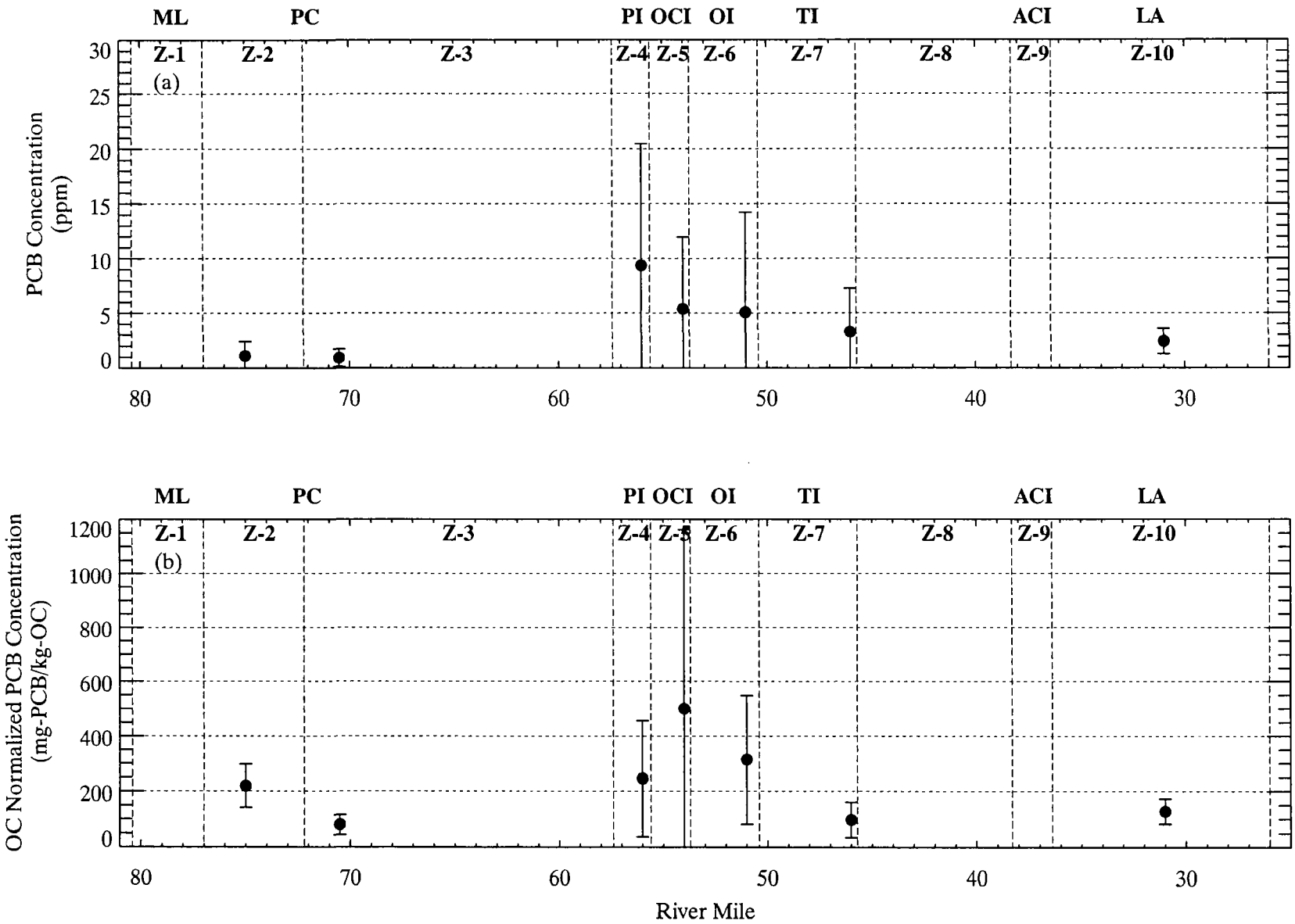

Figure 3-4. Spatial distribution of 1993-94 surficial sediment data: (a) PCB concentration and (b) OC-normalized PCB concentration. Data plotted as +/- 2 standard errors. Sediment data are averaged based on Aquatic Biota Sampling Areas (ABSA).

cfo/HM - E:\CDMkal\documents\Report\cowen\spatial_data_sedconc.pro
Fri Jun 15 12:06:33 2001

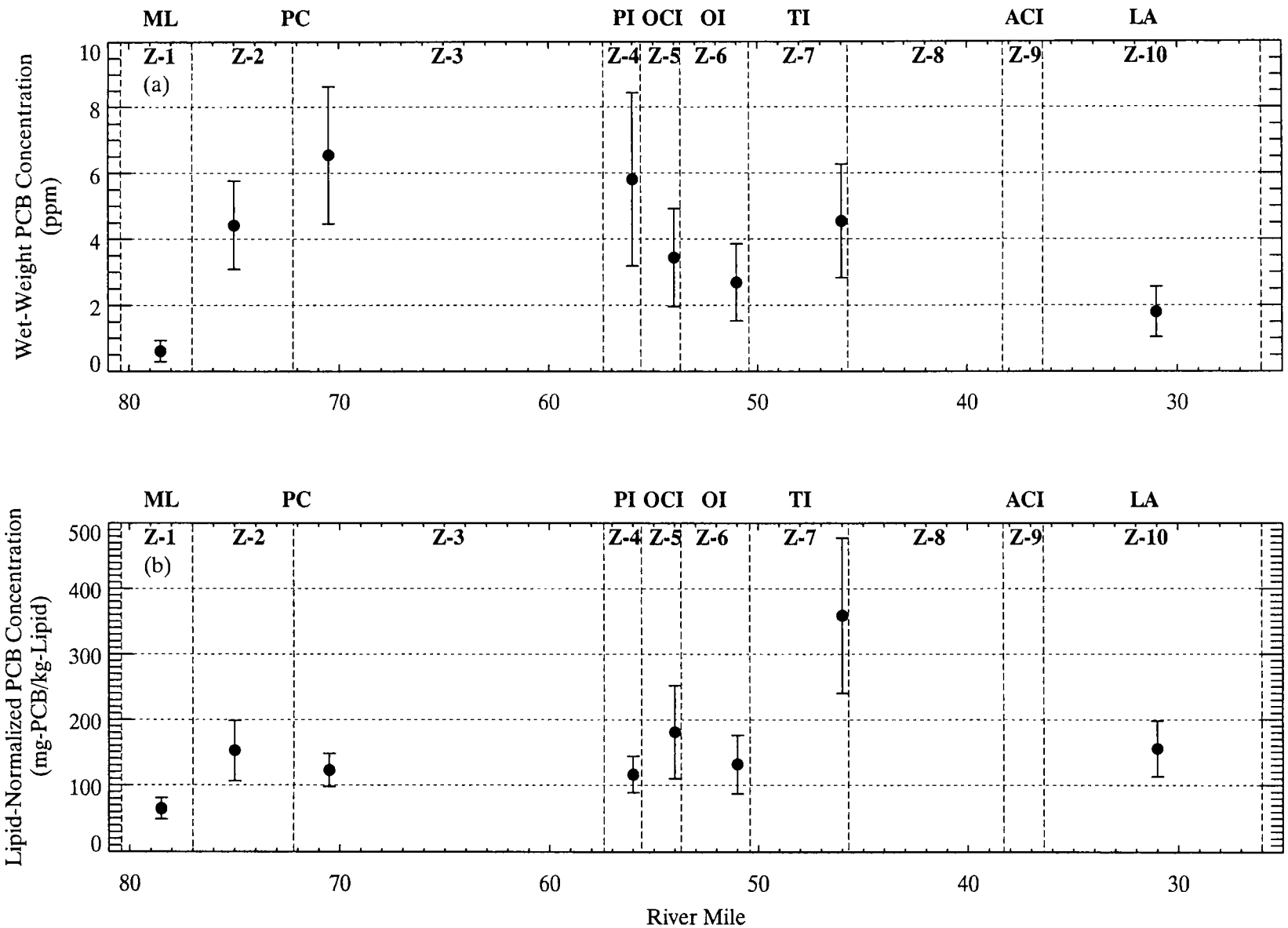

Figure 3-5. Spatial distribution of 1993-94 carp PCB concentrations: (a) wet-weight concentration and (b) lipid-normalized concentration. Data plotted as mean +/- 2 standard errors. Fish data are averaged based on Aquatic Biota Sampling Areas (ABSA).

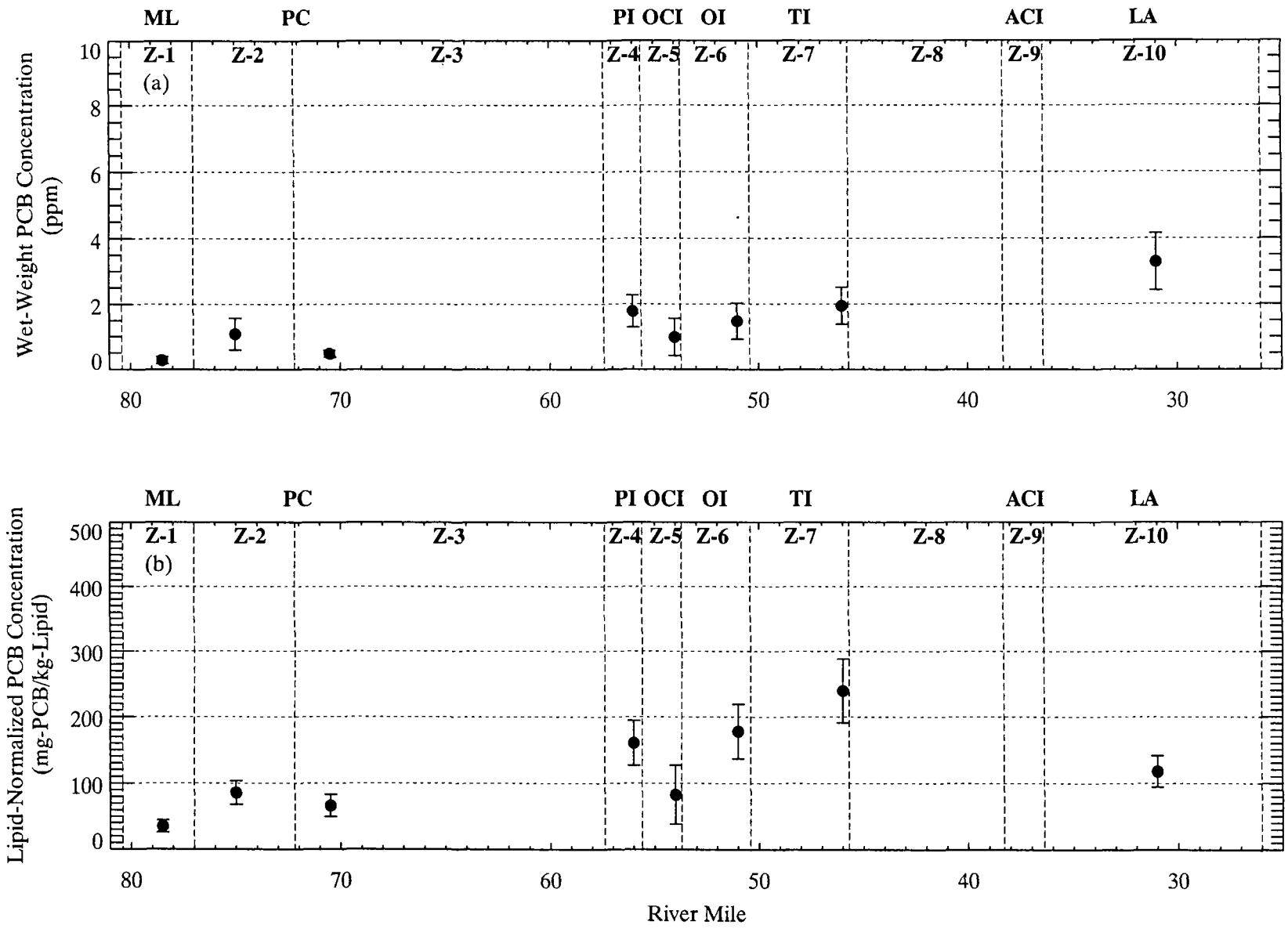

Figure 3-6. Spatial distribution of 1993-94 smallmouth bass PCB concentrations: (a) wet-weight concentration and (b) lipid-normalized concentration. Data plotted as mean +/- 2 standard errors. Fish data are averaged based on Aquatic Biota Sampling Areas (ABSA).

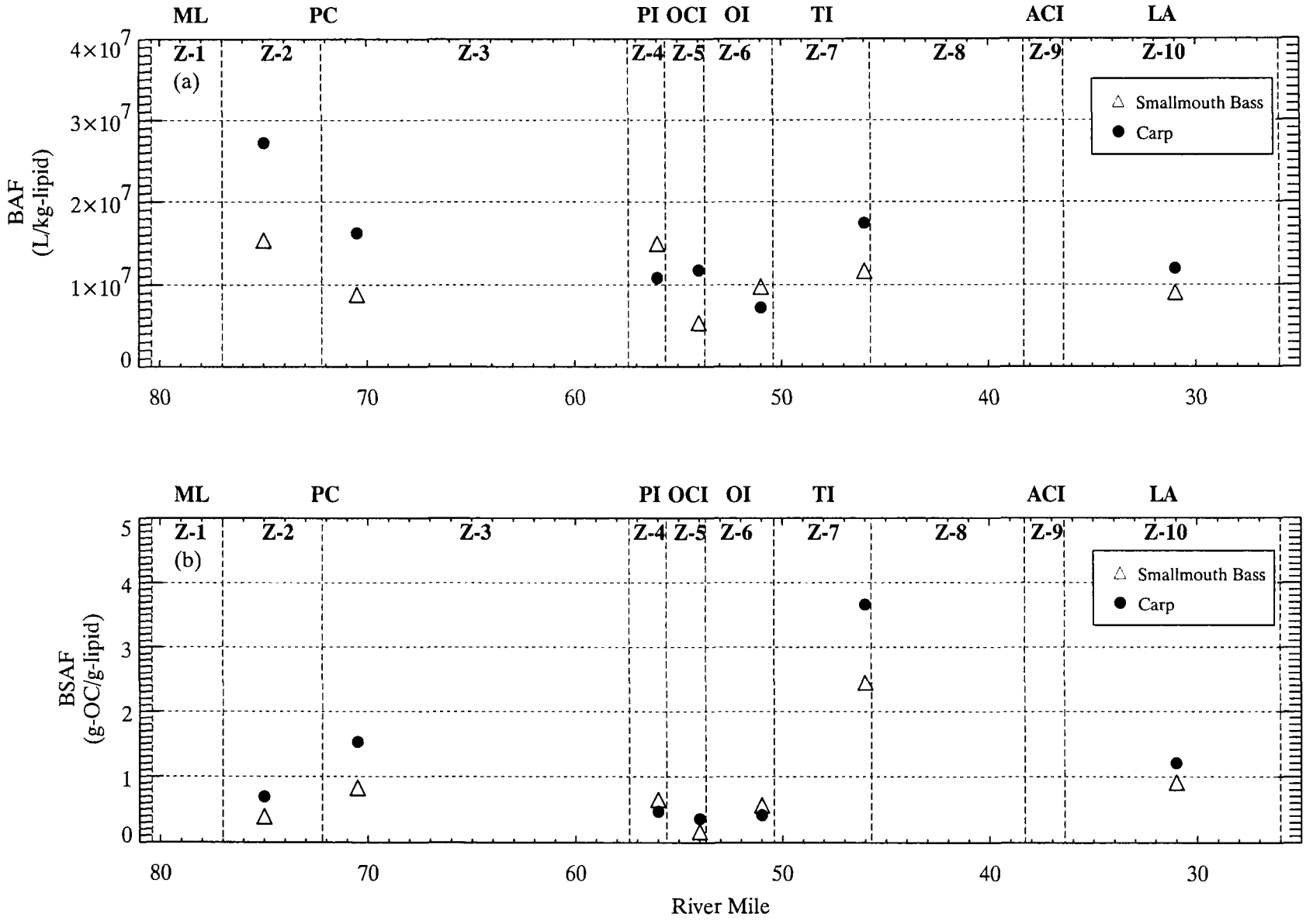

Figure 3-7. Spatial distribution of bioaccumulation factors in carp and smallmouth bass: (a) bioaccumulation factor (BAF) and (b) biota-sediment accumulation factor (BSAF).
Fish data are averaged based on Aquatic Biota Sampling Areas (ABSA).

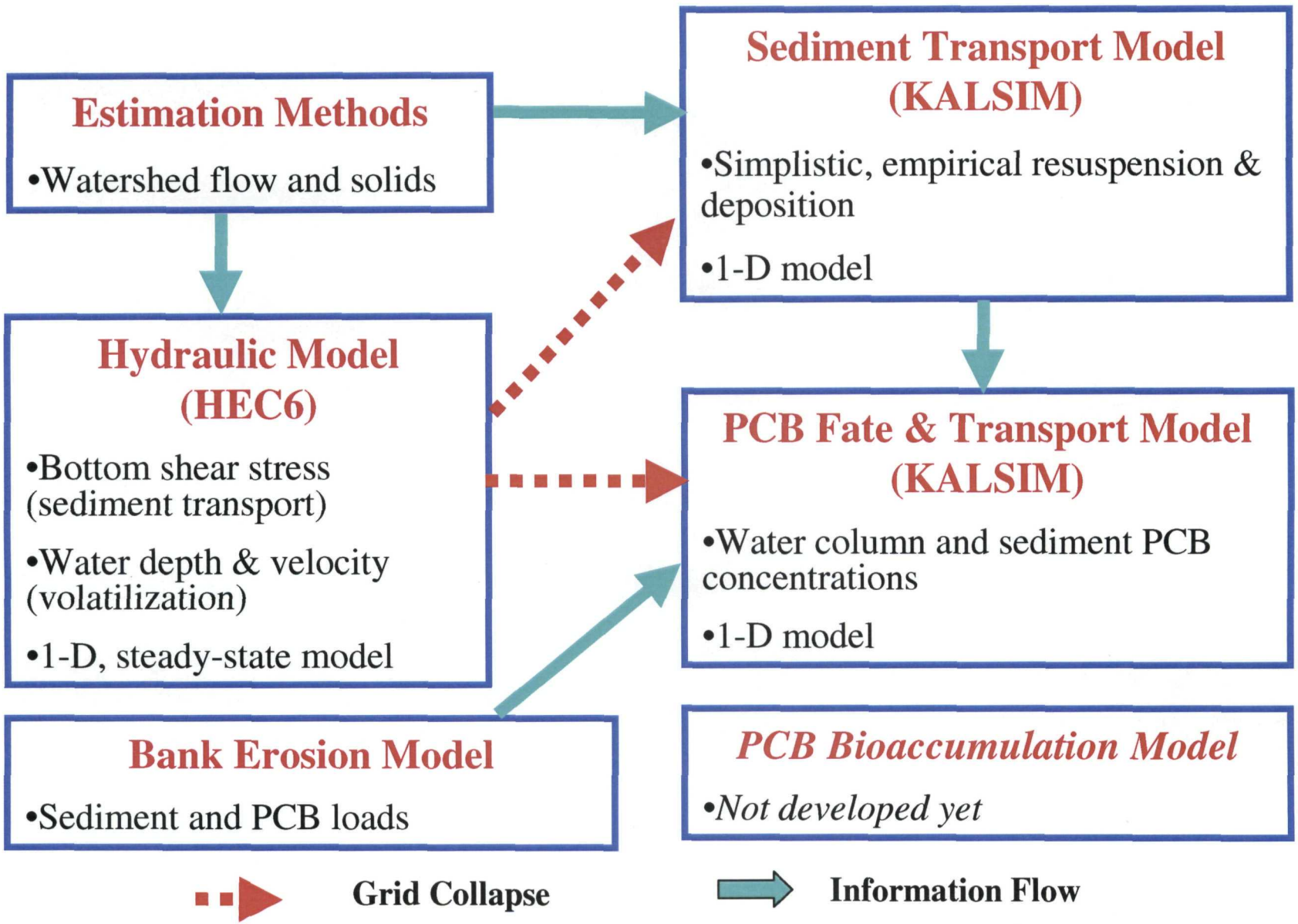

Figure 4-1. Schematic of LTI model framework for the Kalamazoo River.

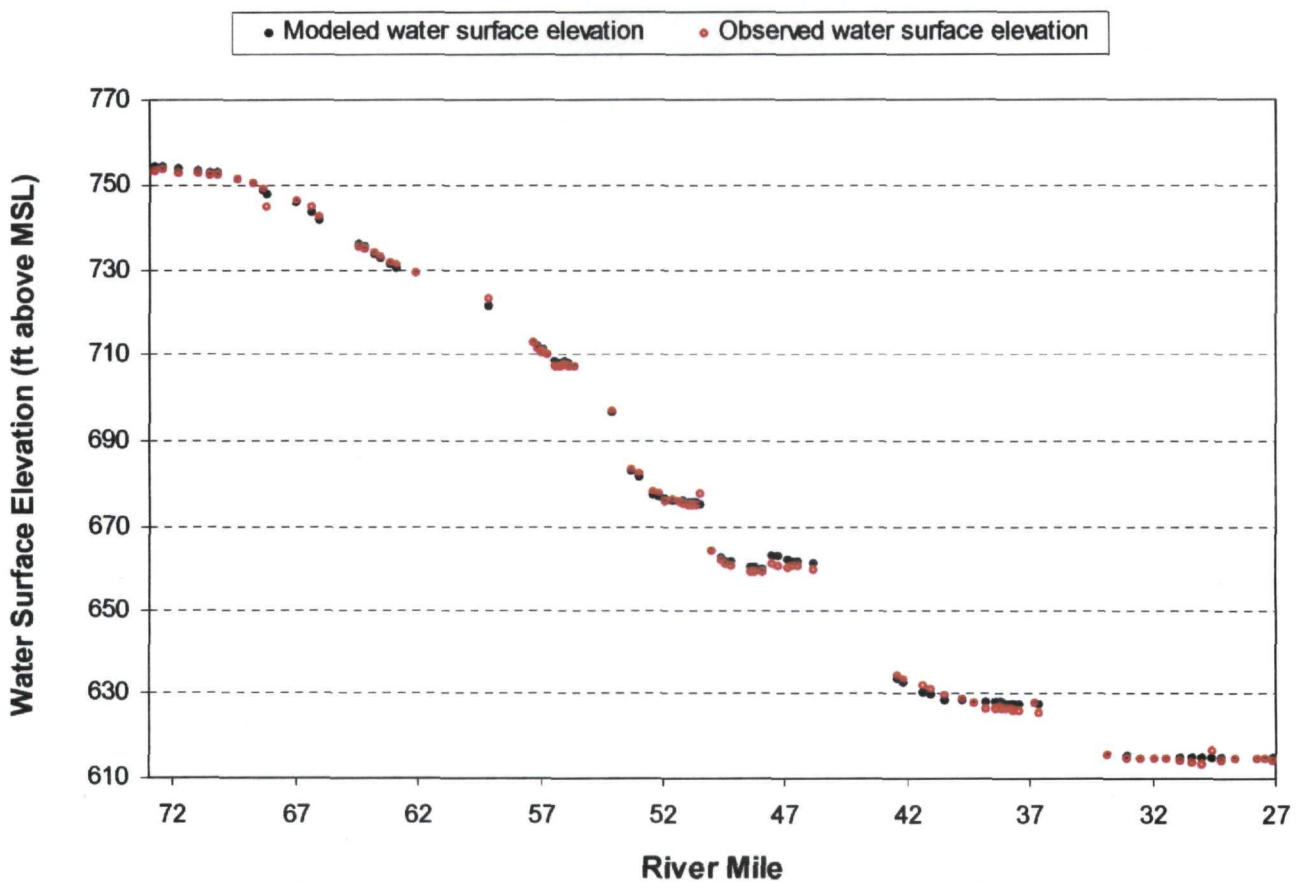

Figure 4-2. Comparison of predicted and measured stage heights for HEC-6 calibration. Reproduction of Figure 5-3 in LTI (2000).

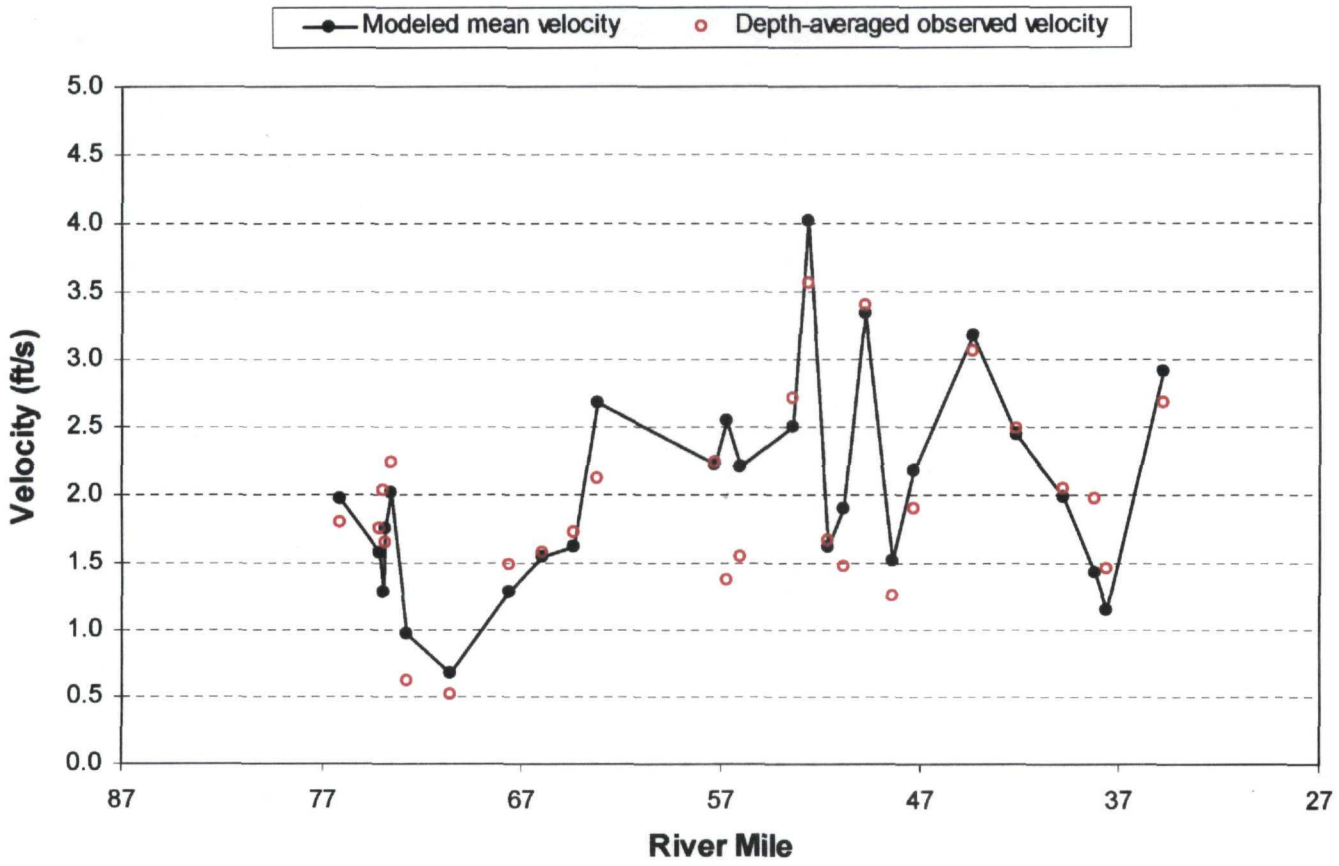

Figure 4-3. Comparison of predicted and measured current velocities for HEC-6 calibration. Reproduction of Figure 5-4 in LTI (2000).

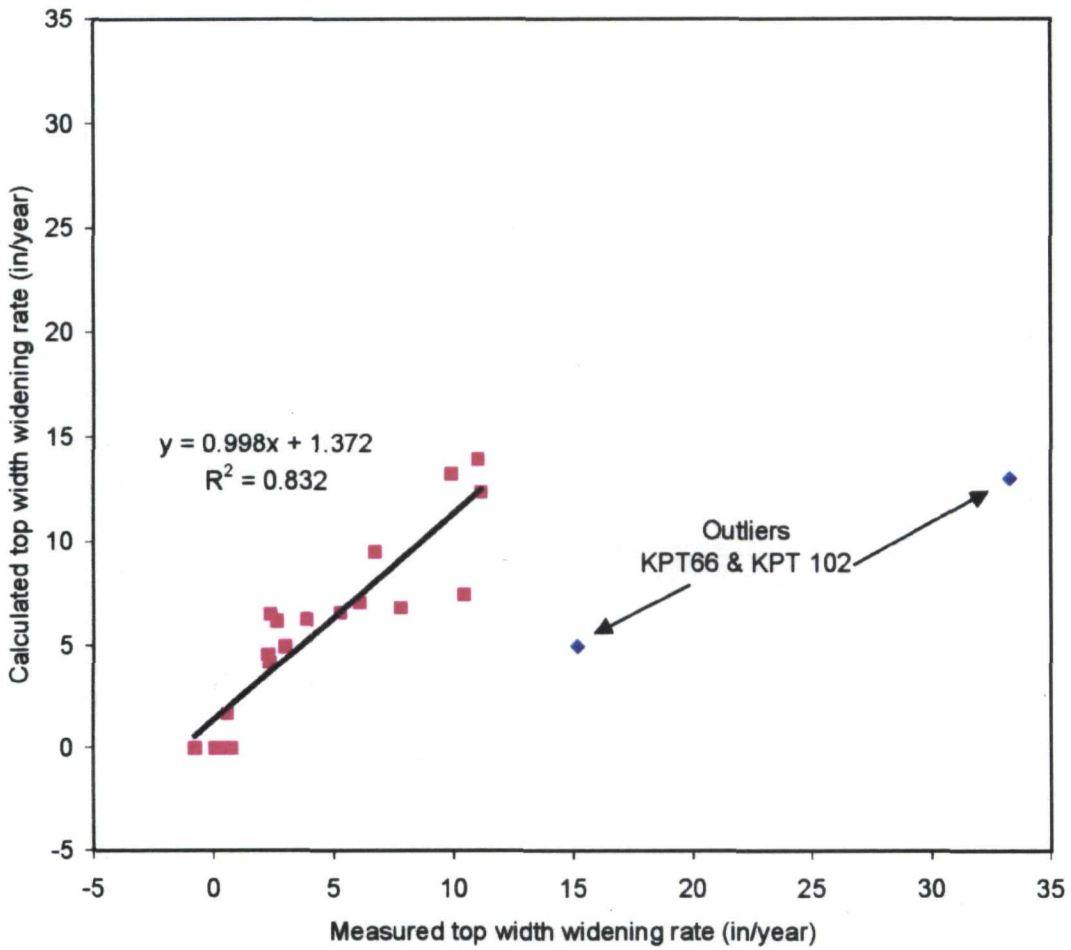

Figure 4-4. Comparison of predicted and measured erosion rates for bank erosion model calibration. Reproduction of Figure 2 in Appendix B of LTI (2000).

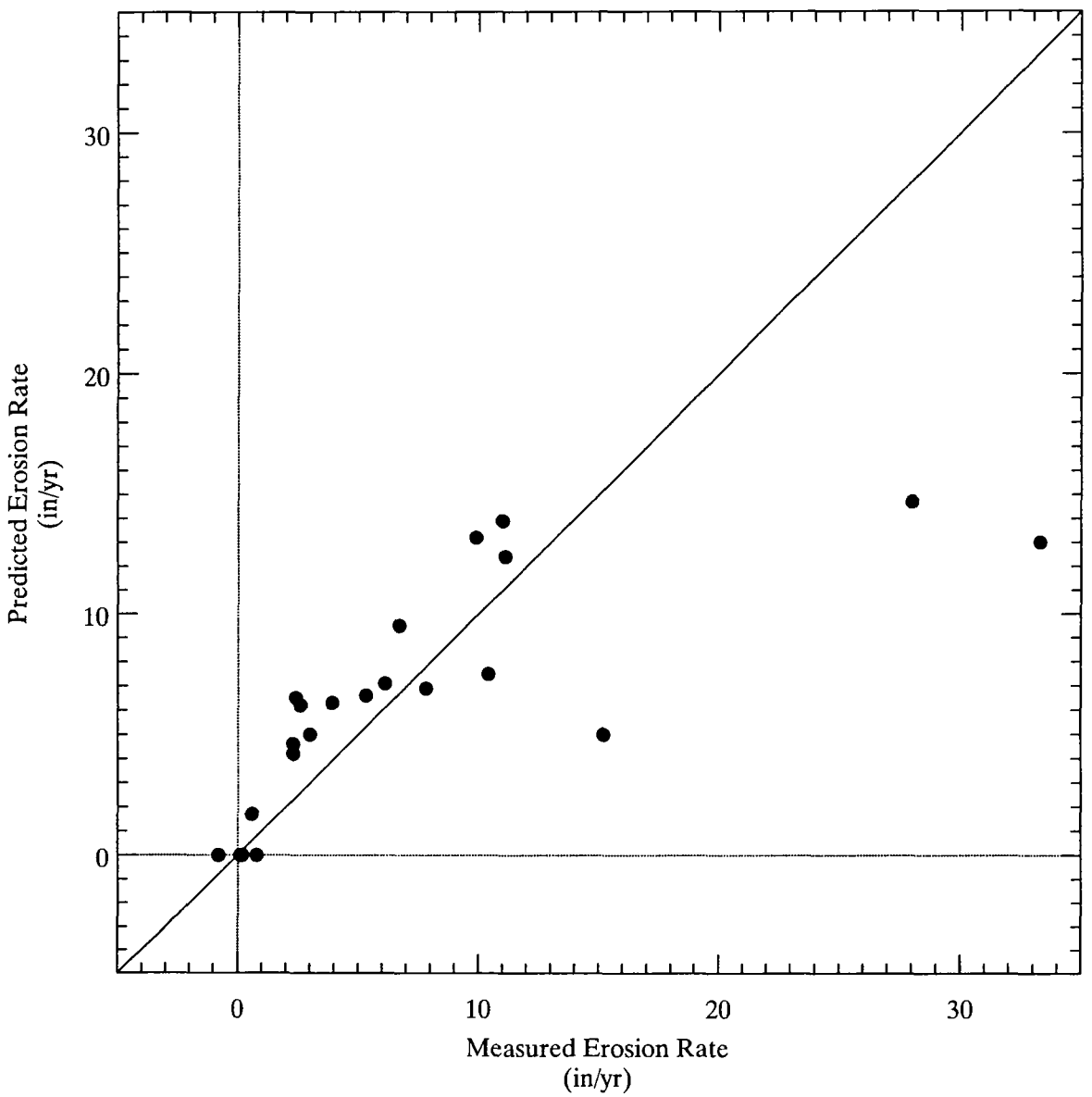

Figure 4-5. Comparison of LTI-provided predictions and measured bank erosion rates for calibration period.

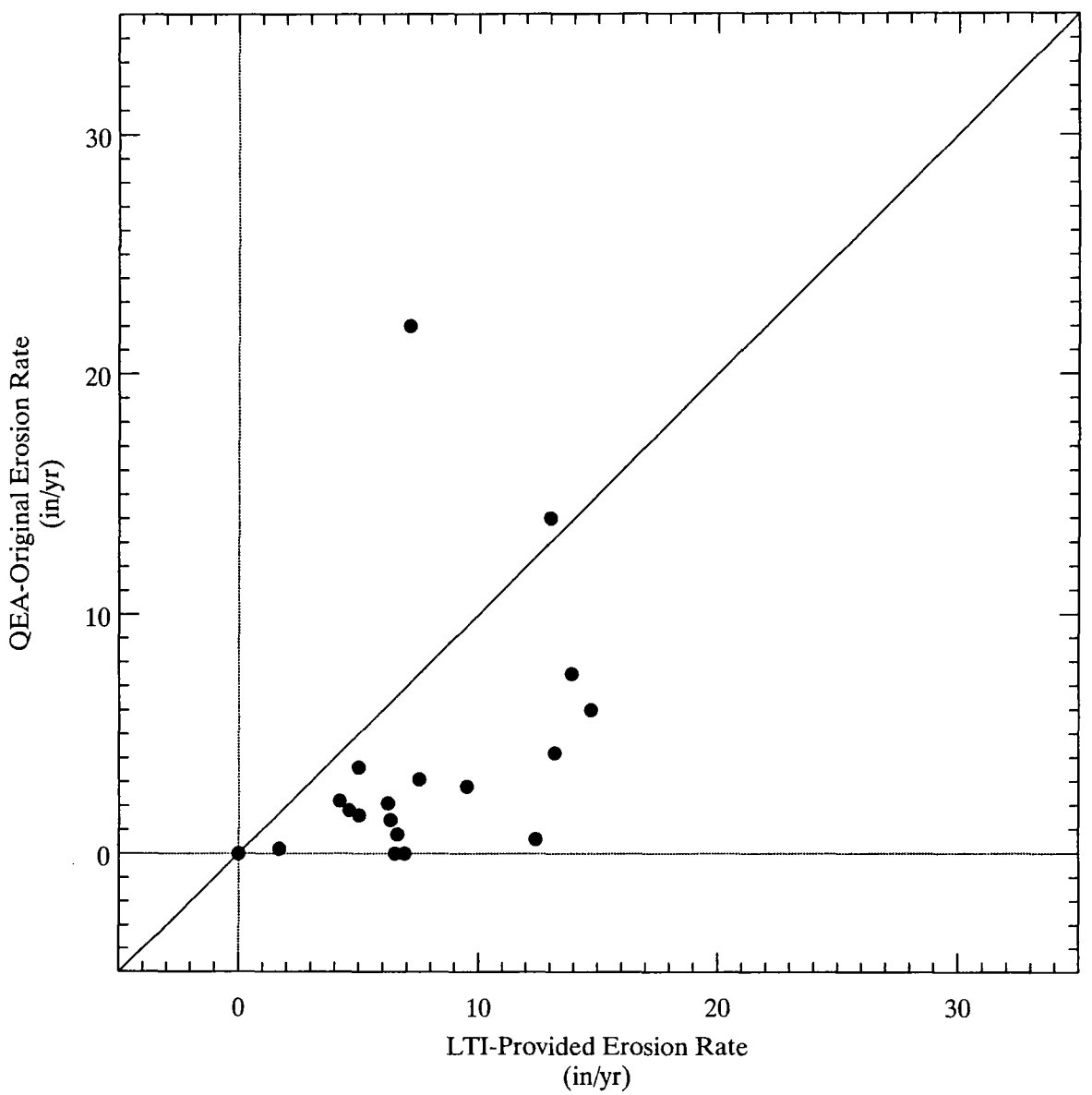

Figure 4-6. Comparison of QEA-original and LTI-provided bank erosion rates for calibration period.

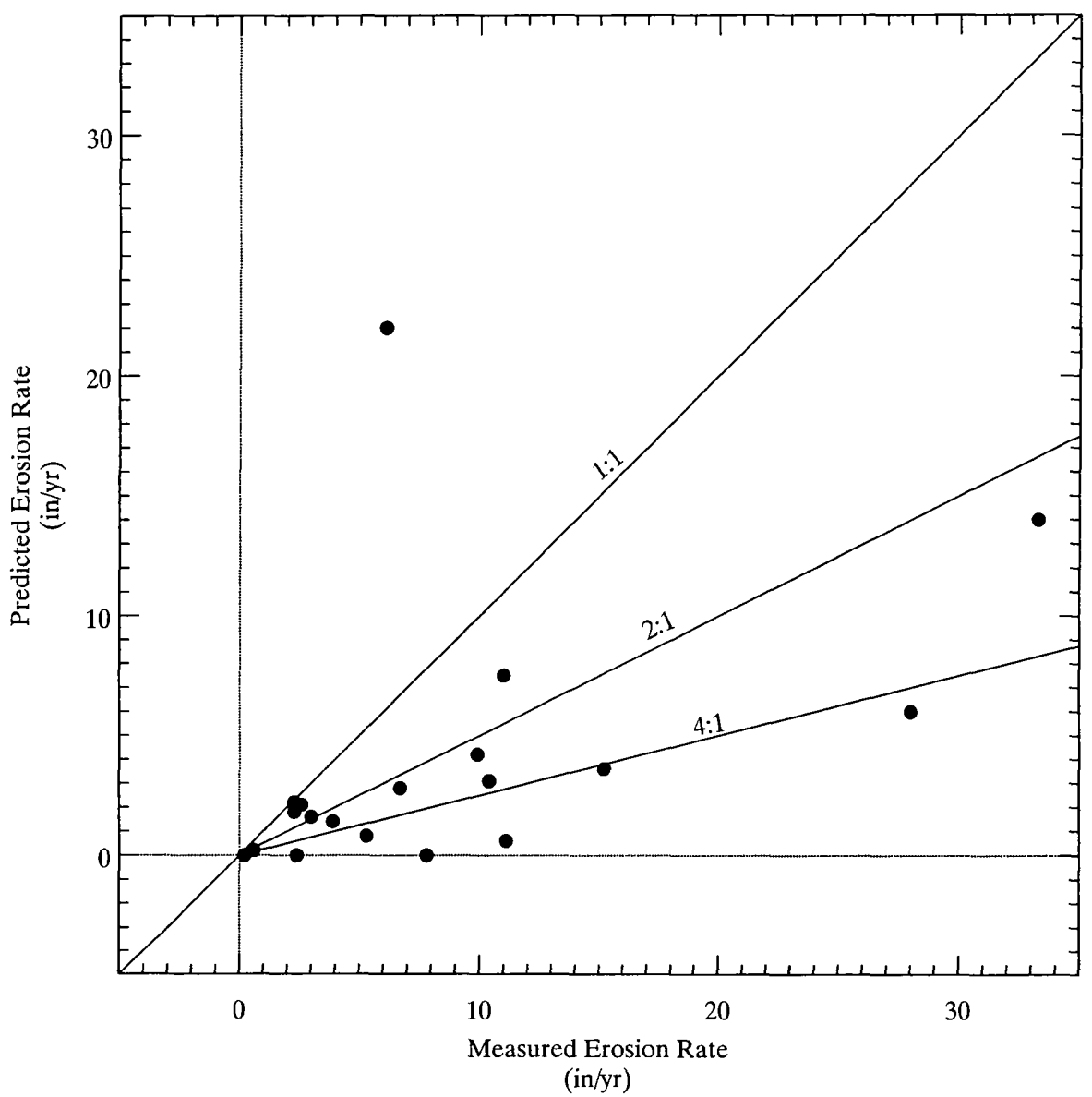

Figure 4-7. Comparison of QEA-original predictions and measured bank erosion rates for calibration period.

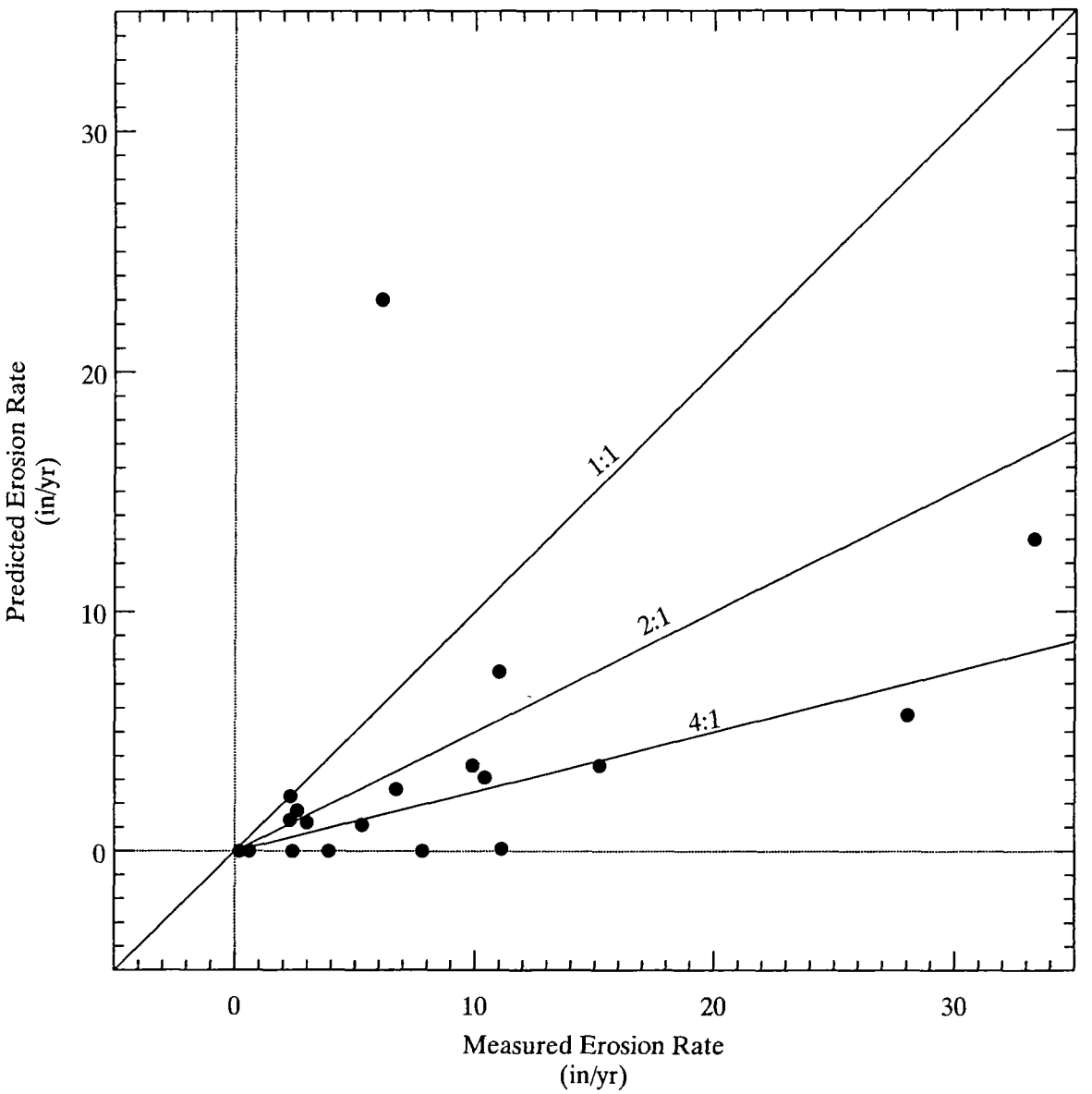

Figure 4-8. Comparison of QEA-corrected predictions and measured bank erosion rates for calibration period.

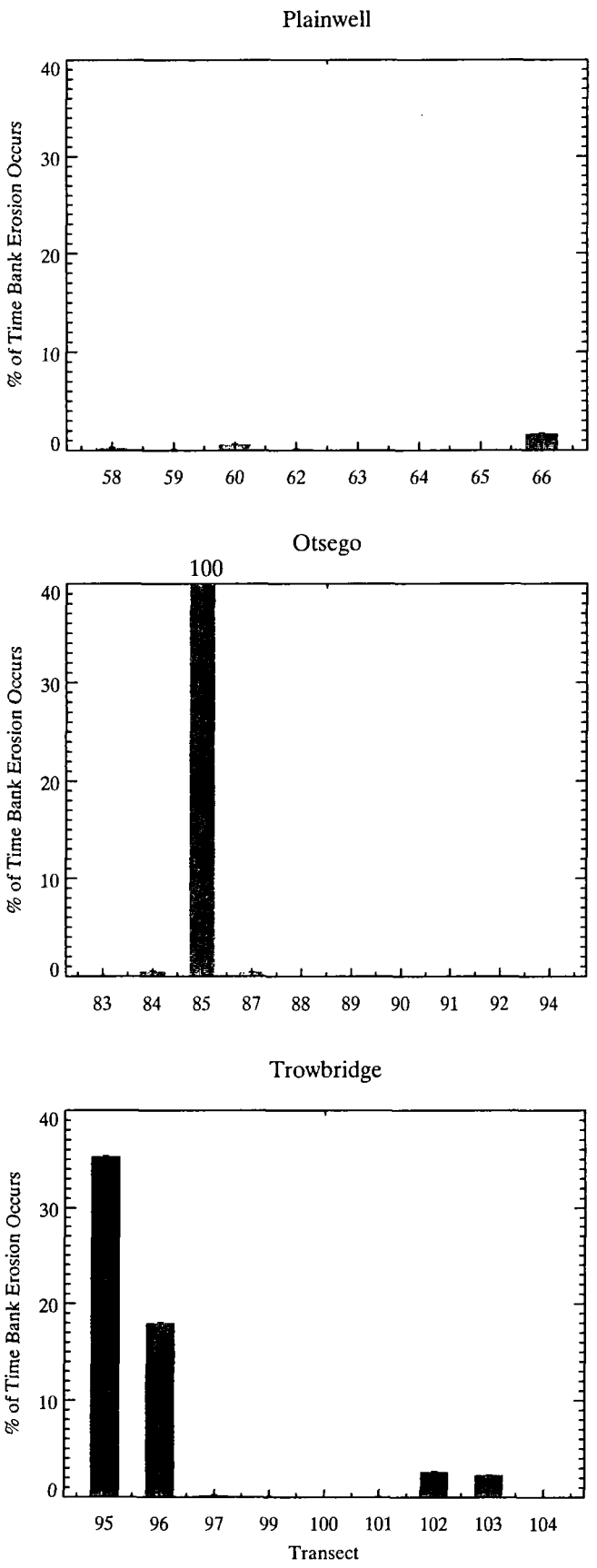

Figure 4-9. Frequency distributions for percent of time that bank erosion is predicted to occur during model calibration period (1994 through 1999) in the three former impoundments.

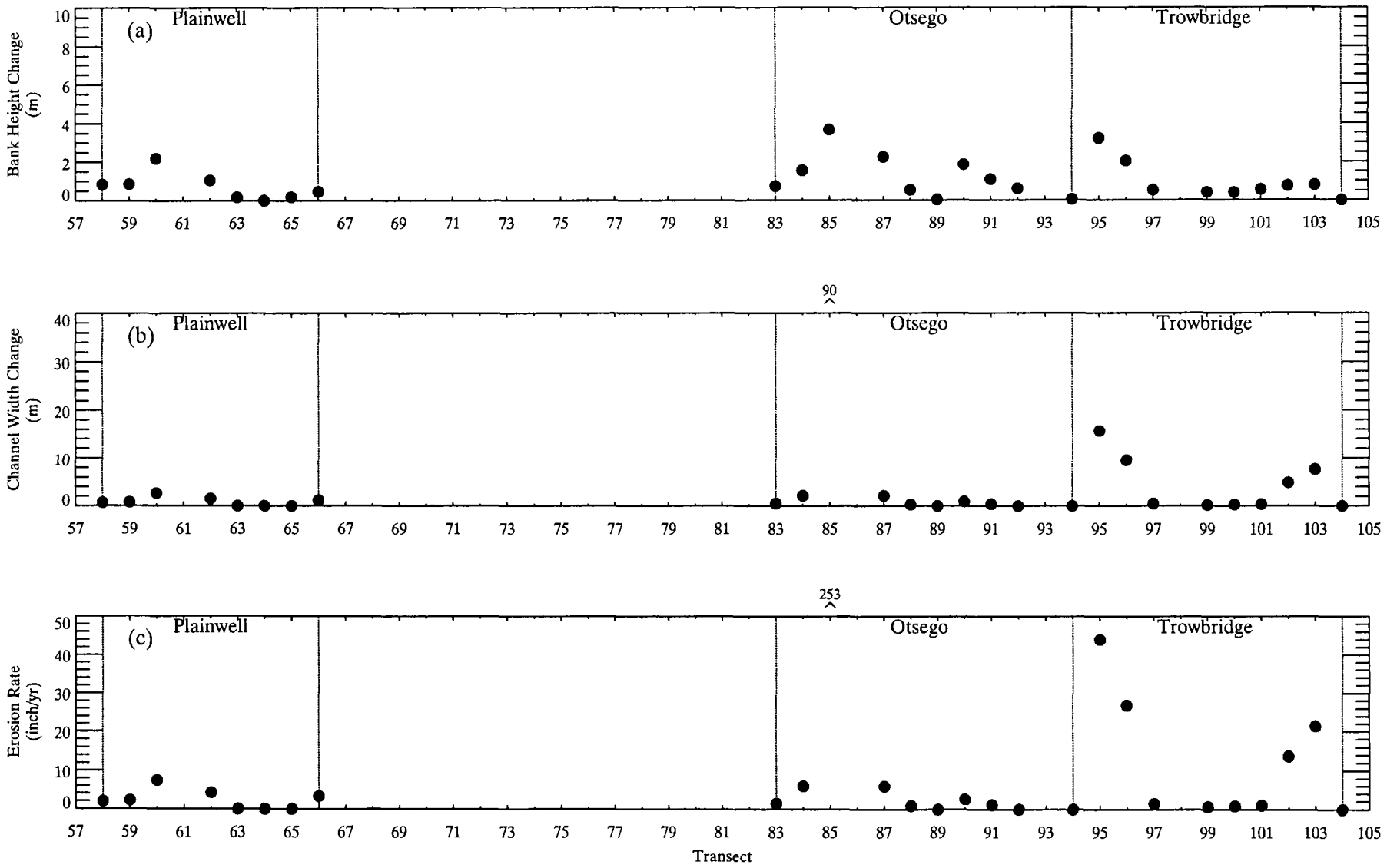

Figure 4-10. Spatial distributions of bank erosion predictions at end of model calibration period (1999) for: (a) bank height change, (b) channel width change and (c) erosion rate.

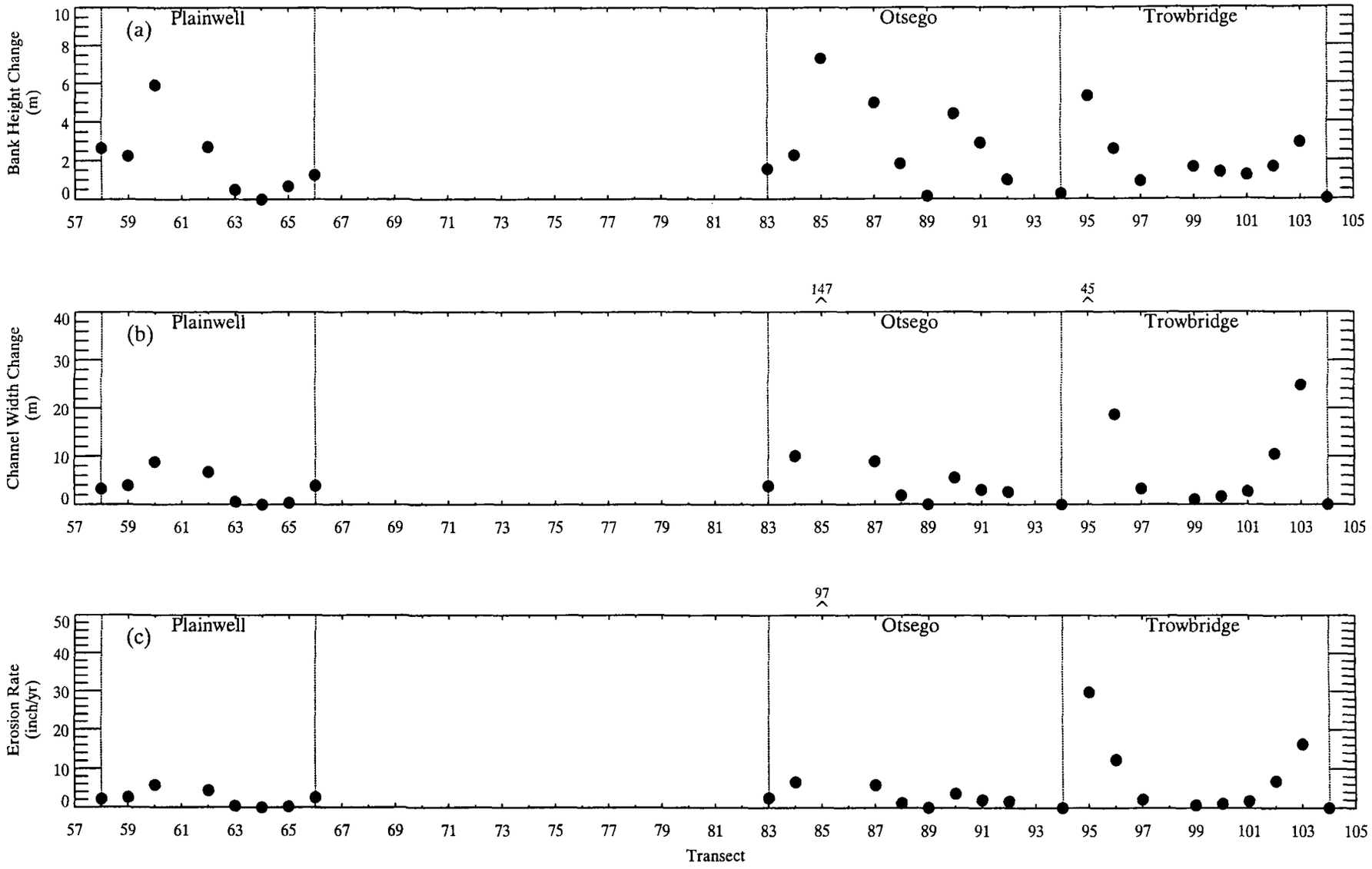

Figure 4-11. Spatial distributions of bank erosion predictions at end of 30-year forecast period for: (a) bank height change, (b) channel width change and (c) erosion rate.

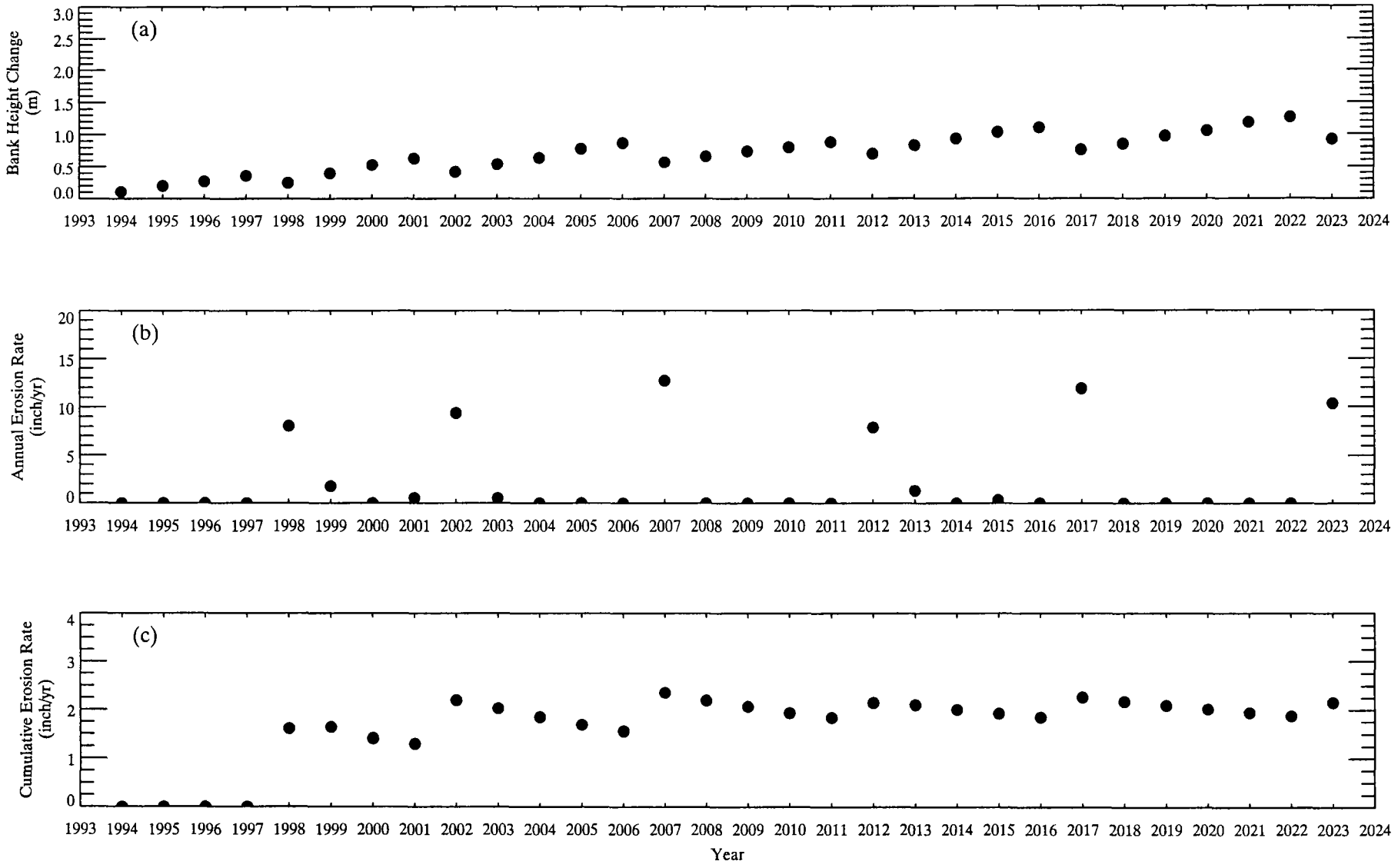

Figure 4-13. Time-series of bank erosion predictions at transect 97 (former Trowbridge Impoundment) for: (a) bank height change, (b) annual erosion rate and (c) cumulative erosion rate.

HM/cfo - E:\CDMkal\documents\Report\cowen\bank_erosion_output_temporal.pro
Fri Jun 15 12:28:20 2001

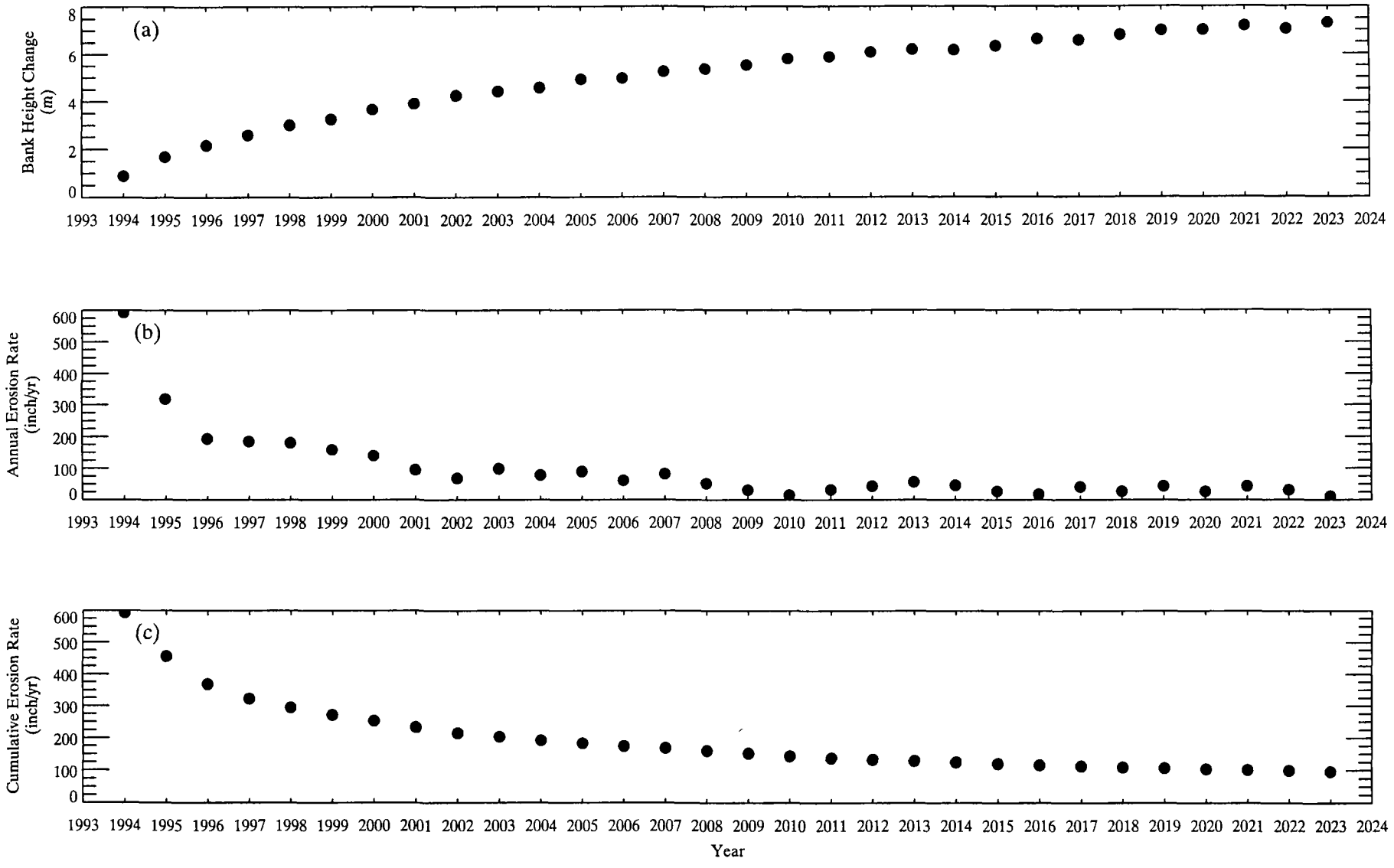

Figure 4-14. Time-series of bank erosion predictions at transect 85 (former Otsego Impoundment) for: (a) bank height change, (b) annual erosion rate and (c) cumulative erosion rate.

HM/cfo - E:\CDMkal\documents\Report\cowen\bank_erosion_output_temporal.pro
Fri Jun 15 12:29:05 2001

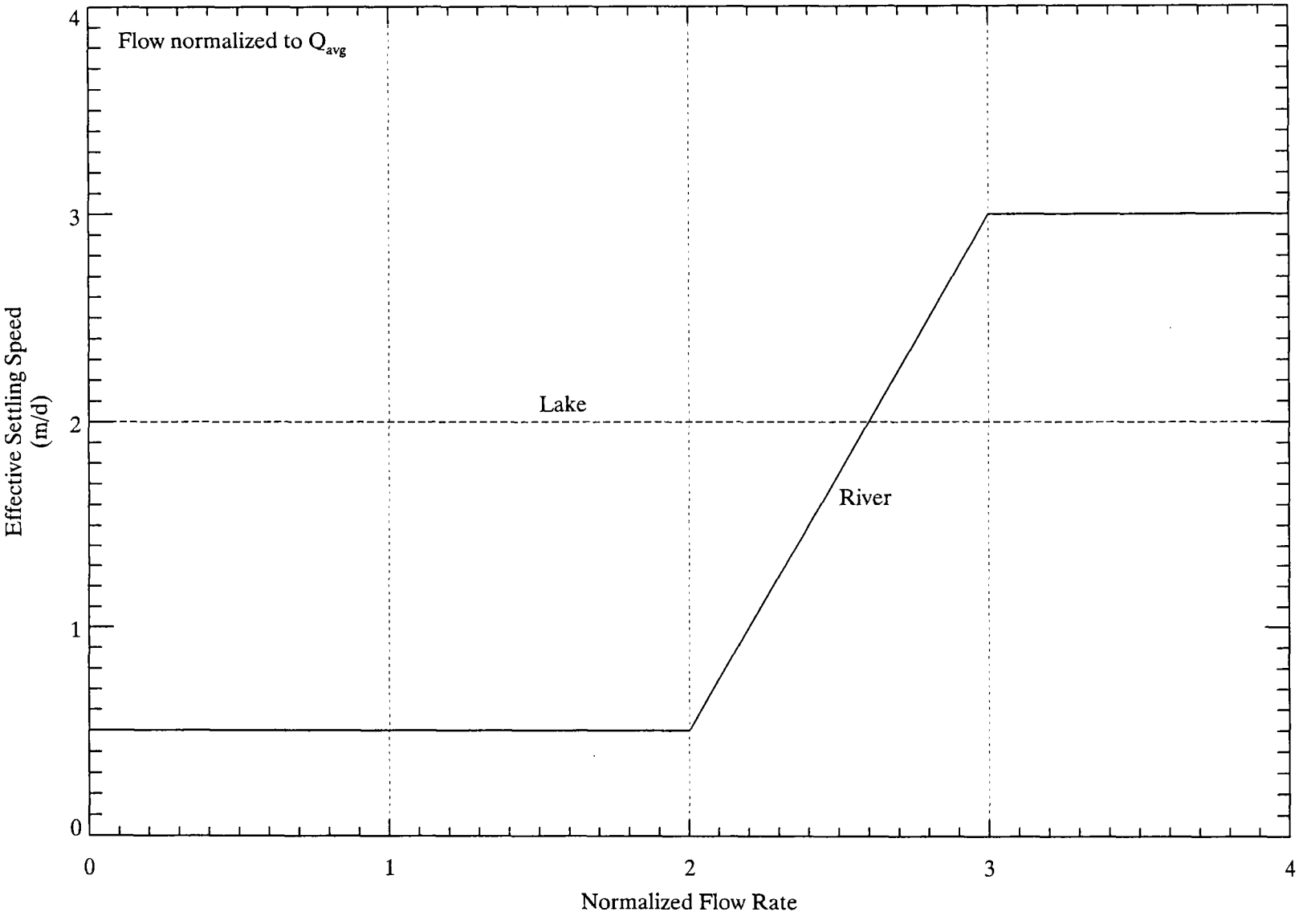

Figure 4-15. Effective settling speed functions used in river and lake sections of the sediment transport submodel.

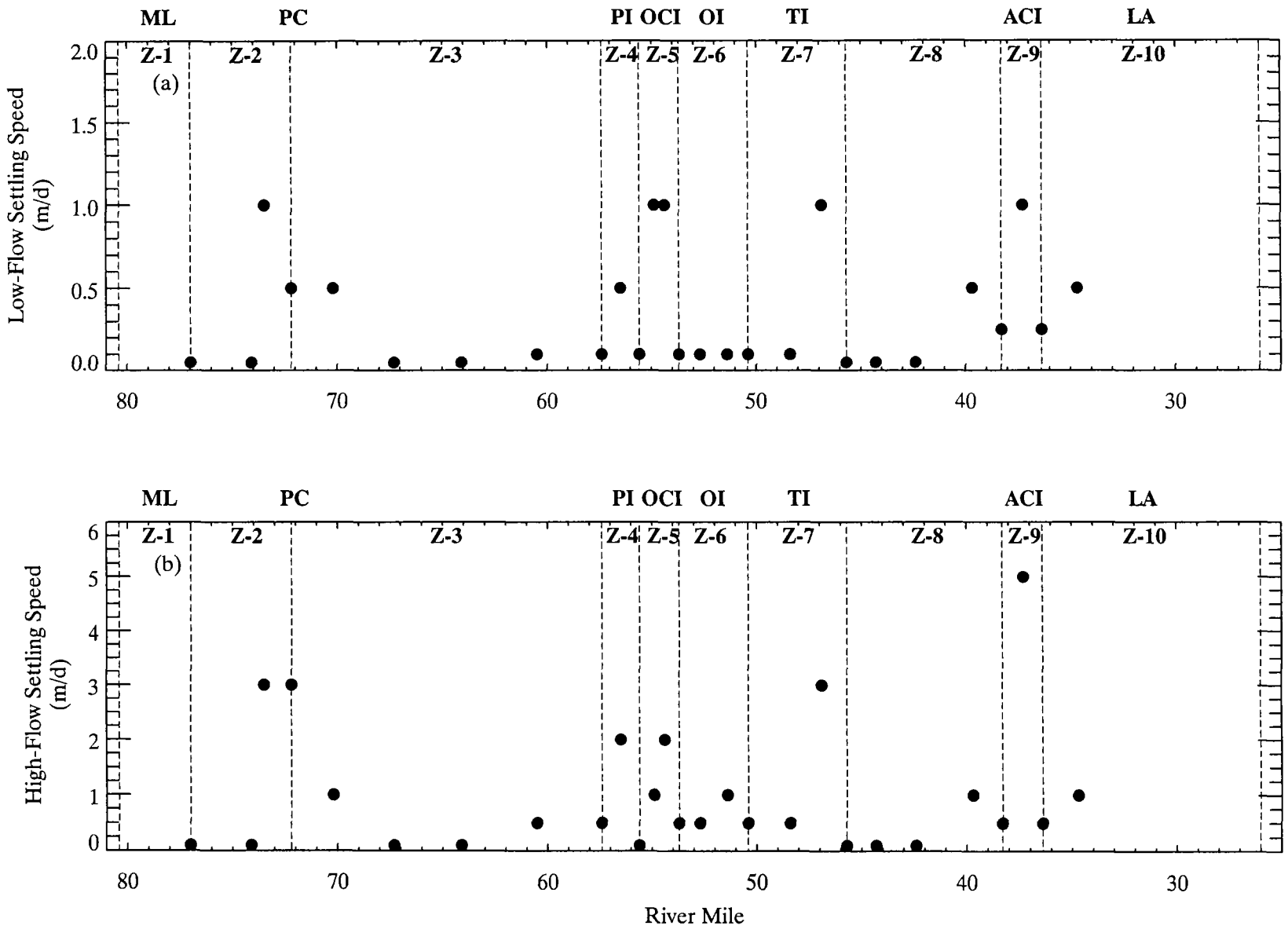

Figure 4-16. Spatial distributions of (a) low-flow and (b) high-flow effective settling speeds.

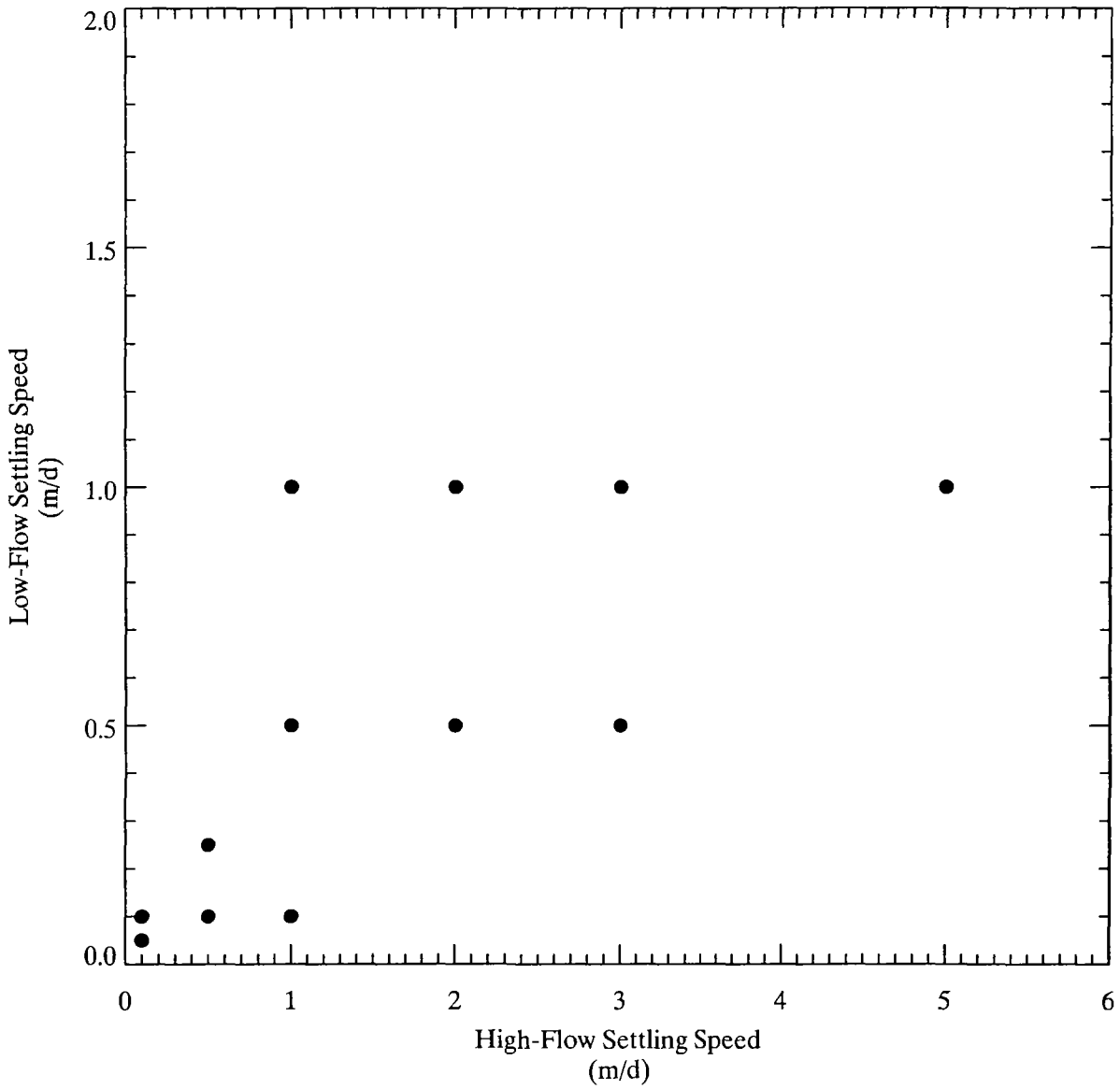

Figure 4-17. Low-flow versus high-flow effective settling speeds in river sections (segments 4-30).

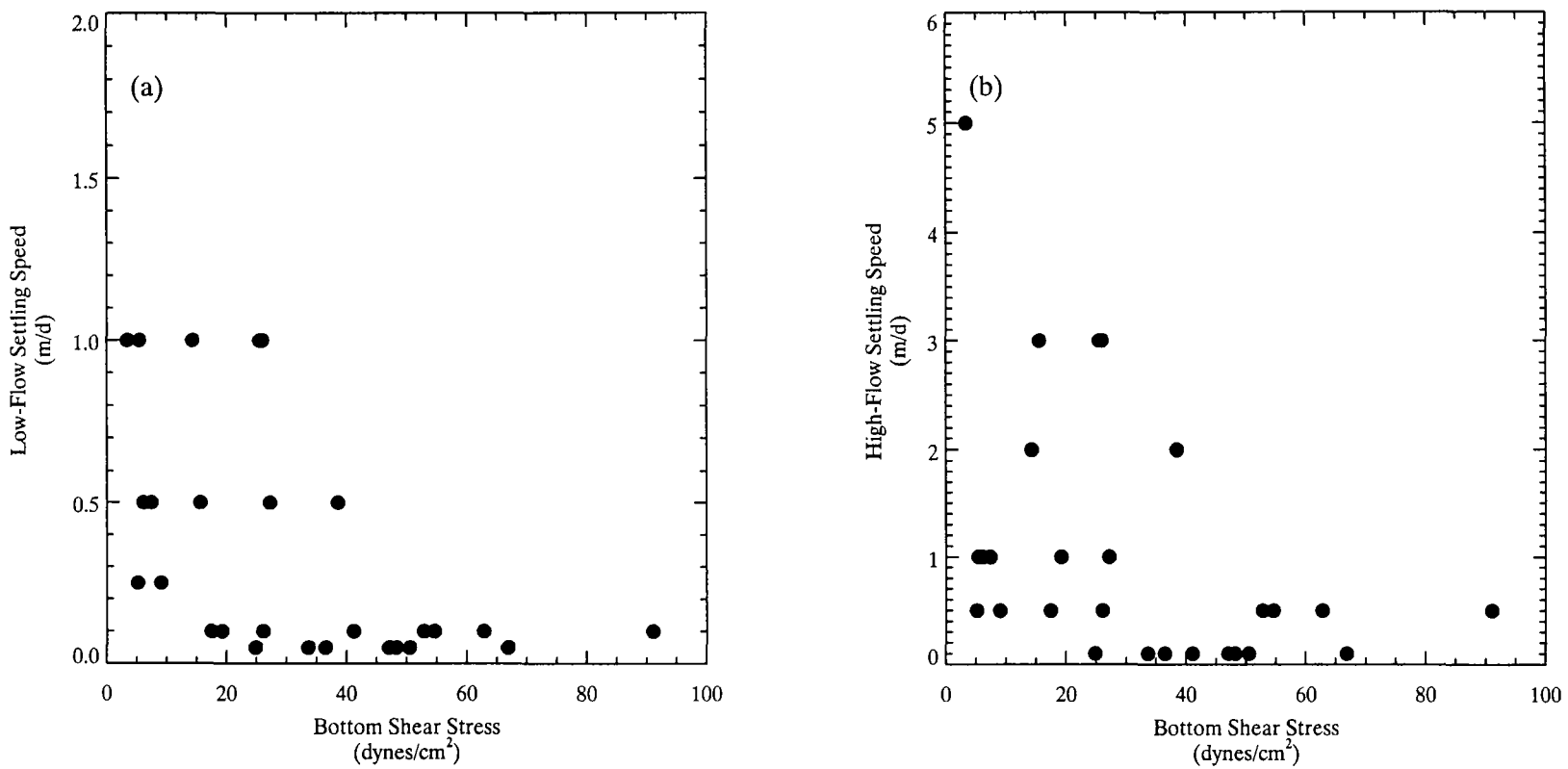

Figure 4-18. Dependence of (a) low-flow and (b) high-flow effective settling speed on bottom shear stress in river sections (segments 4-30).

cfo - E:\CDMkal\documents\Report\cowen\spatial_sedtran_param.pro
Fri Jun 15 12:15:40 2001

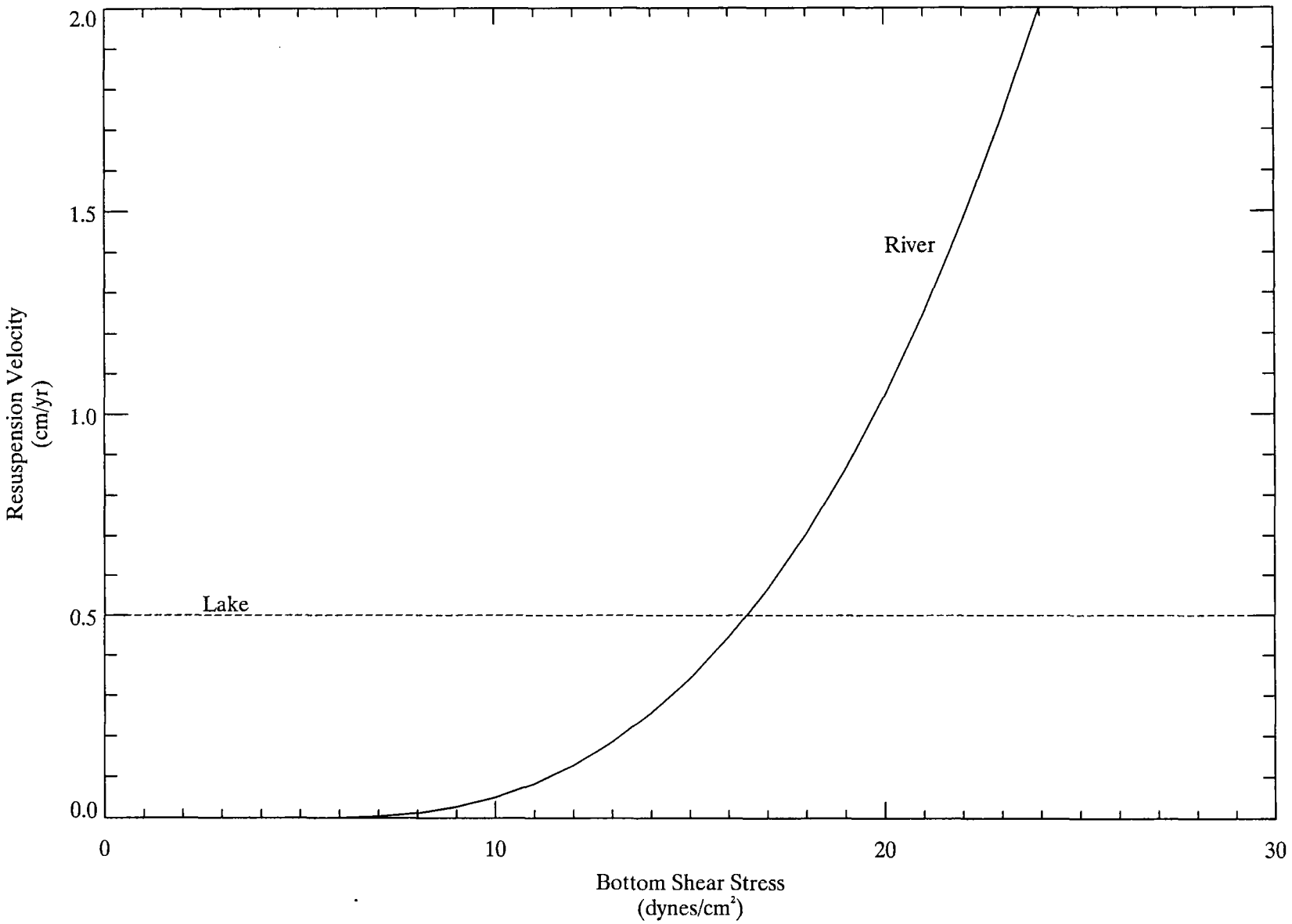

Figure 4-19. Resuspension velocity functions applied to river and lake areas.

HM - E:\CDMkal\documents\Report\Shear_resus.pro
Fri Jun 15 12:16:02 2001

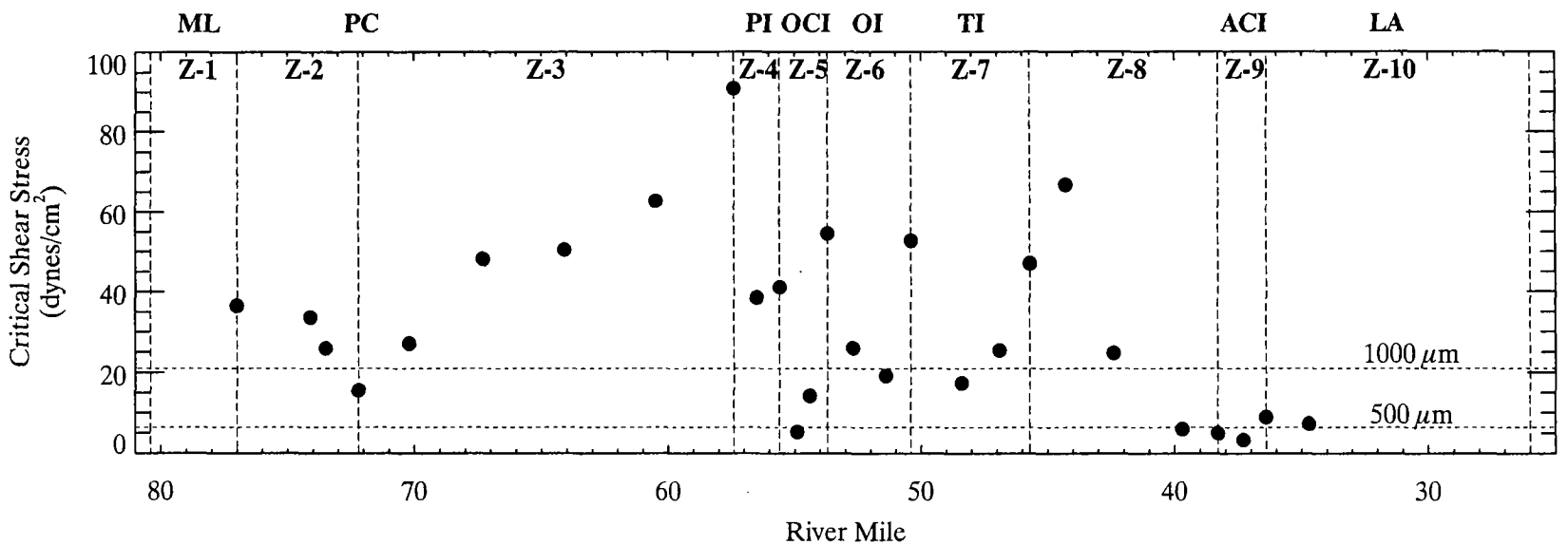

Figure 4-20. Spatial distribution of critical shear stress in river sections (segments 4-30). Critical shear stress for 500 and 1000 μm sand particles shown for comparison.

cfo - E:\CDMkal\documents\Report\cowen\spatial_sedtran_param.pro
Fri Jun 15 12:15:34 2001

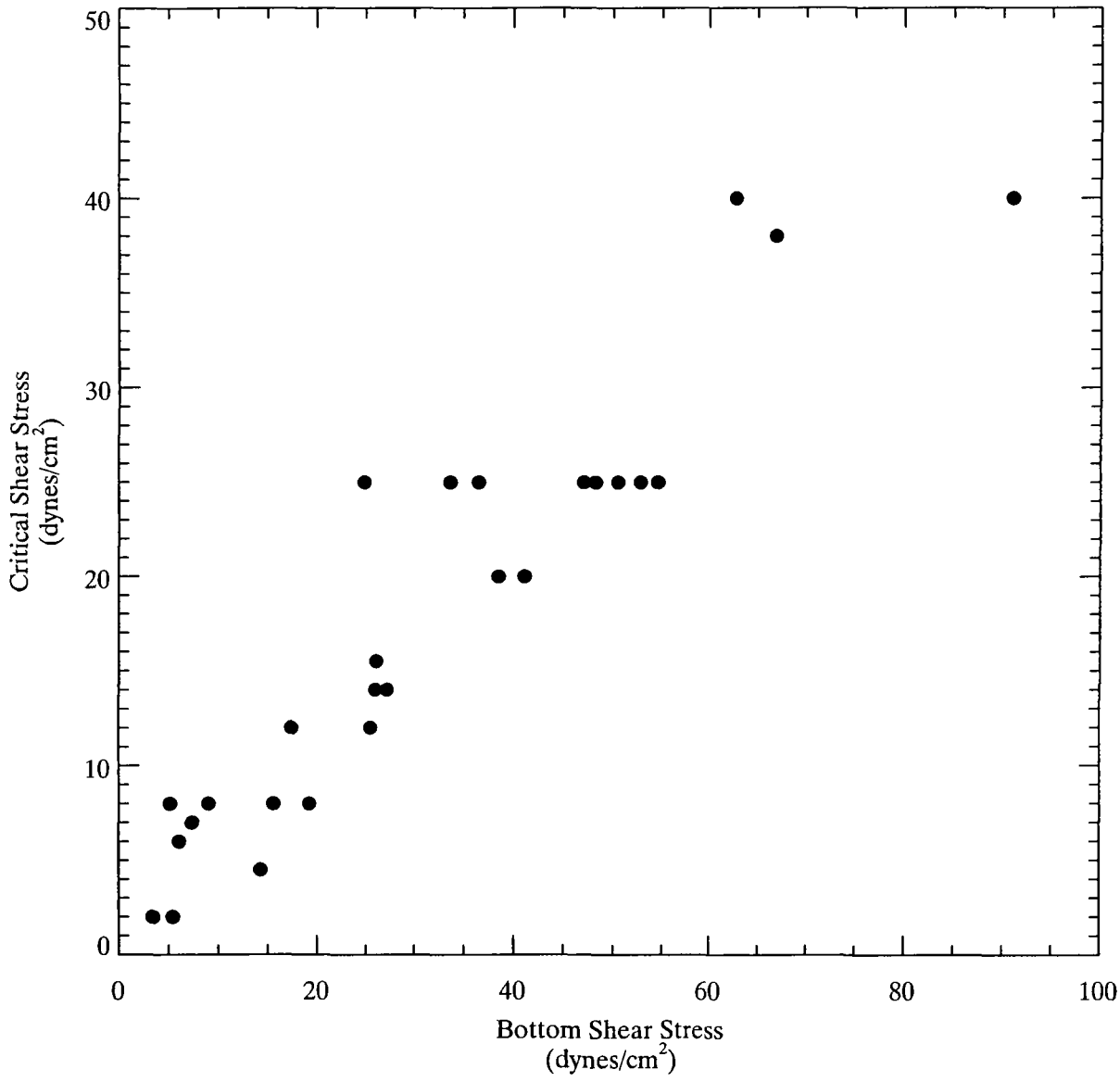

Figure 4-21. Dependence of critical shear stress on bottom shear stress in river sections (segments 4-30).

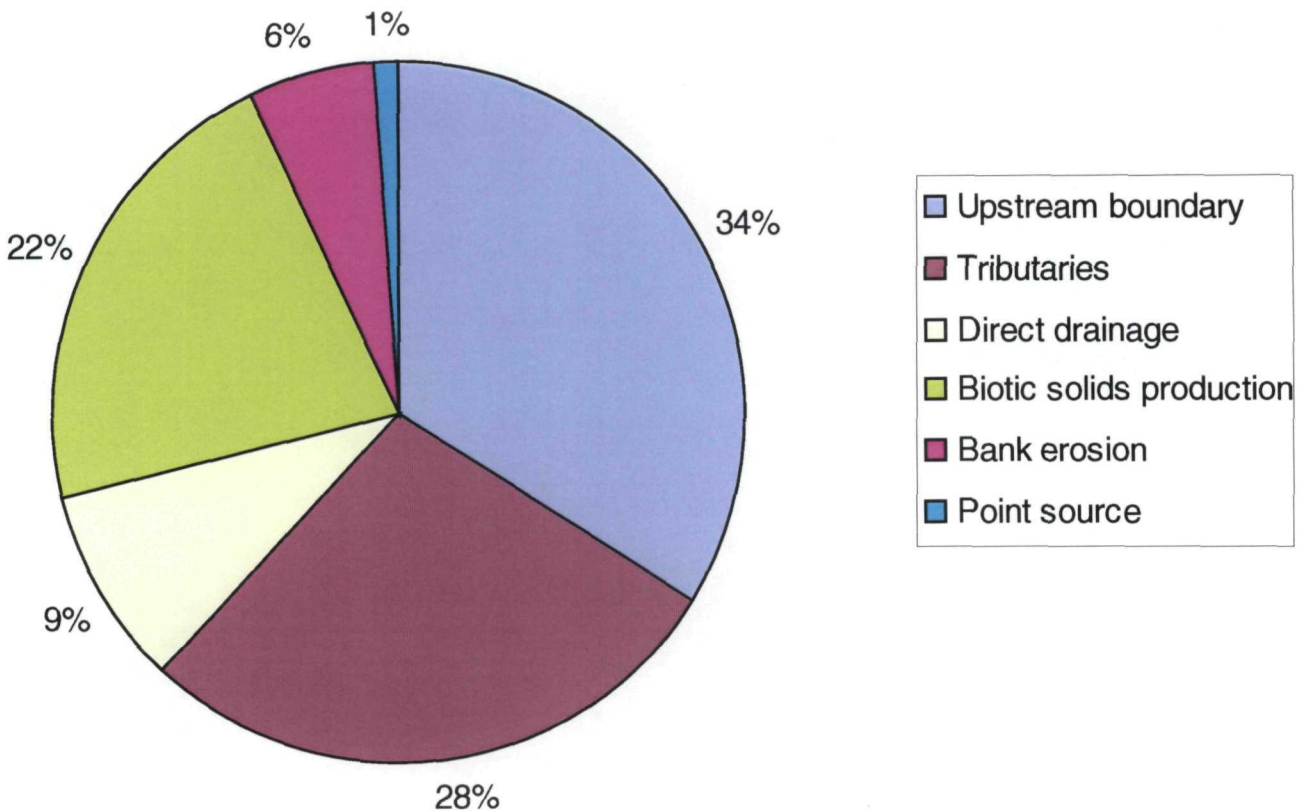

Figure 4-22. Distribution of sediment load sources for model calibration period (1993 through 1999). Total sediment load was 242,200 MT.

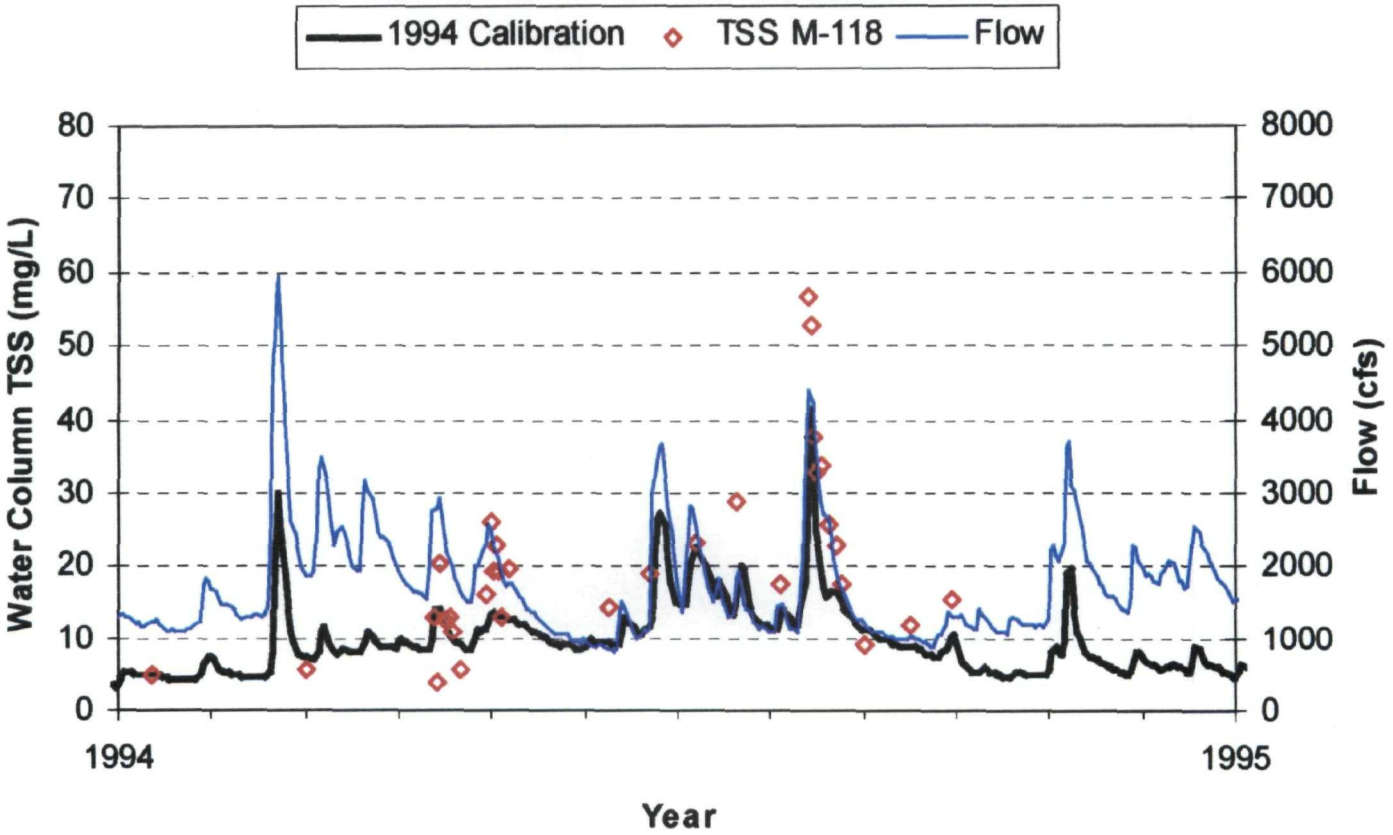

Figure 4-23. Comparison of predicted and measured TSS concentration at M-118 in Allegan City during 1994. Reproduction of Figure 7-3e in LTI (2000).

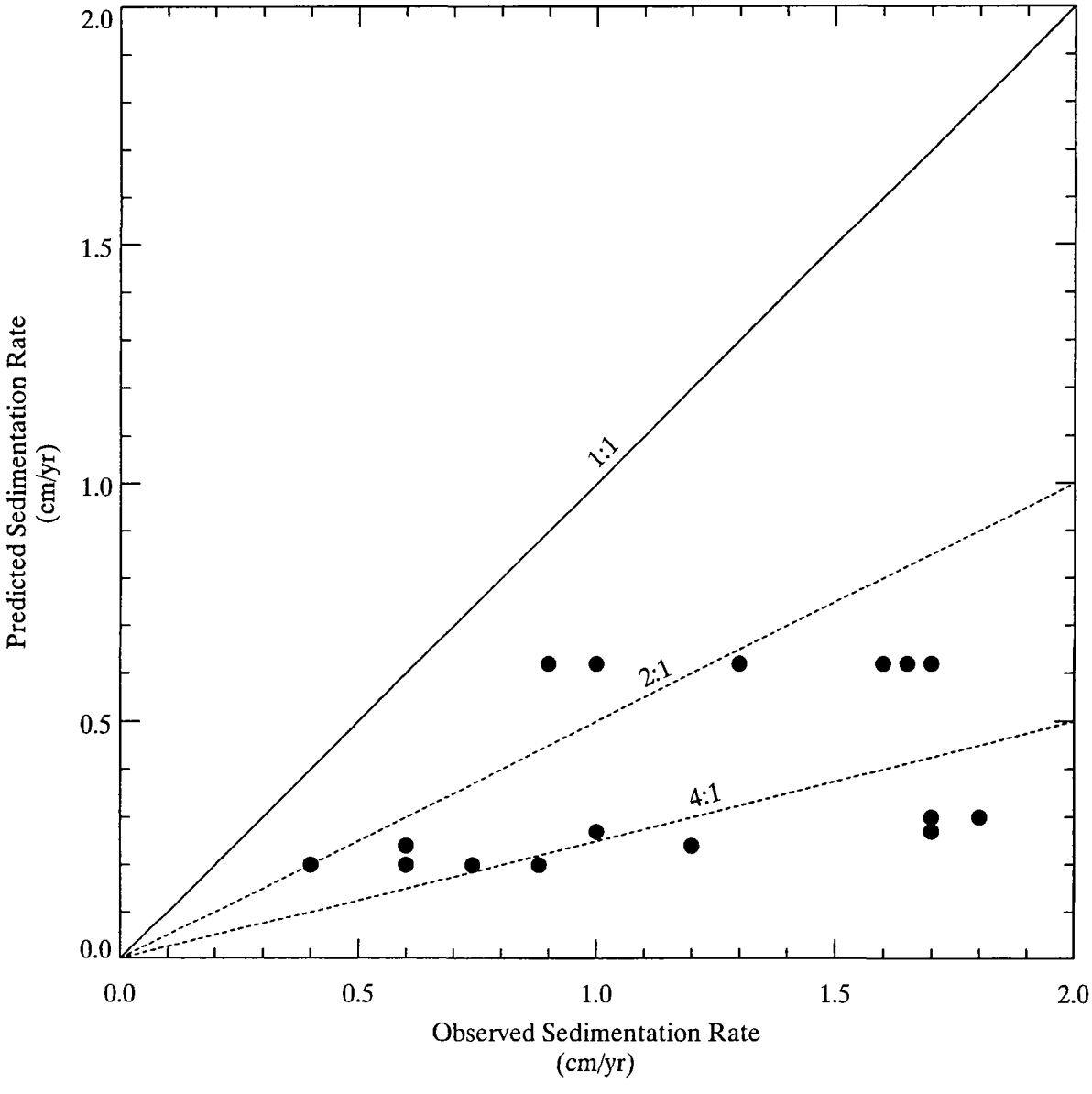

Figure 4-24. Comparison of predicted and observed sedimentation rates for model calibration period (1993 through 1999).

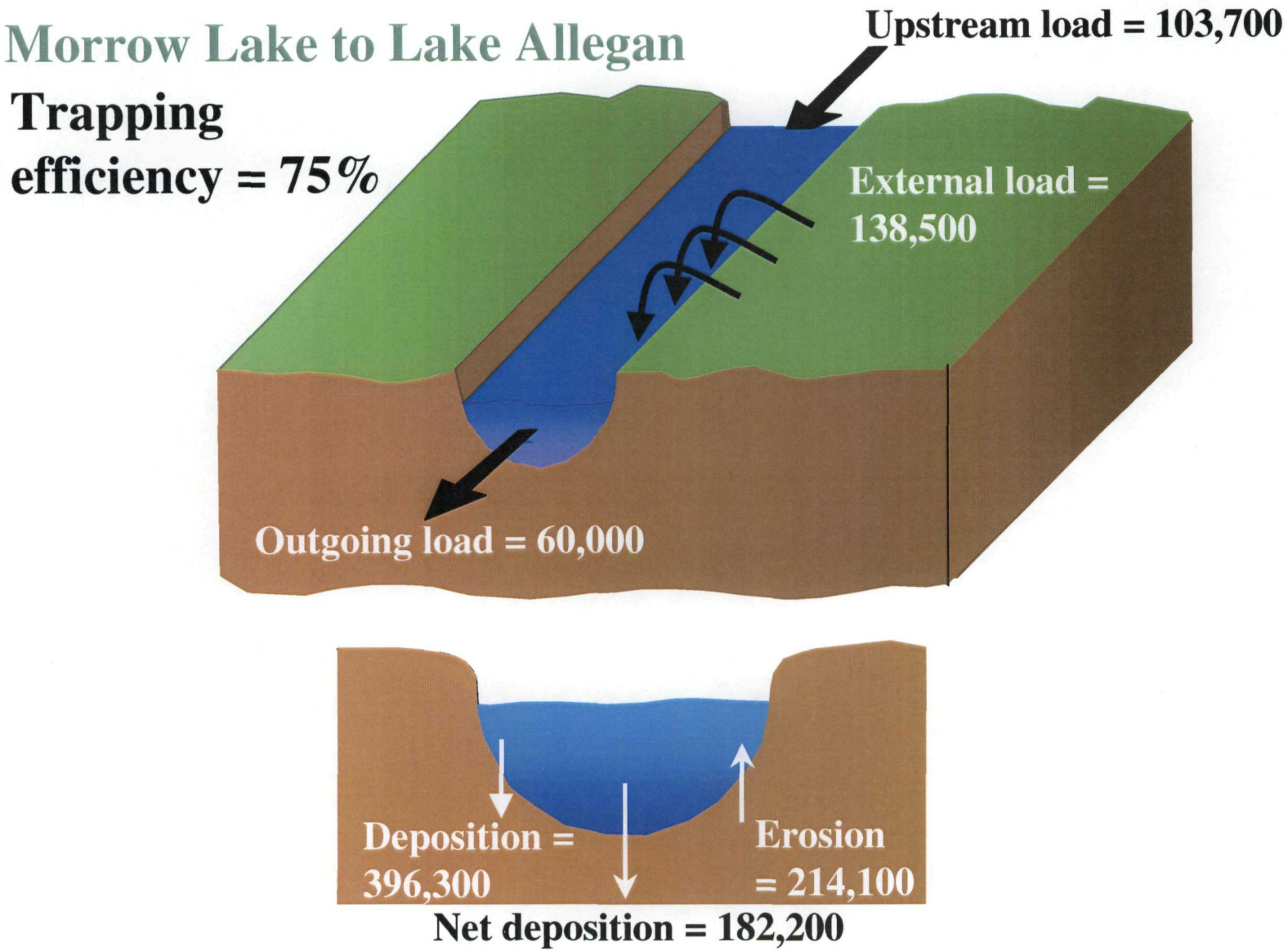

Figure 4-25. Sediment mass balance for Kalamazoo River based on model results during the calibration period (1993 through 1999). All values are in MT.

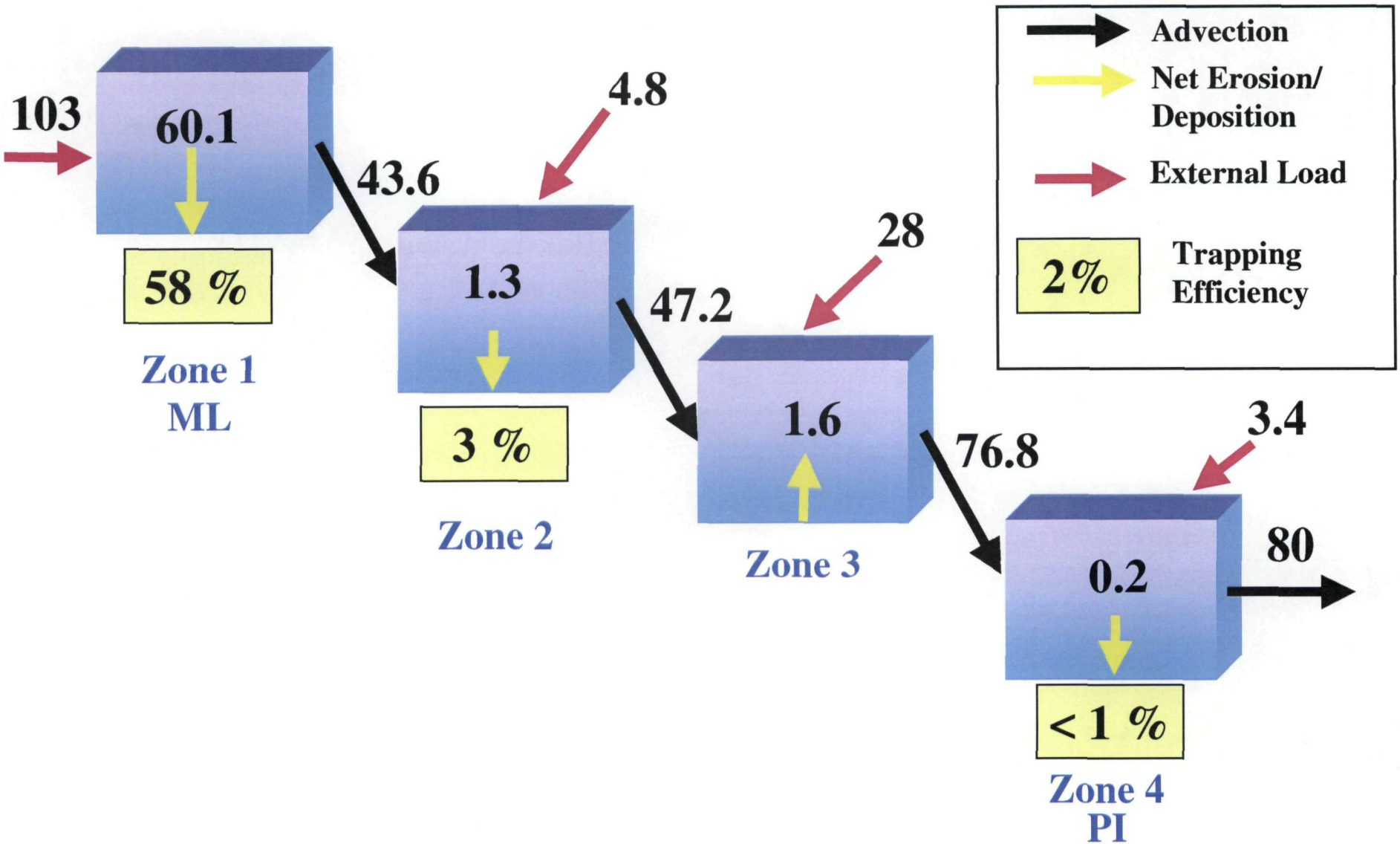

Figure 4-26. Sediment mass balance for zones 1 (Morrow Lake) to 4 (former Plainwell Impoundment) based on model results during calibration period (1993 through 1999). All values are in 1,000 MT.

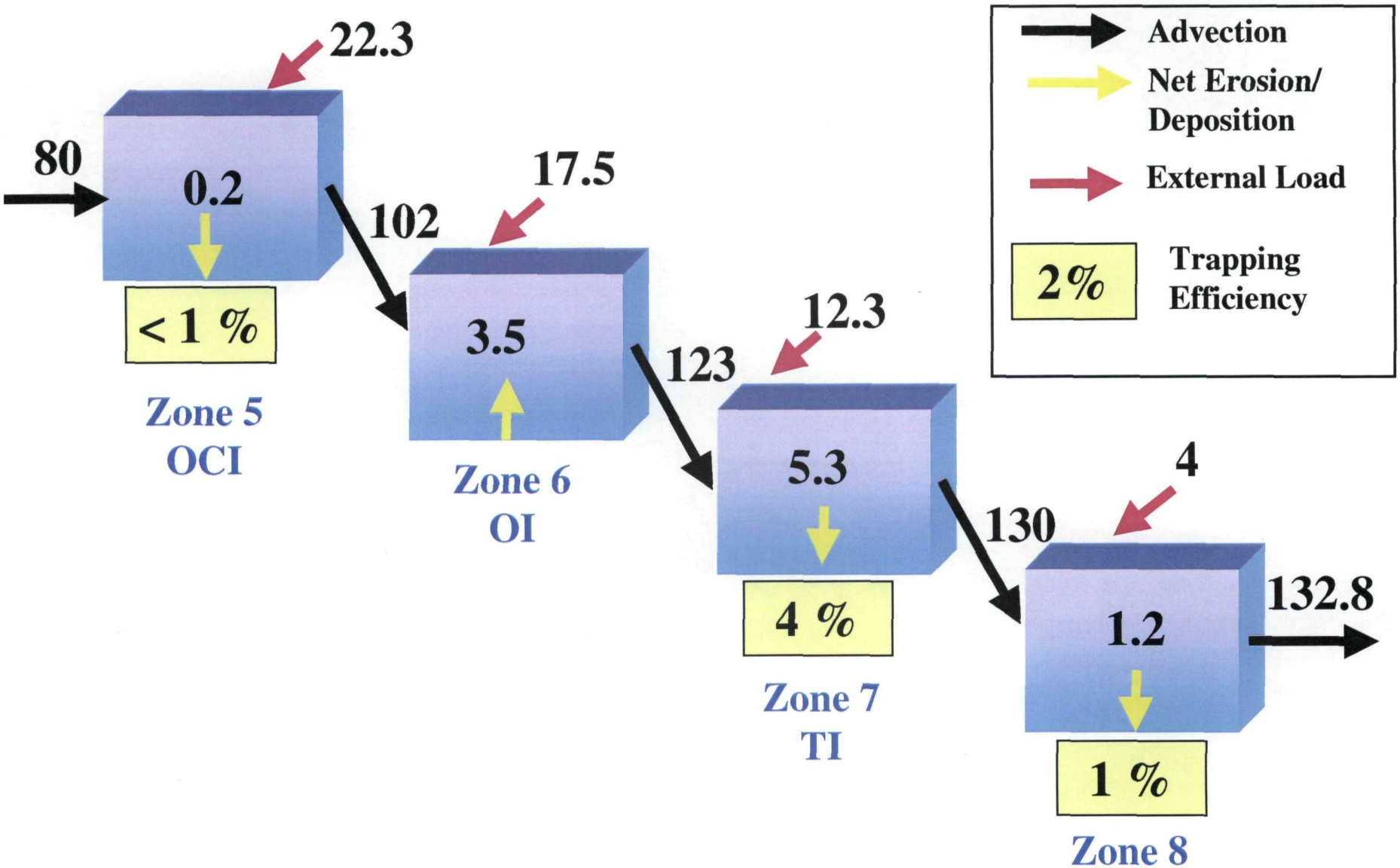

Figure 4-27. Sediment mass balance for zones 5 (Otsego City Impoundment) to 8 based on model results during calibration period (1993 through 1999). All values are in 1,000 MT.

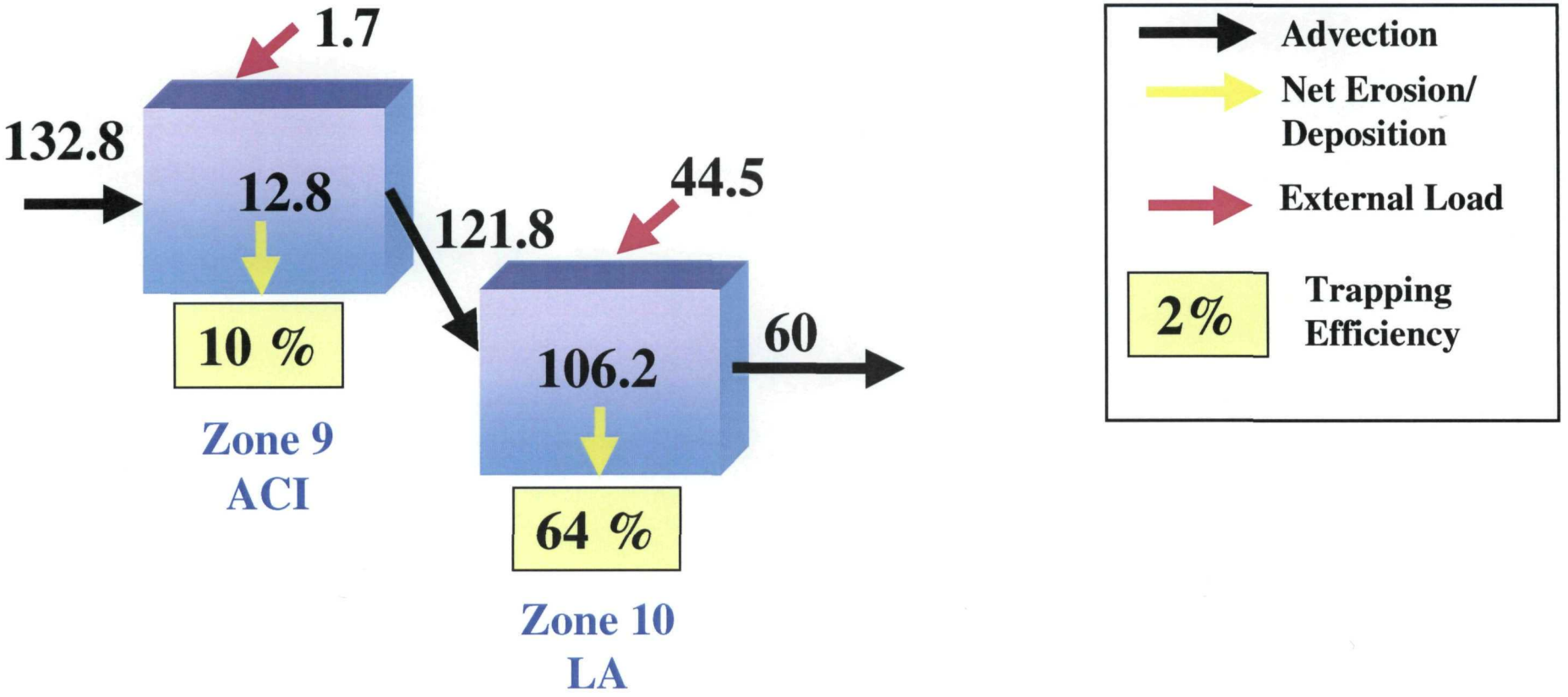

Figure 4-28. Sediment mass balance for zones 9 (Allegan City Impoundment) and 10 (Lake Allegan) based on model results during calibration period (1993 through 1999). All values are in 1,000 MT.

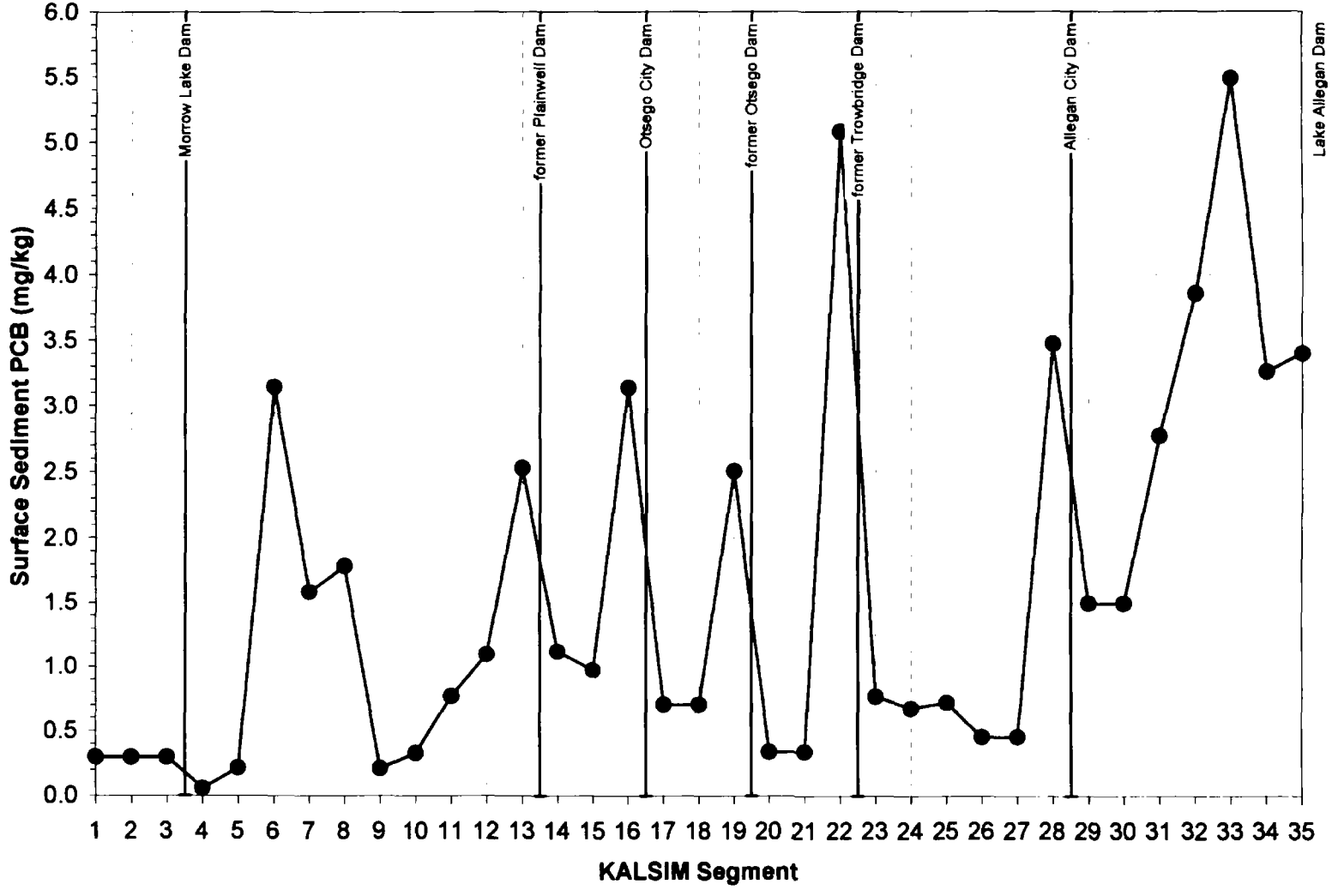

Figure 4-29. Spatial distribution of initial PCB concentrations in surficial sediments. Reproduction of Figure 4-18 in LTI (2000).

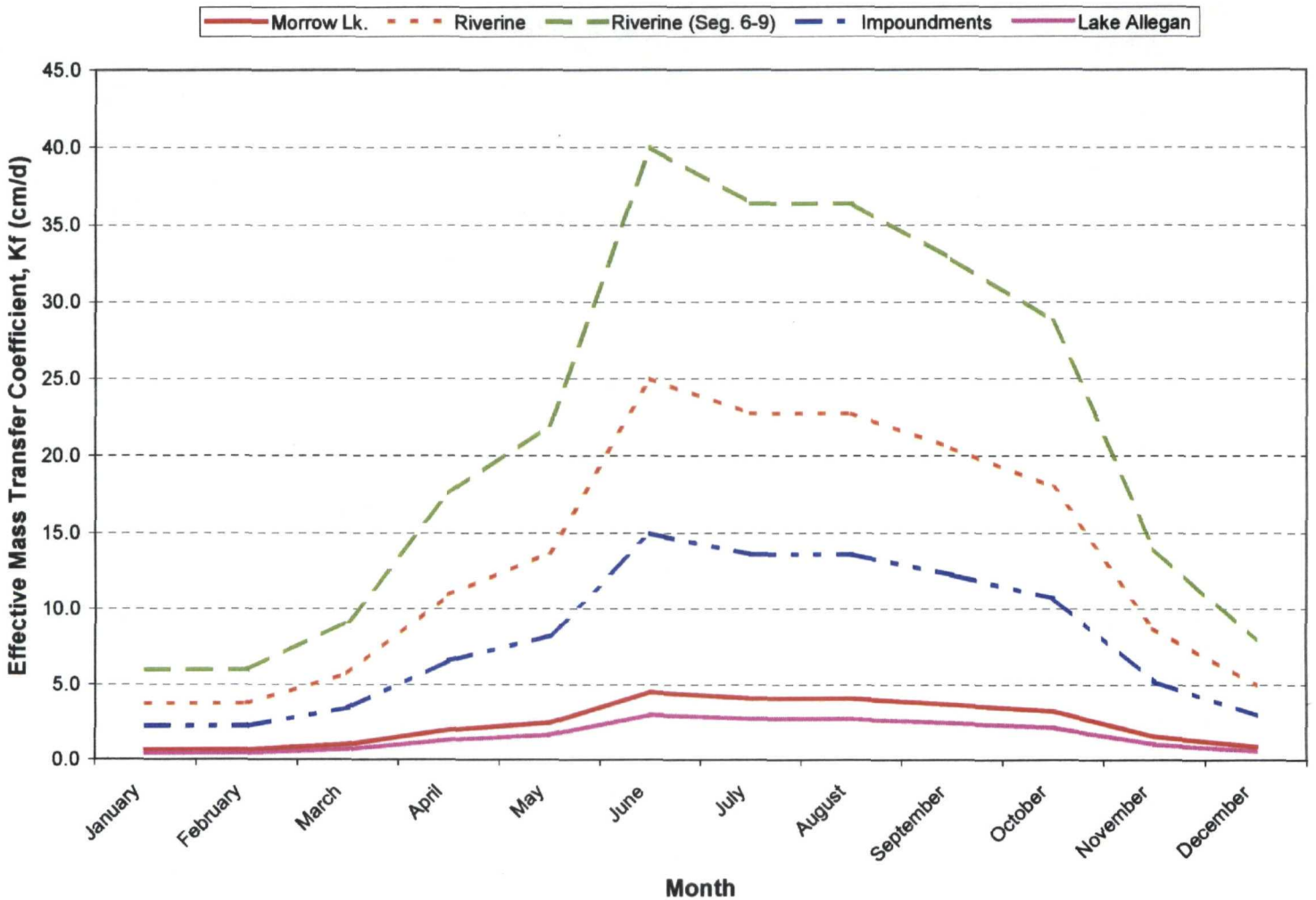

Figure 4-30. Temporal and spatial distribution of sediment-water mass transfer coefficient (K_f). Reproduction of Figure 7-2 in LTI (2000).

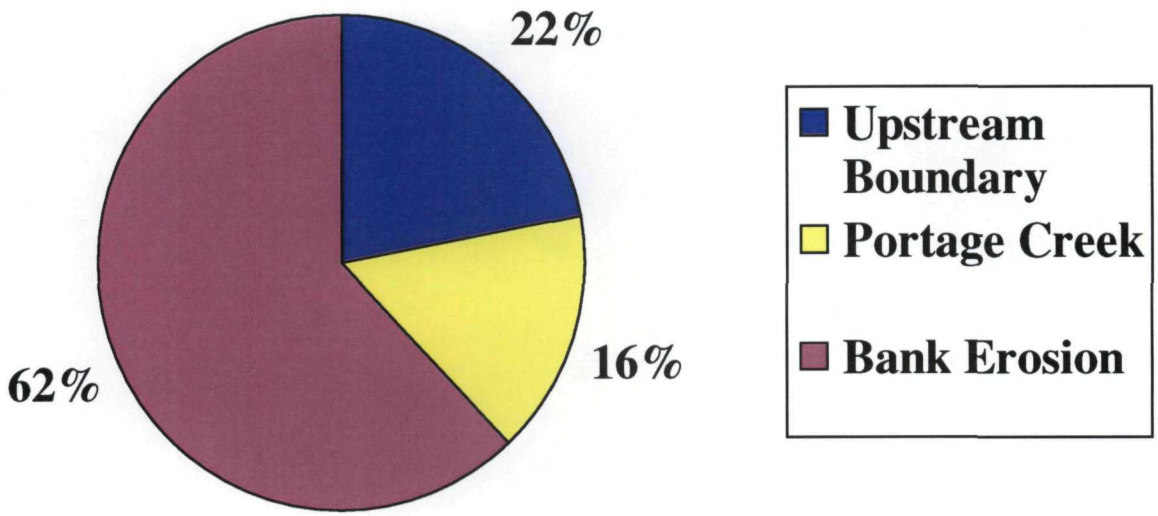

Figure 4-31. Distribution of external PCB loads input during calibration period (1993 through 1999).

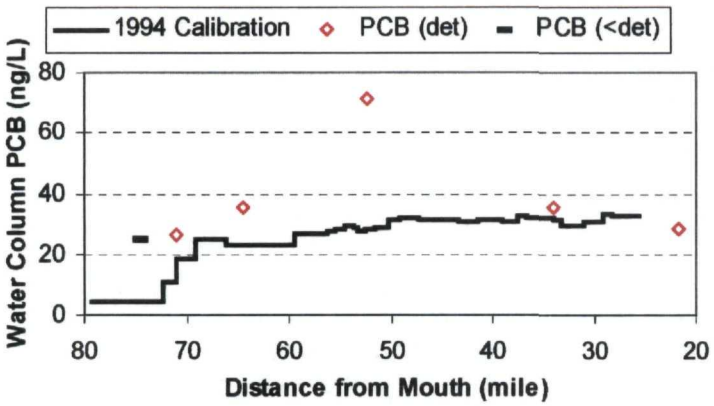

A. 6/9/1994, Segment 1 flow 550 cfs

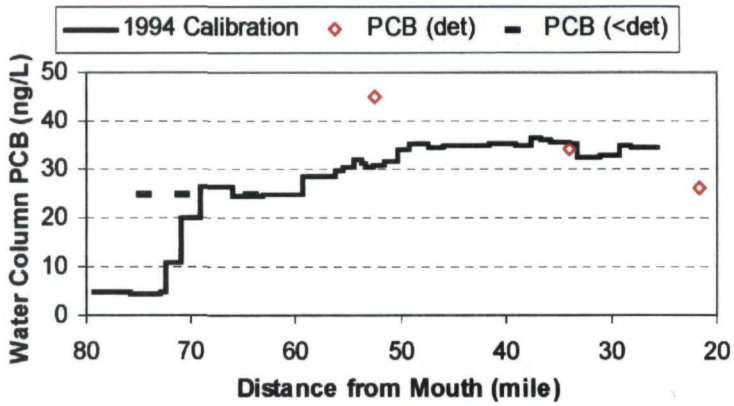

B. 6/22/1994, Segment 1 flow 700 cfs

Figure 4-32. Comparison between predicted and observed water column PCB concentrations during low-flow conditions in 1994. Reproduction of Figure 7-6 in LTI (2000).

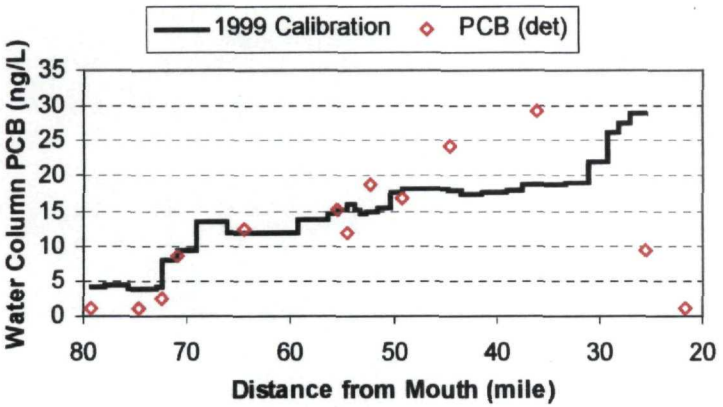

A. 9/9 - 9/10/1999, Segment 1 flow 350 cfs

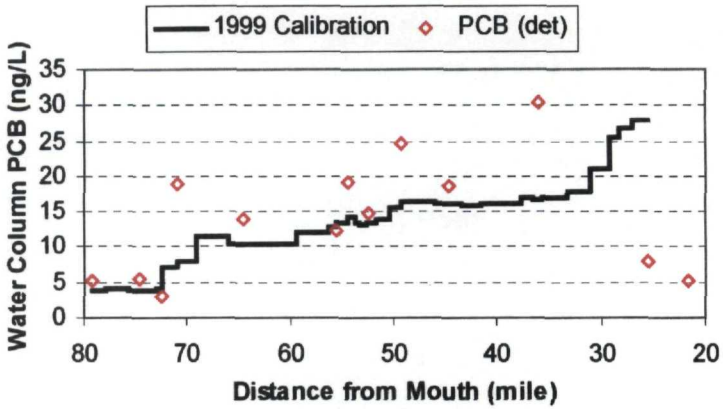

B. 9/20 – 9/21/1999, Segment 1 flow 400 cfs

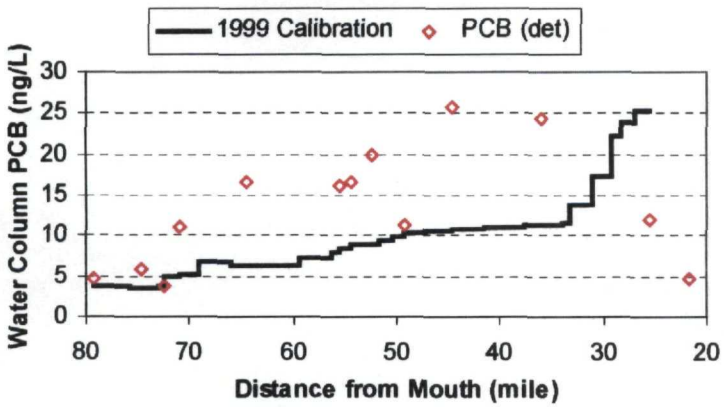

C. 10/20 – 10/21/1999, Segment 1 flow 450 cfs

Figure 4-33. Comparison between predicted and observed water column PCB concentrations during low-flow conditions in 1999. Reproduction of Figure 7-8 in LTI (2000).

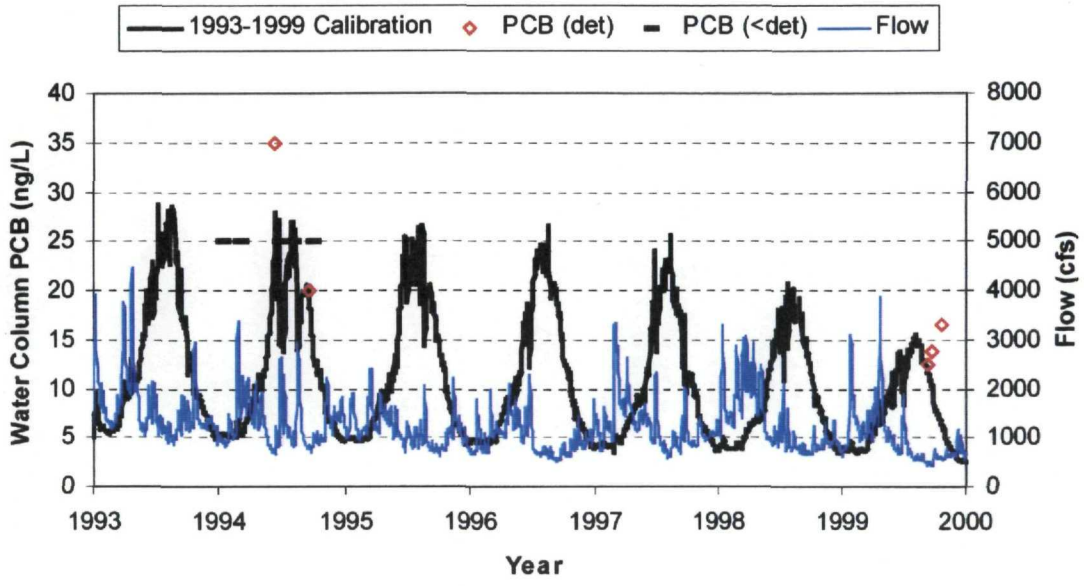

C. D Avenue, Cooper Township

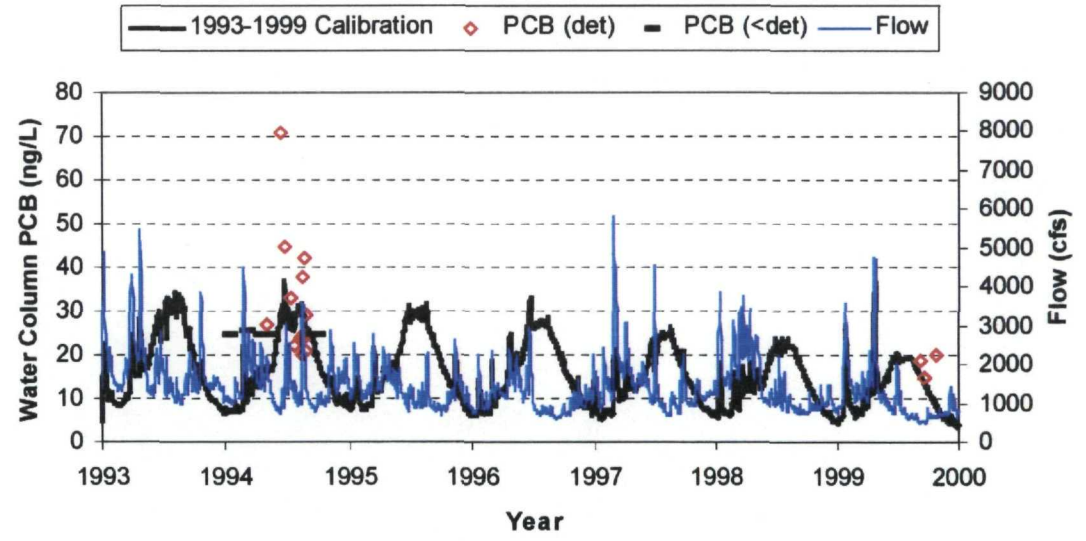

D. Farmer Street, Otsego

Figure 4-34. Comparison between predicted and observed water column PCB concentrations at two locations during the calibration period. Reproduction of Figure 7-11c,d in LTI (2000).

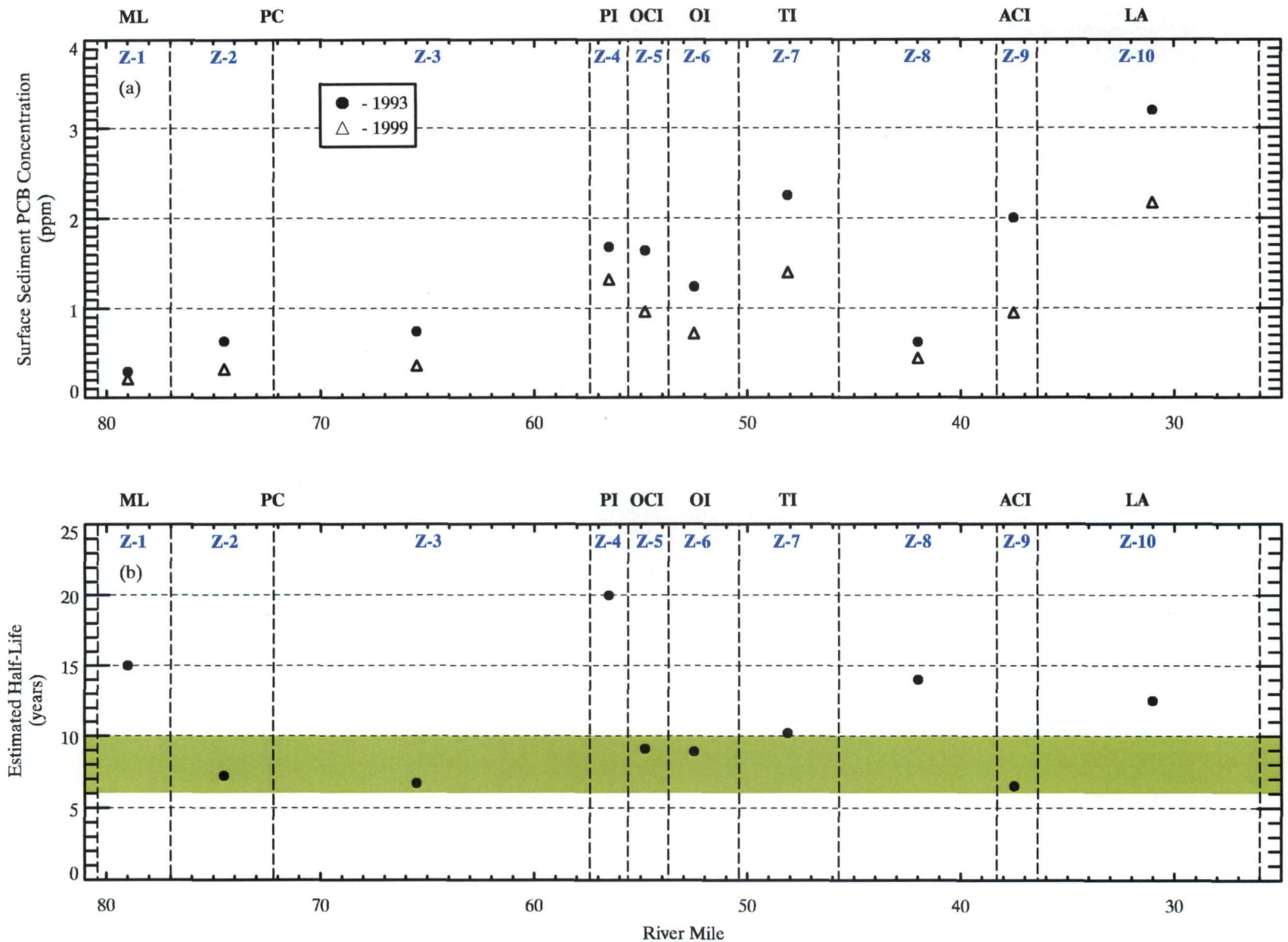

Figure 4-35. Spatial distributions of (a) predicted surficial sediment PCB concentrations in 1993 and 1999 and (b) corresponding PCB half-lives (green band corresponds to PCB half-life range based on temporal analysis of fish data). Average values for zones 1-10 are shown.

HM - E:\CDMkal\documents\Report\half_life.pro
Fri Jun 15 14:48:06 2001

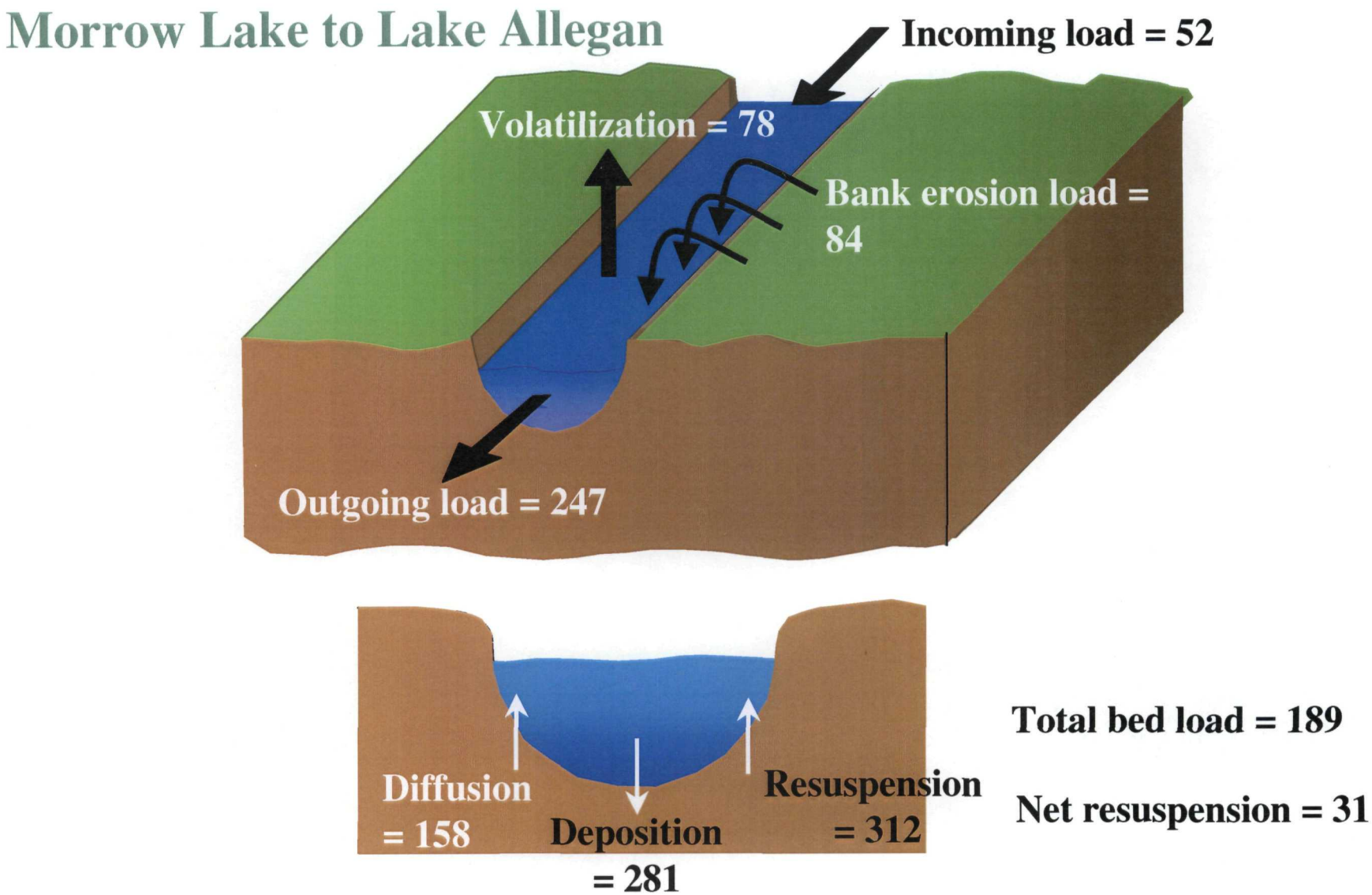

Figure 4-36. PCB mass balance for water column PCBs in the Kalamazoo River based on model results during calibration period (1993 through 1999). All values are in kg.

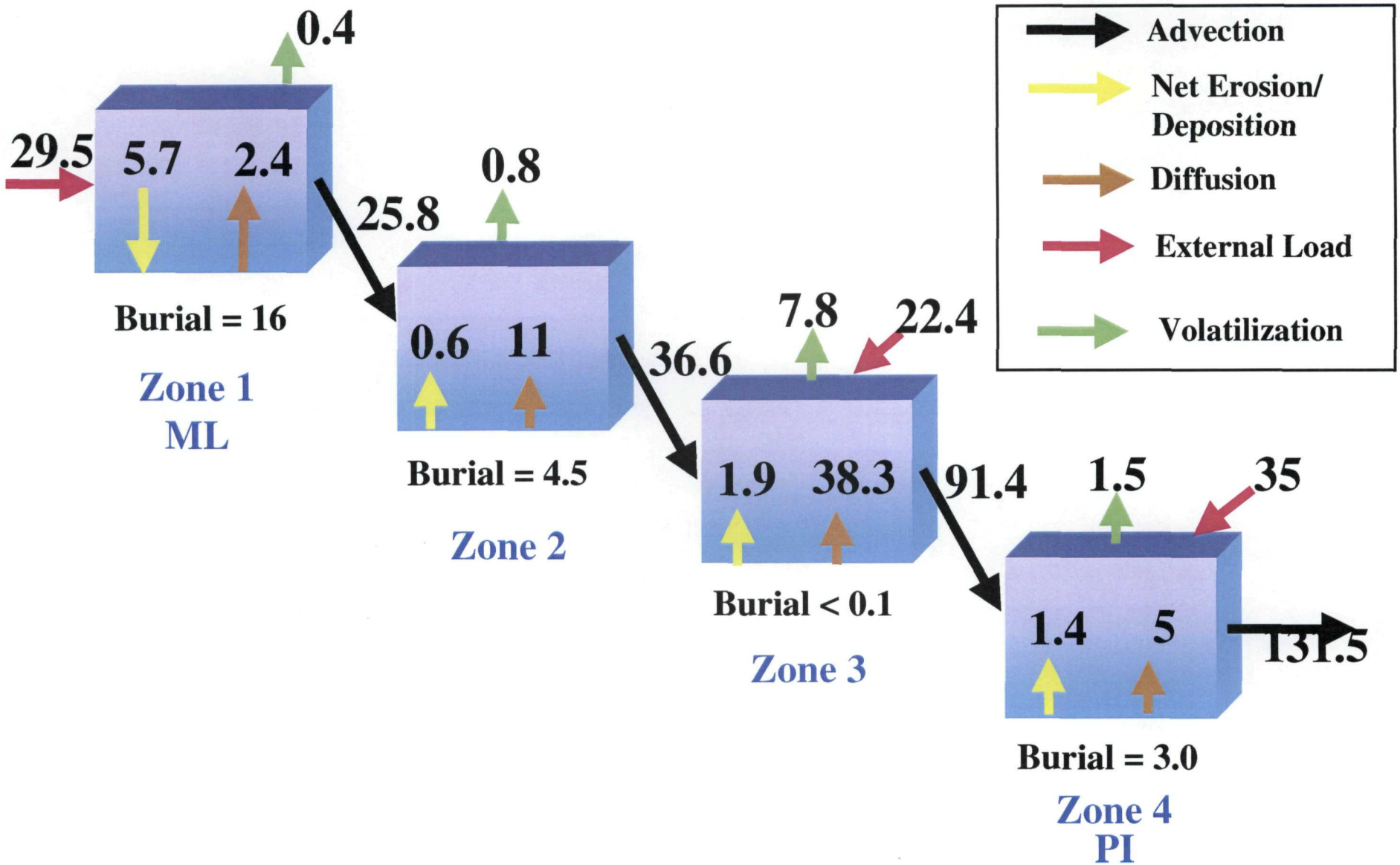

Figure 4-37. Water column PCB mass balance for zones 1 (Morrow Lake) to 4 (former Plainwell Impoundment) based on model results during calibration period (1993 through 1999). All values are in kg.

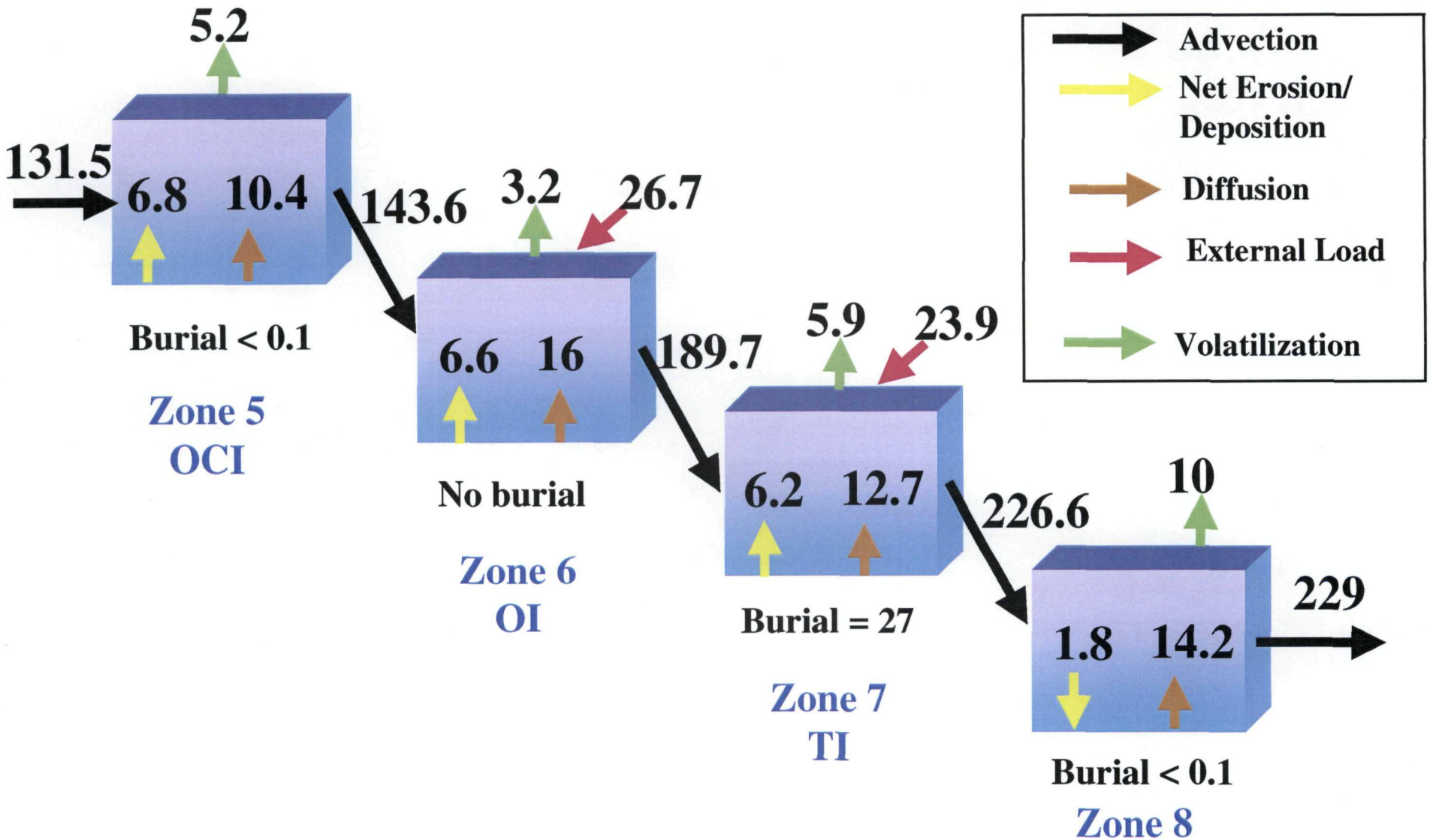

Figure 4-38. Water column PCB mass balance for zones 5 (Otsego City Impoundment) to 8 based on model results during calibration period (1993 through 1999). All values are in kg.

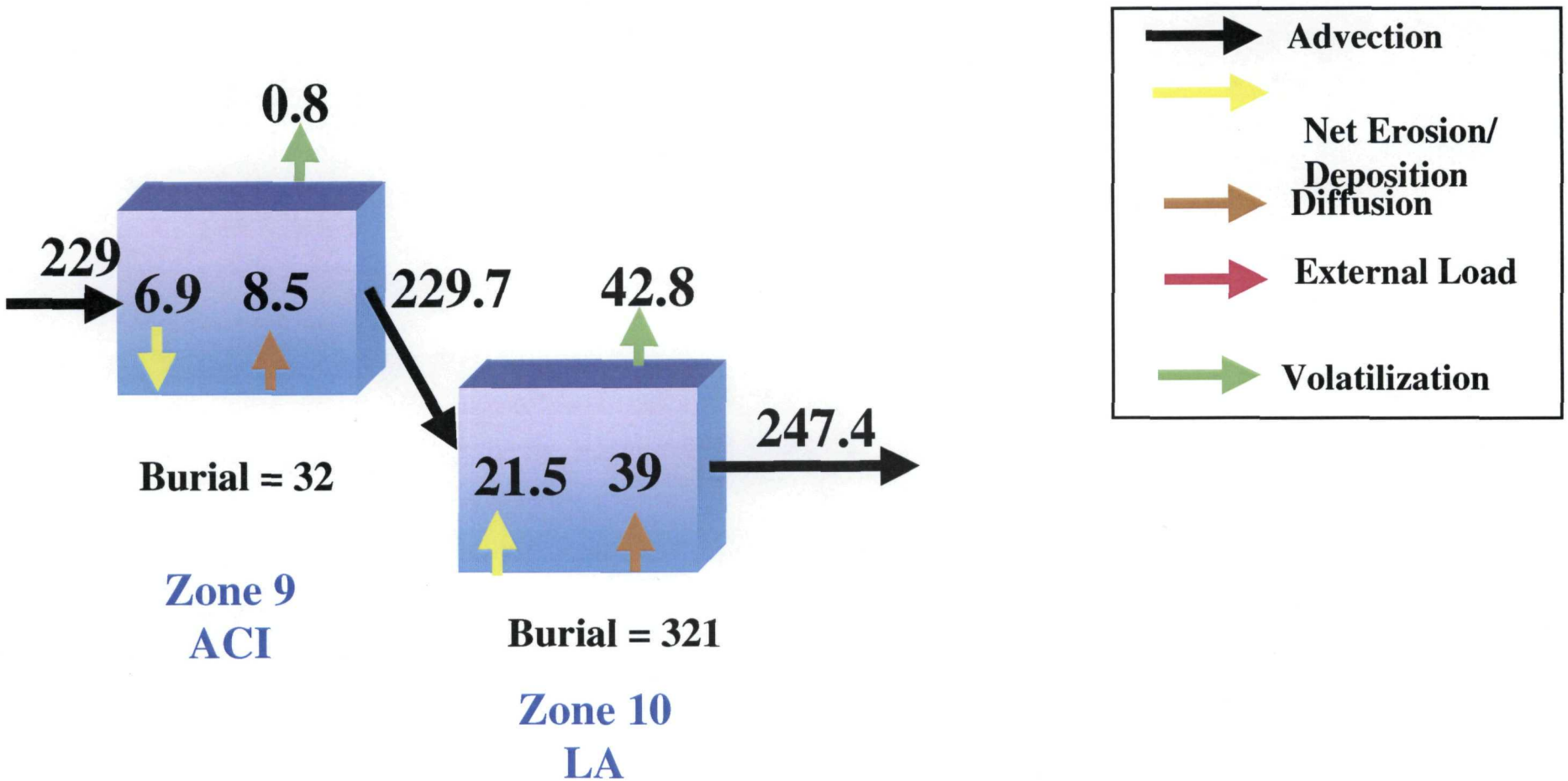

Figure 4-39. Water column PCB mass balance for zones 9 (Allegan City Impoundment) and 10 (Lake Allegan) based on model results during calibration period (1993 through 1999). All values are in kg.

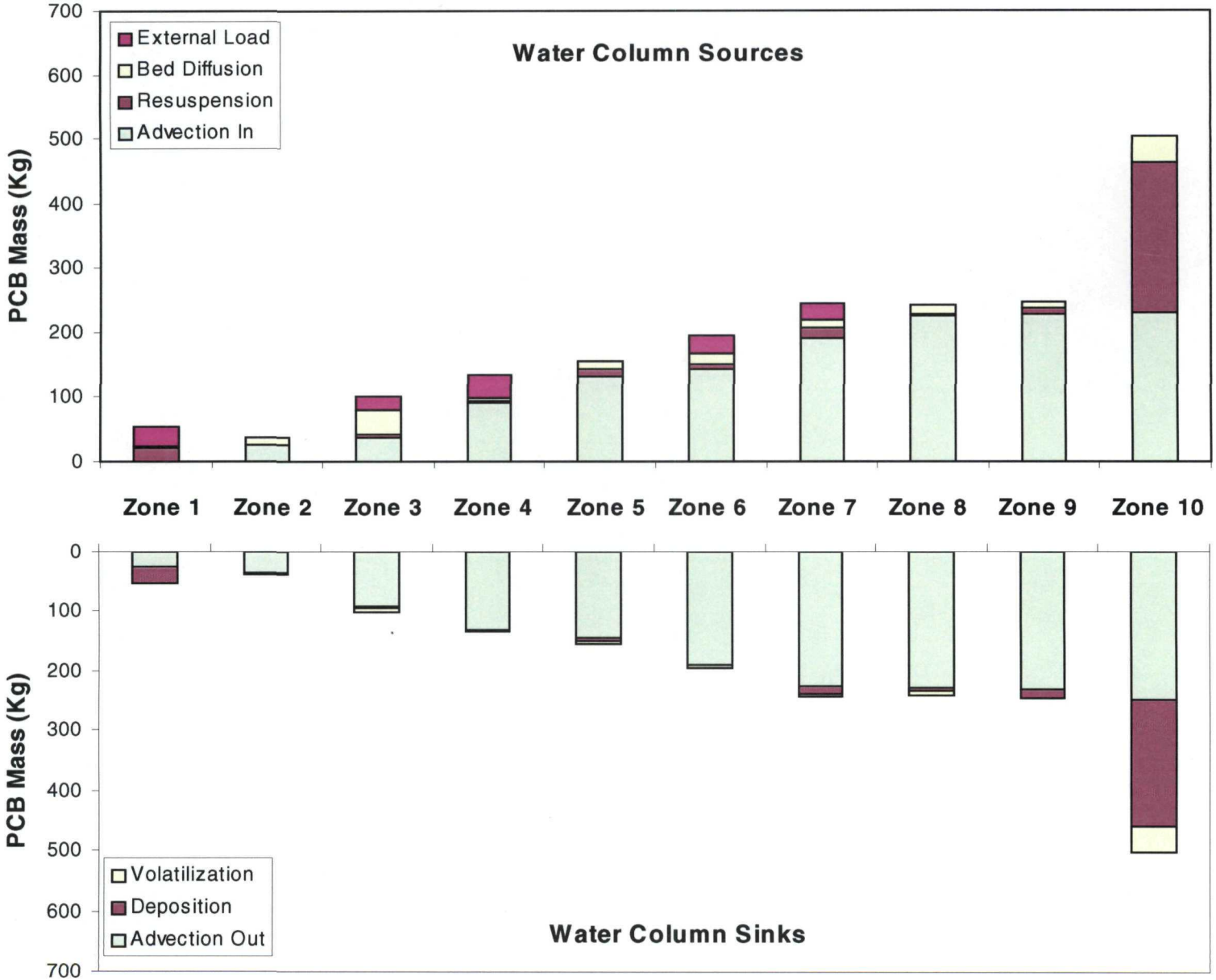

Figure 4-40. Sources and sinks of water column PCBs in zones 1 to 10 based on model results during calibration period (1993 through 1999).

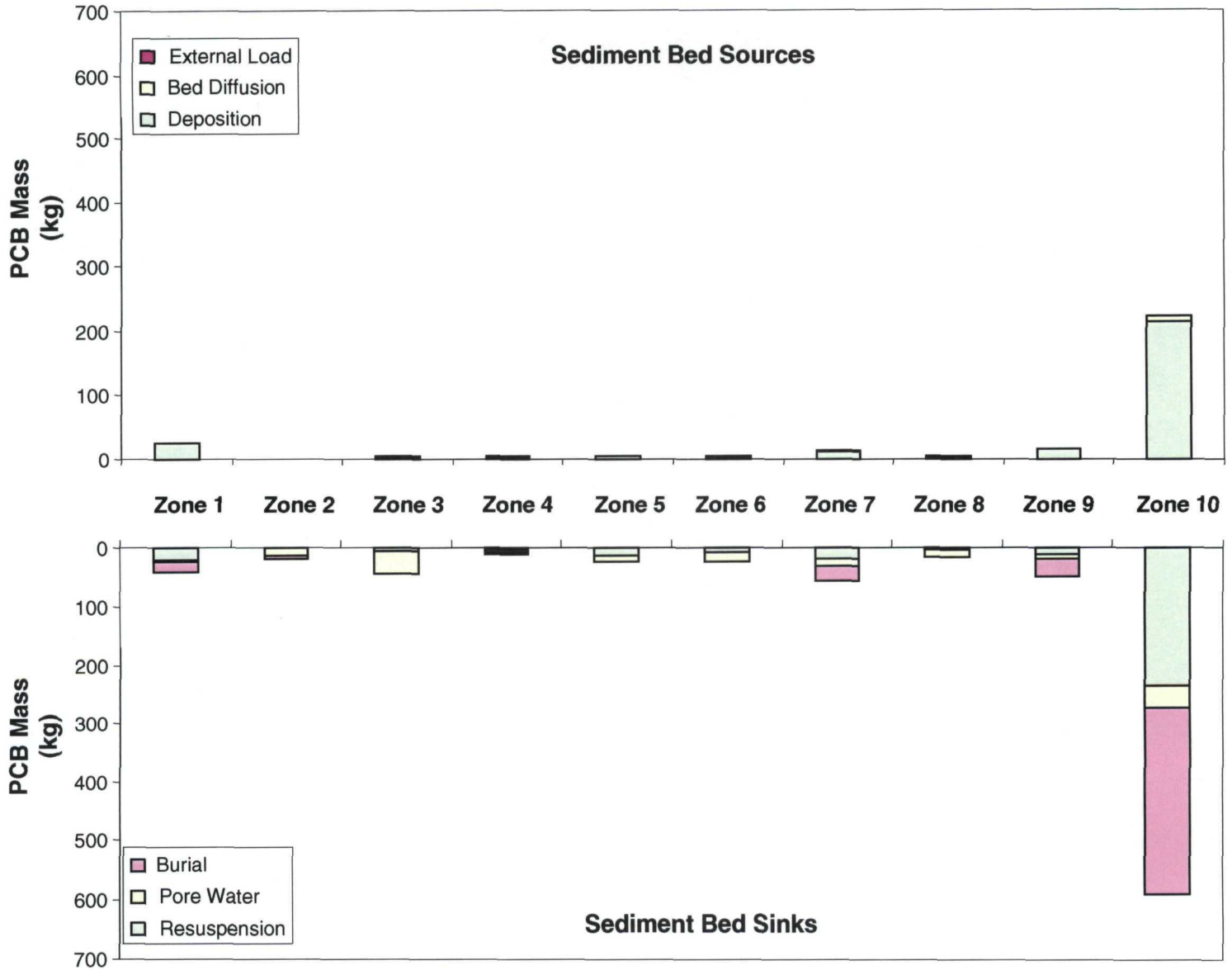

Figure 4-41. Sources and sinks of sediment PCBs in the well-mixed (top 5 cm) layer in zones 1 to 10 based on model results during calibration period (1993 through 1999).

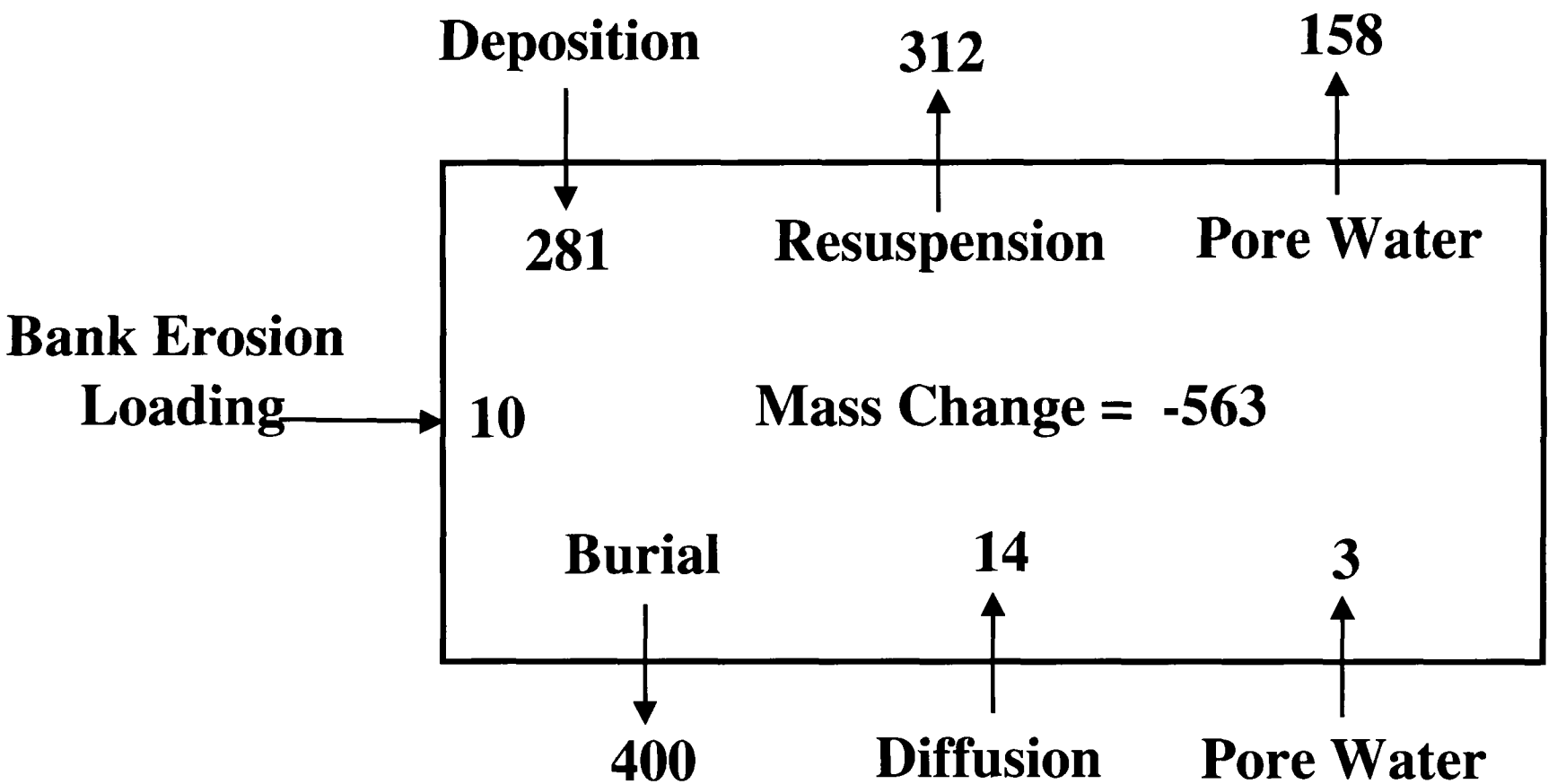

Figure 4-42 Sediment PCB mass balance for the well-mixed (top 5 cm) layer in the Kalamazoo River based on model results during calibration period (1993 through 1999). All values are in kg.